Transportation fuels from biomass fast pyrolysis, catalytic hydrodeoxygenation, and catalytic fast hydropyrolysis

Dabros, Trine M. H.; Stummann, Magnus Zingler; Høj, Martin; Jensen, Peter Arendt; Grunwaldt, Jan-Dierk; Gabrielsen, Jostein; Mortensen, Peter M.; Jensen, Anker Degn

Published in:
Progress in Energy and Combustion Science

Link to article, DOI:
10.1016/j.pecs.2018.05.002

Publication date:
2018

Document Version
Peer reviewed version

Transportation Fuels from Biomass Fast Pyrolysis, Catalytic Hydrodeoxygenation, and Catalytic Fast Hydropyrolysis

Trine M. H. Dabros[a] trina@kt.dtu.dk

Magnus Zingler Stummann[a] mazi@kt.dtu.dk

Martin Høj[a] mh@kt.dtu.dk

Peter Arendt Jensen[a]

Jan-Dierk Grunwaldt[b] grunwaldt@kit.edu

Jostein Gabrielsen[c]

Peter M. Mortensen[c]

Anker Degn Jensen*[,a] aj@kt.dtu.dk

a) Department of Chemical and Biochemical Engineering, Technical University of Denmark (DTU), Søltofts Plads 229, Kgs. Lyngby, DK-2800 (Denmark).

b) Institute for Chemical Technology and Polymer Chemistry, Karlsruhe Institute of Technology (KIT), Engesserstr. 20, Karlsruhe, D-76131 (Germany).

c) Haldor Topsøe A/S, Haldor Topsøes Allé 1, Kgs. Lyngby, DK-2800 (Denmark).

**)* Corresponding author: aj@kt.dtu.dk, Department of Chemical and Biochemical Engineering, Technical University of Denmark (DTU), Søltofts Plads 229, Kgs. Lyngby, DK-2800 (Denmark).

Abstract

This review presents and discusses the progress in combining fast pyrolysis and catalytic hydrodeoxygenation (HDO) to produce liquid fuel from solid, lignocellulosic biomass. Fast pyrolysis of biomass is a well-developed technology for bio-oil production at mass yields up to ~75%, but a high oxygen content of 35-50wt% strongly limits its potential as transportation fuel. Catalytic HDO can be used to upgrade fast pyrolysis bio-oil, as oxygenates react with hydrogen to produce a stable hydrocarbon fuel and water, which is removed by separation. Research on HDO has been carried out for more than 30 years with increasing intensity over the past decades. Several catalytic systems have been tested, and we conclude that single stage HDO of condensed bio-oil is unsuited for commercial scale bio-oil upgrading, as the coking and polymerization, which occurs upon re-heating of the bio-oil, rapidly deactivates the catalyst and plugs the reactor. Dual or multiple stage HDO has shown more promising results, as the most reactive oxygenates can be stabilized at low temperature prior to deep HDO for full deoxygenation. Catalytic fast hydropyrolysis, which combines fast pyrolysis with catalytic HDO in a single reactor, eliminates the need for reheating condensed bio-oil, lowers side reactions, and produces a stable oil with oxygen content, H/C ratio, and heating value comparable to fossil fuels. We address several challenges, which must be overcome for continuous catalytic fast hydropyrolysis to become commercially viable, with the most urgent issues being: *i)* optimization of operating conditions (temperature, H_2 pressure, and residence time) and catalyst formulation to maximize oil yield and minimize cracking, coke formation, and catalyst deactivation, *ii)* development of an improved process design and reactor configuration to allow for continuous operation including pressurized biomass feeding, fast entrainment and collection of char, which is catalytically active for side reactions, efficient condensation of the produced oil, and utilization and/or integration of by-products (non-condensable gasses and char), and *iii)* long-term tests with respect to catalyst stability and possible pathways for regeneration. By reviewing past and current research from fast pyrolysis and catalytic HDO, we

target a discussion of the combined processes, including direct catalytic fast hydropyrolysis. By critically evaluating their potential and challenges, we finally conclude, which future steps are necessary for these processes to become industrially feasible.

Keywords: fast pyrolysis; catalytic hydrodeoxygenation (HDO); catalytic fast hydropyrolysis; bio-oil; transportation fuel

Abbreviations

AC	Activated carbon
ACI	Acid catalyzed reactions
ACP	Phosphorus activated carbon
BFB	Bubbling fluid bed
CAN	Carbonyl number
CFB	Circulating fluid bed
CRA	Cracking
CUS	Coordinatively unsaturated site
daf	Dry ash free basis
db	Dry basis
DCO	Decarboxylation and/or decarbonylation
DDO	Direct deoxygenation
DFT	Density functional theory
DME	Demethylation
DMO	Demethoxylation
DOD	Degree of deoxygenation
EXAFS	Extended X-ray absorption fine structure
FCC	fluid catalytic cracking
GC	Gas chromatography
GHG	Greenhouse gas
GPC	Gel permeation chromatography
HCR	Hydrocracking
HDM	Hydrodemetallization
HDN	Hydrodenitrogenation
HDO	Hydrodeoxygenation
HDS	Hydrodesulfurization
HHV	Higher heating value
HYD	Hydrogenation
IR	Infrared
LCA	Life cycle assessment
LHSV	Liquid hourly space velocity

OECD	Organization for Economic Co-operation and Development
MS	Mass spectrometry
MT	Methyl transfer
NMR	Nuclear magnetic resonance
ppm	Parts per million
Q-EXAFS	Quick extended X-ray absorption fine structure
SNG	Synthetic natural gas
STM	Scanning tunneling microscopy
TAN	Total acid number
TEM	Transmission electron microscopy
TGA	Thermogravimetric analysis
TOF	Turn over frequency
WHSV	Weight hourly space velocity
XAS	X-ray absorption spectroscopy

Contents

1. Introduction

Today's production and use of energy is responsible for 60% of the global greenhouse gas (GHG) emissions (2016 number) [1]. With an increasing world population and the continued industrialization of developing countries the energy consumption will keep increasing in the near future [2–4]. In addition, the depletion of fossil resources and the wide awareness of anthropogenic global warming have intensified the search for renewable and sustainable energy resources that can support our modern way of living [5].

The increase in the anthropogenic CO_2 emissions can be traced back to the industrialization that accelerated through the 20^{th} century [5]. In 2010, CO_2 released from fossil fuels and industrial processes constituted 65% of anthropogenic GHGs emitted [5]. Regarding the total GHG emissions, the transport sector contributed to 14% with the energy supply sector covering 35%, industry 21%, agriculture and forestry 24%, and buildings 6%, respectively [5]. In 2016, 20% of the human population still lived outside the electrical grid and around 40% relied on wood, coal, or animal waste for cooking and heating [1]. This is expected to change and, hence, as projected by the U.S. Energy Administration in 2016, the global energy consumption of non-OECD countries will increase significantly from $330 \cdot 10^6$ TJ in 2012 to $560 \cdot 10^6$ TJ in 2040 (see Figure 1a) [4].

In 2011, The World Bank estimated that there were 176 vehicles per 1000 people on average in the world. The number was 55 for low and middle income countries, 620 for high income countries, and 797 in the U.S. alone [6]. Especially for non-OECD countries, the liquid fuel consumption is expected to increase (see Figure 1b) [4]. In order to accommodate the increasing demand from developing countries it is crucial to develop technologies for a sustainable production of renewable transportation fuels. Fluctuations in the crude oil prices [4,7], which in 2016 were historically low [7], affect the economy of emerging technologies immensely.

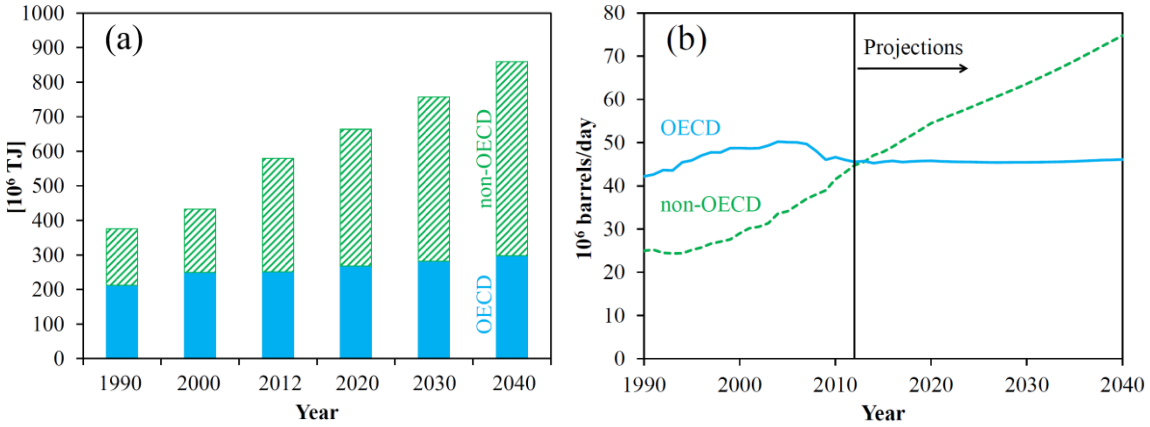

Figure 1 (a) Global energy consumption reported and projected by the U.S. Energy Information Administration in 2016. (b) Petroleum and other liquid fuel consumption. By OECD (Organization for Economic Co-operation and Development) and non-OECD countries. Redrawn from [4].

Today, the infrastructure of the modern society is almost solely based on carbon based fuels due to their very high energy density and their availability from the still large oil reserve. At the same time, wind and solar based electricity production is reaching a mature stage and is today cost competitive with the fossil based in some regions of the world [8]. The major threshold for both fuel-cell and battery driven vehicles is the necessity to build a new fuel infrastructure with charging stations for H_2 or electricity, respectively [9]. Battery driven vehicles also struggle with a low energy density and instability of the currently dominant lithium batteries [9]. Another obstacle lies in the availability of wind and solar based electricity and lack of good storage technologies, e.g. chemical energy storage via hydrogen is not yet economically feasible [10]. Electricity production from photovoltaic cells peaks during the day, whereas power consumption typically peaks in the morning and afternoon, which results in the so-called duck-curve [11]. Consequently, carbon based fuels currently appear as an attractive candidate for the principal part of the transportation energy, and biomass appears as the most promising renewable source. Additionally, for aviation, heavy duty road transport, and shipping industries, it is unlikely that these will be fueled by electricity in the near future. The earth's biomass production capacity can however not be increased to cover the total

global energy demand [12], and it is important to stress that the future energy supply system is most likely to be based on several synergetic technologies, which can complement each other, for example in order to fill the gap in the duck-curve.

Biomass can be used as a raw material for the production of fuels with low (potentially zero) carbon footprint [13–15]. First generation biofuel processes such as bio-ethanol (from sugar cane and corn) and bio-diesel (from vegetable oils) convert biomass into fuel through well-established technologies [16]. However, since the applied biomass types are edible, a political and ethical dilemma may arise when considering that many people (e.g. 13% in 2008-2010 [17]) in the world are starving. Additionally, the energy efficiency per unit land is markedly lower for food grade biomass compared to energy crops [15]. Therefore, development of second generation biofuels is based on utilization of non-edible biomasses such as wood, energy crops, algae, and waste material from agriculture, paper production, and municipalities [18,19].

Mortensen et al. [20] reviewed the competitiveness of various routes for biofuel generation. Based on an assessment of the fuel price per mass of oil equivalent, it was concluded that a viable route for renewable liquid fuel production is fast pyrolysis coupled with catalytic hydrodeoxygenation (HDO). While fast pyrolysis is used to increase the biomass energy density by producing a liquid product commonly referred to as bio-oil, which can be transported more easily than solid biomass, catalytic HDO is used to enhance the fuel properties through oxygen removal in a H_2 atmosphere using a suitable catalyst. Another promising technology is the coupling of fast pyrolysis and HDO in catalytic fast hydropyrolysis, where the HDO is performed directly in the pyrolysis reactor [21]. The H_2 required for these processes could possibly be provided by electrolysis of water powered by wind or solar energy.

This review provides an overview of the principles of biomass pyrolysis (section 2) followed by an extensive review of catalytic HDO (section 3), which leads to the discussion of coupled fast pyrolysis and catalytic HDO in a continuous process such as catalytic fast hydropyrolysis (section 4). With respect to HDO (section 3), the reader is also referred to the review by Mortensen et al. [20], which includes literature up until 2011. Compared to this former review, section 3 in this work expands and updates the part on catalytic HDO. Each section (2, 3, and 4) begins with an introduction to published reviews within pyrolysis, catalytic HDO, and catalytic fast hydropyrolysis, respectively. The aim of this review is to comprehensively cover all three topics at once, in order to couple the knowledge from fast pyrolysis and HDO (sections 2 and 3) in the discussion and evaluation of proposed processes for production of transportation fuels from biomass fast pyrolysis, catalytic HDO, and catalytic fast hydropyrolysis (section 4).

2. Fast Pyrolysis of Biomass

Fast pyrolysis of solid biomass is done by fast heating to 400-600 °C in an inert atmosphere whereby a large fraction of the biomass is converted to a liquid product (after condensation) with a typical energy recovery of 45-75% [22]. The produced oil, which is commonly referred to as pyrolysis oil or bio-oil is a dark homogeneous liquid, which contains water and a wide range of oxygenates [22]. The energy recovery of the oil can be defined as:

$$Y_H = \left(\frac{h_{oil} \cdot m_{oil}}{h_{biomass}}\right) \cdot 100\% \quad (1)$$

Here, Y_H is the energy recovery, and h is the heat of combustion (MJ/kg) of the produced oil and the feed biomass, typically defined as the higher heating value (HHV), and m_{oil} is the mass of bio-oil formed per kg biomass. Typically, the heating value of bio-oil is similar to the feedstock and approximately half the heating value of crude oil [23]. In this section, the principles of fast pyrolysis and selected reactor technologies will be discussed with emphasis on the pyrolysis of woody

biomass. More information on fast pyrolysis of biomass can be found in the reviews by Bridgwater [23–26], Mohan et al. [27], Butler et al. [28], Yaman [29], and Venderbosch and Prins [30].

Pyrolysis is the thermal decomposition of biomass in the absence of oxygen, which generates gas, condensable vapors (the bio-oil), and char. The pyrolysis temperature, heating rate, and the residence time of the vapors and char have a significant influence on the liquid, solid, and gas yields [30]. Fast pyrolysis operating conditions have been optimized to obtain a maximum liquid yield of 55-80wt% for wood [22,31–35]. The main features of fast pyrolysis are [23]:

- High heating rate of the biomass surface, with orders of more than 100 °C/s.
- Short residence time of the gas and vapors, preferably below 2 s. This minimizes the extent of secondary reactions that would decrease the bio-oil yield and increase the gas yield. Fast cooling of the vapors is used to collect the bio-oil and avoid secondary reactions.
- The temperature in the reactor is carefully controlled and is in the range of 400-600 °C. In this temperature range high conversion to a liquid can be achieved, while vapor cracking is minimized.

If fast pyrolysis is performed in the presence of a catalyst, it is called catalytic pyrolysis. This is typically performed in an inert atmosphere at ambient pressure with a (potentially modified) cracking catalyst such as HZSM-5 [36–43], or with other materials such as red mud [44] and alumina based catalysts [45,46]. As this review deals with catalytic HDO and coupling of fast pyrolysis with HDO, catalytic pyrolysis with non-HDO catalysts and upgrading of pyrolysis oil with zeolites without hydrogen in the gas phase is outside the scope of this review. For an overview of the work performed within this field, we refer to the reviews of Venderbosch [47] and Yildiz et al. [48] for catalytic fast pyrolysis, and to the review of Rezaei et al. [49] and Mortensen et al. [20] for upgrading of pyrolysis oil with zeolites.

2.1. Fast Pyrolysis Reactor Technology

In this section, we review two well-known fast pyrolysis reactor designs; the fluid bed reactor and the ablative reactor. Descriptions of other designs such as vacuum pyrolysis or auger pyrolysis reactors can be found in the reviews of Bridgwater [23], Mohan et al.[27], and Garcia-Nunez et al. [50].

2.1.1. Fluid Bed Reactors

In a fluid bed reactor, an inert gas is sent upwards through a particulate bed consisting of an inert heat transfer material and biomass, which is continuously fed, whereby the entire bed is fluidized. Hereby high rates of mixing and heat transfer are obtained [23,27,30]. Fluid beds are divided into bubbling fluid beds (BFB) where the bed is contained in the bottom part of the reactor, and circulating fluid beds (CFB), where the gas velocity is comparatively higher and the bed material is continuously entrained out of the reactor and returned using a cyclone [23,27,30]. For fast pyrolysis of biomass, the BFB design shown in Figure 2 is often used [23]. The produced char can be combusted in a separate reactor to provide the necessary heat to the process. Alternatively, the char could potentially also be exported as a soil improvement agent or used for other purposes [51–53], but the composition and properties of the char should be critically addressed. Especially carcinogenic compounds such as heavy metals and polyaromatic hydrocarbons are an issue. In the BFB it is fairly easy to control the temperature and an efficient heat transfer to the biomass is obtained by using sand as heat carrier [23,30,54]. The residence time for the char and vapor is controlled by the flow rate of the carrier gas. The solid particles have a higher residence time than the vapors [27]. As shown in Figure 2 the char is separated by cyclones, and the bio-oil is separated from the gas by condensation and electrostatic precipitation of the aerosol vapors [23,27].

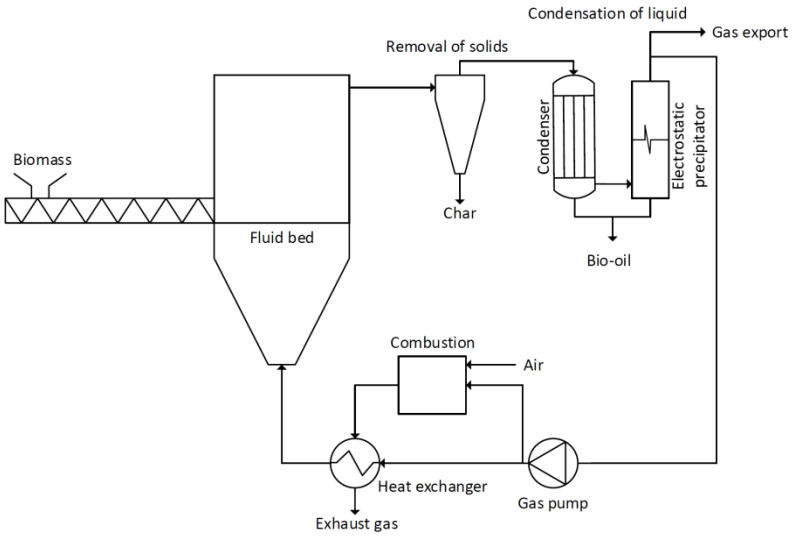

Figure 2 Bubbling fluid bed (BFB) reactor for biomass fast pyrolysis and product recovery.

In the CFB, sand leaves the reactor together with the products [23,27,30]. The sand and char particles are separated from the gas by cyclones and sent to a combustor, before some of the gas is recycled back to the fluid bed reactor. The heat generated through combustion of char is used to heat the sand, which is then recycled back to the pyrolysis reactor [23,27,30,55]. However, with this reactor configuration solid ash can be recycled back to the pyrolysis reactor, which can lead to undesirable ash build-up in the system, which may decrease the liquid yield [56]. The gas velocity in the CFB reactor (5-15 m/s or higher) is larger than in the BFB reactor (1-3 m/s), with the choice of velocity depending on the particle size and density. The high gas velocity leads to attrition of the char particles hence decreasing the particle size [23,27]. Since smaller particles are more difficult to separate from the product gas stream, this may lead to an increased char content in the bio-oil [23,27].

An important advantage of the CFB reactor is that it is suitable for upscaling, which makes it possible to have high throughputs with this technology compared to competing technologies [23]. Thus, the CFB reactor is the most widely used type of fast pyrolysis reactor for large scale plants.

The CFB has been operated at commercial scale and the technology (RTP) is sold by Envergent Technologies [57].

2.1.2. Ablative Reactors

In the ablative reactor the biomass particles are pressed against a hot surface whereby a high heating rate is obtained [27]. Biomass melts on the surface forming an oil film, which vaporizes and gives access to fresh biomass [23,27,28,30]. An ablative reactor design is shown in Figure 3. In the ablative reactor the outer part of each particle is rapidly heated, and the generated char is then shredded from the biomass particle. The ablative reactor is consequently limited by the rate of heat transfer to the surface of the particle, and larger particles can therefore be used [23,58]. The heat transfer, and thereby the heating rate, increases with increasing pressure of particles onto the reactor wall. Similarly, increasing the relative velocity between the particles and the wall also increases the heat transfer rate [23,27]. The process is controlled by the available surface area [23] and the capacity is therefore a linear function of the available heat transfer area [27], which limits the capacity of this technology. Some of the more developed ablative reactors are the rotating cone [30,59], the auger bed reactor [28,30], and the pyrolysis centrifuge reactor [60]. One of the advantages of the ablative reactors is that they are independent of an inert energy carrier and a gas for fluidization [30]. In terms of commercial use, there are (to the authors' knowledge) currently no ablative reactors operating with a feed capacity above 1 ton/h.

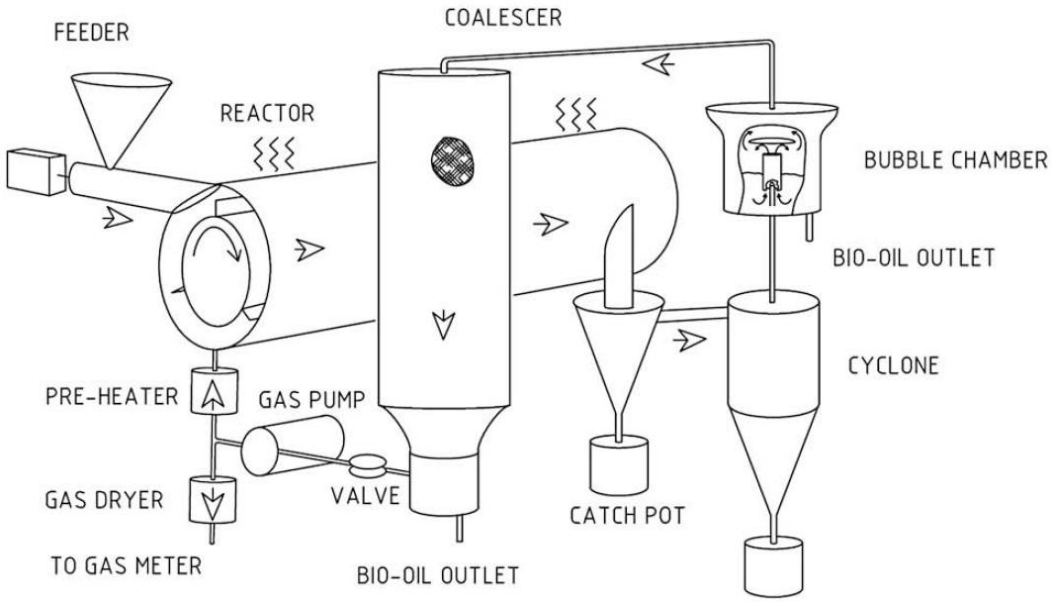

Figure 3 An ablative reactor design: The pyrolysis centrifuge reactor used by Bech and Trinh et al. [22,60–62]. Reprinted from [60] (copyright 2009) with permission from Elsevier.

2.2. Influence of Feedstock and Operating Conditions

The main constituents of biomass are cellulose, hemicellulose, and lignin [19,63–67]. The distribution between these components varies for the different types of biomass [65]. Cellulose is a linear polymer consisting of β-(1→4)-D-glucopyranose units [27], which is thermally defragmented at 270-400 °C [68–70]. Hemicellulose consists of different polymerized monosaccharides such as glucose, mannose, galactose, xylose, arabinose, 4-O-ethylglucuronic acid, and galacturonic acid residues [27]. The number of repeating units is significantly smaller than for cellulose and thermal decomposition takes place at 220-400 °C [30,70]. Lignin is a three-dimensional, highly branched, phenolic polymer [19,27,30], which has a broad thermal decomposition range of 160-900 °C [30,70].

The yield, composition, and properties of bio-oil from fast pyrolysis are influenced by the composition of the biomass, the residence time in the reactor, inorganic constituents, and the temperature. Most studies of biomass fast pyrolysis have been performed using wood, however, other feedstocks such as straw, lignin, sewage sludge, and macroalgae have also been used

[22,61,62,71]. A high ash content decreases the oil yield, while increasing the char and gas yield [30,31]. Alkali metals in the ash are generally considered to decrease the oil yield by catalyzing cracking reactions (producing gas) and condensation reactions (producing char). Since the produced char is rich in ash, it is catalytically active and should be removed from the pyrolysis reactor to limit side reactions. Especially potassium, calcium, and sodium have been reported to have a negative impact on the oil yield [30–32,72]. Cracking increases the water content in the oil and thereby decreases its heating value [31]. Alkali metals have furthermore been reported to accelerate bio-oil aging during storage [73]. Silicon and other non-alkali metals have been reported to be inactive during the pyrolysis [30]. Biomass with a high concentration of lignin has also been found to give a relatively low bio-oil yield [74].

In the following, the effect of using different feedstocks will be discussed. However, not all of the conducted research is performed at conditions, which are optimal for bio-oil production. Consequently some of the reported liquid yields are lower than what can be obtained with optimized conditions.

When using wood the bio-oil yield is typically between 55-75wt% on dry ash free basis (daf) [22,31–35]. This is due to the low ash content of 0.4-3wt% dry basis (db), a low potassium content of 0.04-0.4wt% db, and a low lignin content of 10-30wt% daf [22,31–33,75–79]. Because of the high liquid yield and a high liquid energy recovery (~75%) [22,31–33,75], wood is considered an optimal feedstock for fast pyrolysis oil production.

Generally, the bio-oil yields from fast pyrolysis of agricultural biomass such as wheat straw is 40-65wt% daf [22,31,35,80–83] with an energy recovery of approximately 55% [22,31,32]. The lower yield compared to wood can be ascribed to the higher ash (4-10wt% db) and particularly potassium (0.9-1.5wt% db) content in straw [22,31,35,80–84]. Rice straw gives a slightly higher bio-oil yield

(40-70wt% daf) than wheat straw, despite the fact that it has a high ash content of 9-20wt% db [72,83,85,86]. However, the major fraction of the ash is silicon, which has no or low catalytic cracking activity.

Lignin can be obtained as a byproduct from paper production and the production of second generation bio-ethanol [74,87]. Lignin is more difficult to process than straw or wood, since lignin swells and becomes sticky during heating. At the same time, the bio-oil yield is lower, typically 30-60wt% daf, while the char yield is higher, 25-50wt% daf [22,62,74,87]. The energy recovery in bio-oil from lignin is therefore also moderate (~45%) [22], which makes it a less attractive feedstock for fast pyrolysis. Macroalgae have also been considered for fast pyrolysis. However, the ash content is very high (up to 50wt% db) [22,88–93], and the bio-oil yield is therefore only around 50-65wt% daf [22,93,94]. Furthermore, macroalgae need to be dried before they can be used in fast pyrolysis. Interestingly the energy recovery for macroalgae is between 25 and 76% [22,61], as high as for wood. The high energy recovery for macroalgae could be due to the relatively high protein and lipid content which is easily converted to liquid oil compared to woody biomass [95].

It is also possible to produce bio-oil from sewage sludge by fast pyrolysis and thereby both reduce the volume of solid waste and produce bio-oil. However, there are large variations in the ash content (25-50wt% db) in sewage sludge, thus the bio-oil yield varies between 30-60wt% daf [61,76,96–98]. Sewage sludge additionally has a high moisture content and drying is needed before it can be used [96,97].

The temperature is an important parameter in fast pyrolysis and must be carefully controlled in order to achieve maximal bio-oil yield [34,75,99–101]. Generally, it is observed that increasing the temperature increases the gas yield and decreases the char yield [34,60,75,101,102]. The optimal temperature for bio-oil production for fast pyrolysis is 450-550 °C for most types of biomass, as

indicated in Figure 4. Above 550 °C the bio-oil yield decreases significantly and the gas yield increases [99], because the higher temperature leads to cracking of the formed vapors [25,26,60].

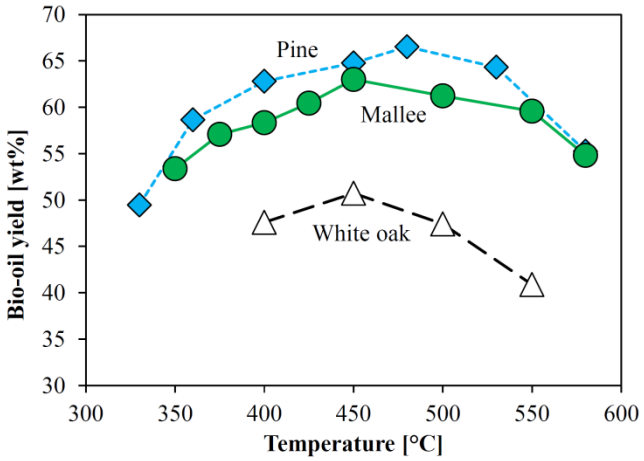

Figure 4 Bio-oil yield for different types of wood as a function of temperature in a fluid bed fast pyrolysis reactor. Data from [34,75,103].

The residence time of the pyrolysis vapors is also an important parameter. If the residence time is too high secondary reactions such as thermal cracking will take place, which decreases the bio-oil yield [100,104]. The pyrolysis vapor consists of many reactive species and thus, a high residence time can increase the size of the molecules due to polymerization [105]. The gas residence time should normally be below 2 s in order to achieve a maximum liquid yield [106], and several studies have shown a decrease in the bio-oil yield when the residence time is increased [56,59,80,104]. The heating rate is also an important parameter; a too low heating rate leads to a higher char yield [23]. The heating rate in fast pyrolysis is more than 100 °C/s at the biomass particle surface. In fluid bed reactors, the fluidization velocity is also an important parameter, because it determines the gas residence time and influences the mixing between the cold biomass particles and the hot sand [101]. In order to achieve a high oil yield with the fluid bed reactor, the biomass particles should preferably

be smaller than a few mm in diameter [107–111]. A low moisture content of the feed biomass is also preferred, because a high moisture content limits the heat transfer and thereby increases the char yield [112,113].

2.3. Bio-oil Properties

Bio-oil is a complex mixture, consisting of hundreds of different compounds [32,114]. It has a dark brown color and is a viscous, but freely flowing liquid [23,30]. The water content is typically around 15-30wt% [23,24,115], but can be as high as 60wt% [116]. The water cannot be removed through conventional distillation, because rapid polymerization occurs when bio-oil is heated resulting in the formation of 30-50wt% residual solid [115]. The most important properties of bio-oil are compared to different types of conventional fossil oils in Table 1. It is clear that bio-oil is very different from crude oil. Bio-oil has a high oxygen content, typically 35-50wt% [22–24,115], which significantly decreases the HHV. The resulting HHV for bio-oil is 16-21 MJ/kg; less than half the HHV for conventional petroleum oils [22,24]. Because of the high oxygen content bio-oil has a high polarity and is consequently immiscible with conventional petroleum oils [23,27,30]. The density of bio-oil is approximately 1.2 kg/L [23,24], which is significantly higher than the density of diesel (0.82-0.85 kg/L) [117,118]. This means that on a mass basis (MJ/kg), the energy content in bio-oil is 37-49% of that of diesel, but on a volumetric basis (MJ/L), the energy content in bio-oil is 53-71%. The viscosity of bio-oil varies between 13 and 100 cSt depending on the water content and the composition [24,115]. Trace amounts of ash, alkali, chlorine, and sulfur may also be present in bio-oil.

Table 1 Common properties of wood derived bio-oil and fossil derived oils. Based on data from [22–24,115,117–119].

Physical property		**Bio-oil**	**Diesel**	**Heavy fuel oil**
Water	[wt%]	15-30	0-0.001	0.1-7
Ash	[wt%]	0-0.2	0-0.01	0.03-0.1
Carbon	[wt%]	44-58	86	85-86
Hydrogen	[wt%]	5.5-7.2	13	11-12
Nitrogen	[wt%]	0-0.2	-	0.3
Oxygen[a]	[wt%]	35-50	0	0-0.1
Sulfur	[wt ppm][b]	<400	10-500	10,000-21,000
Stability	-	Unstable	Stable	Stable
Viscosity (40-50 °C)	[cSt]	13-100	1.9-4.5	140-380
Density (15-40 °C)	[kg/L]	1.1-1.3	0.82-0.85	0.96-1.02
Flash point	[°C]	50-100	≥52	65-100
Pour point	[°C]	-36 to -9	-20	15-21
HHV	[MJ/kg]	16-21	43	38-41
pH	-	2.4-3.2	-	-

a) Includes oxygen from water. b) Parts per million.

Gas chromatography mass spectrometry (GC-MS) [32,120] and nuclear magnetic resonance (NMR) spectroscopy [114,120] analysis of different bio-oils have revealed that the bio-oil contains acids, non-aromatic aldehydes, nonaromatic ketones, furans, pyrans, sugars, benzenes, catechols, lignin derived phenols, guaiacols, and syringols. A list of common molecules found in bio-oil produced from fast pyrolysis of wood is shown in Table 2.

Table 2 Common compounds in wood derived bio-oil. Primarily adapted with permission from [121] (copyright 2013, American Chemical Society). Modified and updated based on refs. [23,24,30,32,115,122–129].

Functional groups		Typical compounds	Structure[a]
Water		Water	H_2O
Simple oxygenates (non-aromatic)	**Acids**	Acetic acid, formic acid, propanoic acid, methyl propanoic acid, butanoic acid, pentanoic acid, glycolic acid, hexanoic acid, ...	
	Esters	Methyl acetate, ethyl acetate, methyl formate, …	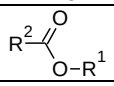
	Alcohols	Methanol, 2-propene-1-ol, butanol, ethylene glycol, propylene glycol, 2,3-butandiol, cyclopentanol, cyclohexanol, 1,2-cyclohexanediol, ...	
	Ketones	2-butanone, cyclopentanone, methylcyclopentanone, 3-methyl-1,2-cyclopentanedione, 2-petanone, cyclohexanone, …	
	Aldehydes	2-butenal, glyoxal, formaldehyde, benzaldehyde, …	
Miscellaneous oxygenates		2-hydroxyacetaldehyde	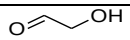
		1-hydroxy-2-propanone	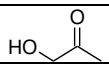
		Methyl-2-oxopropanoate, 1-hydroxy-2-butanone, ...	
Sugars and sugar derivatives		Levoglucosan	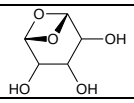
		Xylose, arabinose, glucose, fructose, sorbitol, …	
		Cellobiosan	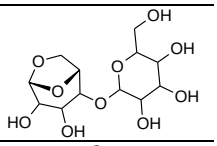
Furans		Furan	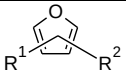
		Furfural	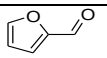
		2-furanone, butyrolactone, methyl-2-furanone, furfuryl alcohol, 2-acetyl furan, 5-methyl furfural,5-hydroxymethyl furfural, tetrahydrofuran, 2,5-dimethyltetrahydrofuran, …	
Aromatics	**Oxygen free**	Toluene, benzene, xylene…	
	Phenols	Phenol, methylphenol, dimethylphenol, ethyl phenol, …	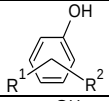
	Catechols	Catechol	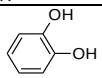
		Methylcatechol, ethylcatechol, methoxycatechol, …	
	Guaiacols	Guaiacol	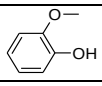
		Methylguaiacol, ethylguaiacol, eugenol, vanillin, …	
	Syringols	Syringol	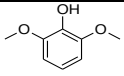
		Methylsyringol, ethylsyringol, 4-propenylsyringol, …	
	Others	Vanillic acid, sinapaldehyde, syringaldehyde, acetosyringone, …	
High molecular weight species		Dimers, trimers, oligomers and cellulose, hemicellulose and lignin pyrolysis products	

a) R denotes H, CH_3 or other aromatic/aliphatic groups.

Figure 5a shows a typical carbon distribution in the compounds present in oak bio-oil and illustrates that the organics in bio-oil are mainly composed of a lignin-derived fraction as well as a cellulosic/hemicellulosic fraction (C_{5-6}), and short C_2 compounds. In Figure 5b, the organic content is divided based on compound types.

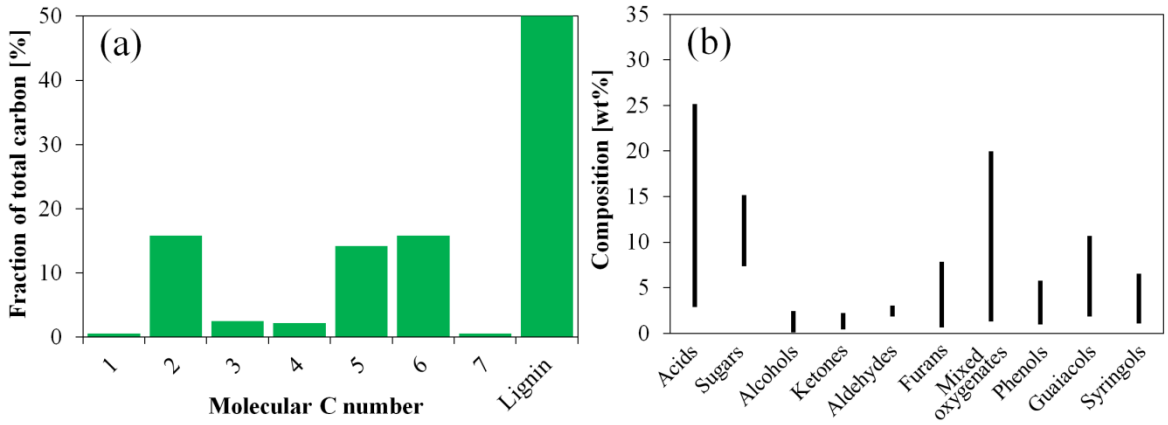

Figure 5 (a) Carbon distribution for compounds present in an oak derived bio-oil. Adapted with permission from [129] *(copyright 2017). (b) Composition ranges in wood bio-oil, reproduced from Ruddy et al.* [130] *(with permission of the Royal Society of Chemistry), who used the data collected by Milne et al.*[131].

Bio-oil derived from wood has been reported to have a high concentration of hydroxyacetaldehyde and levoglucosan, which are degradation products from cellulose [32,132]. The cellulosic and hemicellulosic part of biomass is responsible for the corrosive character (from acids) and instability (from light and reactive oxygenates) of bio-oil, see section 3.1. The pH of bio-oil is around 2.4-3.2 (see Table 1) [22,24,25,115], and acid proof materials should be used for storage [133]. Due to the high oxygen content, bio-oil contains reactive functional groups, which make the bio-oil unstable and polymerize when stored. This increases the molecular weight, which in turn increases the viscosity and density of the oil. The water content also increases over time, which can lead to phase separation [24,115,134,135].

Bio-oil contains small amounts of char (entrained from the pyrolysis process), wax derived compounds and heavy molecules. The waxy compounds tend to crystallize in the upper layer of bio-

oil or on cold surfaces [136]. The heavy compounds typically form networks in the bottom layer, while the water can form droplets over time [136]. These features are part of the reason for the phase separation that sometimes occur during storage [136]. Chlorine, sulfur, nitrogen, and alkali metals in the bio-oil can act as poisons on catalysts used for upgrading of bio-oil [23,137,138].

The phenolic content consists of aromatics with a lower O/C content compared to the cellulose and hemicellulose derived compounds. Additionally, these aromatics are stable and do not readily react. In conclusion, the negative influence of aromatic oxygenates on the fuel quality of bio-oil is less significant compared to cellulose and hemicellulose fragments. It is therefore interesting that bio-oil model compounds upgrading studies have mainly focused on oxygen removal from phenolic species. They may be the most difficult compounds to upgrade, but they are also the least problematic compounds with respect to stability upon storage and heating. This discussion is revisited and elaborated in section 3.

2.4. Commercial Aspects of Bio-oil Utilization

Bio-oil can in many aspects replace crude oil as fuel in boilers and experiments have shown that it can be used for shorter periods in diesel engines [139–143]. However, when using bio-oil in diesel engines the following problems have been reported: ignition difficulties, fuel injection problems, corrosion of injector needles, and coking of combustion chamber, exhaust valve, and injection nozzles leading to clogging [116,140–145]. Consequently, further upgrading of the bio-oil is necessary in order to use it as a liquid transportation fuel. Bio-oil can also be used in gas turbines [24,116,146,147], but corrosion of the turbine blades and deposit build-up makes it necessary to modify the turbines in order to run on pure bio-oil [24,116]. It is common to use furnaces and boilers for power generation, and bio-oil has therefore been tested as a possible fuel for this application [24,148,149].

Even though fast pyrolysis technologies to some extent are commercially available and even used in Finland for combined heat and power generation [57,150,151], the market for bio-oil in power plants and small boilers is currently limited. Solid biomass, such as wood chips or pellets, is already used in power plants in Europe with a minimum requirement for pretreatment [152], which limits the interest in biomass pyrolysis processes that produce a fuel with limited applicability.

Bio-oil can be mixed with the produced char and gasified to form synthesis gas, which can be converted into liquid fuels [153,154]. It is also possible to co-process the bio-oil with conventional fuels in a refinery fluid catalytic cracking (FCC) unit [155,156], but co-feeding is highly challenged in hydrotreating units due to the high content of oxygen in bio-oil, which makes it immiscible with fossil feeds and causes severe coking [157]. It should be further noted that the alkali metals in the bio-oil can decrease the lifetime of catalysts in both the FCC and hydrotreating processes [48,155–157]. It should also be mentioned that zeolites, which are used as commercial FCC catalysts [158], typically have a high cracking activity, which limits the oil yield. There are, however, some promising results on co-feeding catalytic pyrolysis oil to FCC units at both small [159,160] and larger scale [161,162].

3. Catalytic Hydrodeoxygenation

Catalytic HDO is known from hydrotreating (also called hydroprocessing) of crude oil, where it is used to remove the <1% oxygen present in the feed [24,163]. Hydrotreating covers the removal of sulfur (hydrodesulfurization, HDS), nitrogen (hydrodenitrogenation, HDN), oxygen (HDO), and metals (hydrodemetallization, HDM) from fossil crudes [163]. Since the oxygen content in bio-oil is significantly higher than in fossil feedstocks, the requirements for catalysts for hydrotreating of bio-oil is significantly different from those for hydrotreating a fossil feed.

The literature on bio-oil upgrading by HDO and other techniques has experienced a massive increase within the last decades. Saidi et al. [164] counted the number of bio-oil related HDO papers and found 5, 16, 73, and 131 publications for the years 2006, 2008, 2010, and 2012. Reviewing the literature published after 2012 indicates a near exponential growth as seen from Figure 6. There are 447 publications in total on “hydrodeoxygenation” in 2017 of which 189 are also within the topic "bio-oil" and 155 publications also within the topic "model compound”.

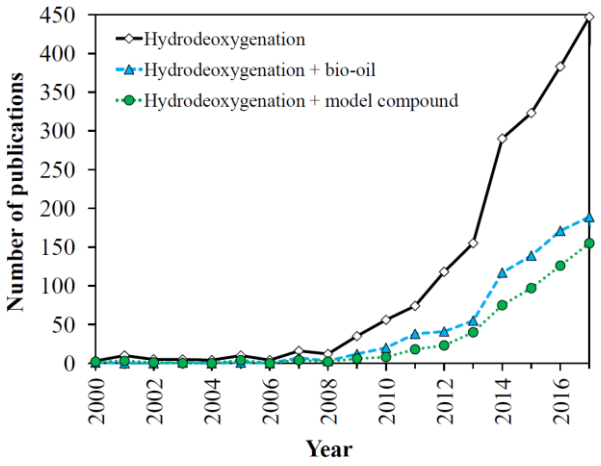

Figure 6 Number of HDO related publications according to Web of Science [165] based on a search on the topic “hydrodeoxygenation” and a refinement of this search with “bio-oil” and “model compound”, respectively. Data retrieved on January 13, 2018.

In conclusion, bio-oil upgrading by HDO is a hot topic, which has called many researchers to contribute to the complex task of converting biomass into high quality liquid fuels. The scope of this section is not to give an exhaustive review of the HDO literature, but rather to provide a comprehensive overview of the most important concepts, results, and trends.

In 2007, Elliott [166] reviewed the historical development in hydrotreating of bio-oil produced via different pyrolysis and liquefaction techniques. In 2014, this review was followed up by a critical review including perspectives on industrial process integration and evaluation of techno-economic analyses [167]. Furimsky [168] has provided a comprehensive review on catalytic HDO chemistry

in terms of reaction mechanisms and kinetics for both petrochemical and biomass derived model oxygenates with a focus on conventional hydrotreating catalysts. A more general review by Furimsky [169] focuses on hydrotreating of various bio-feeds with vegetable oil, lignocellulosic, algae, and sewage sludge origin over different catalyst classes. A number of recent reviews focus on catalytic HDO of lignocellulosic bio-oil and model oxygenates including descriptions of the HDO chemistry over different catalytic systems [20,121,130,170].

The majority of studies on catalytic HDO involve the conversion of model compounds chosen to represent selected functionalities present in bio-oil. The results from these studies aid the understanding of individual reaction mechanisms for a given catalyst and set of reaction conditions. Even though these results provide some insight into catalytic HDO, they cannot be used to draw general conclusions for HDO of real bio-oil due to the complexity of its composition and impurities present. Also, the evaluation of catalytic HDO activity should include considerations on catalyst properties such as active phase dispersion (or particle size), surface area, and pore volume as these features will affect the observed HDO activity.

3.1. Reactions, Reactivity, and Reaction Mechanisms

The complex structure of biomass results in bio-oil compositions with very high diversity as mentioned in section 2.3 and shown in Table 2. As a result of the complex composition, catalytic HDO of bio-oil entails a comprehensive reaction network. An overview of reactions that can occur during upgrading of bio-oil is shown in Figure 7 together with commonly applied acronyms.

Decarboxylation and decarbonylation (DCO) especially occur in upgrading of vegetable oils due to a high content of fatty acids and fatty acid esters [171]. HDO covers the removal of oxygen with H_2 and has the deoxygenated compound and water as products. HDO can occur as direct deoxygenation (DDO) or with saturation of double bonds or aromatic functional groups by hydrogenation (HYD)

prior to deoxygenation. It should be noted that HYD has also been used as an acronym for combined hydrogenation and deoxygenation [172–174]. Cracking reactions (CRA or HCR) are dominant in upgrading processes with zeolites and are well-known from the FCC of petrochemical oils [158]. Demethylation (DME), demethoxylation (DMO), and transalkylation reactions such as methyl transfer (MT) are acid catalyzed and are thus observed when using acidic supports such as Al_2O_3 [172,173,175,176]. Coking and polymerization reactions typically occur as well, and the extent depends largely on the acidity of the catalyst support [177–180], on the temperature [181], and on the oxygenate functionality [166,168].

C-C and C-O bond cleavage is the common route for upgrading of simple oxygenates and furans, while phenols can undergo either DDO or hydrogenation (HYD) prior to deoxygenation [121,175]. The acid catalyzed reactions have previously been assigned the acronym ACI to distinguish these reactions from the HDO pathways [172,173].

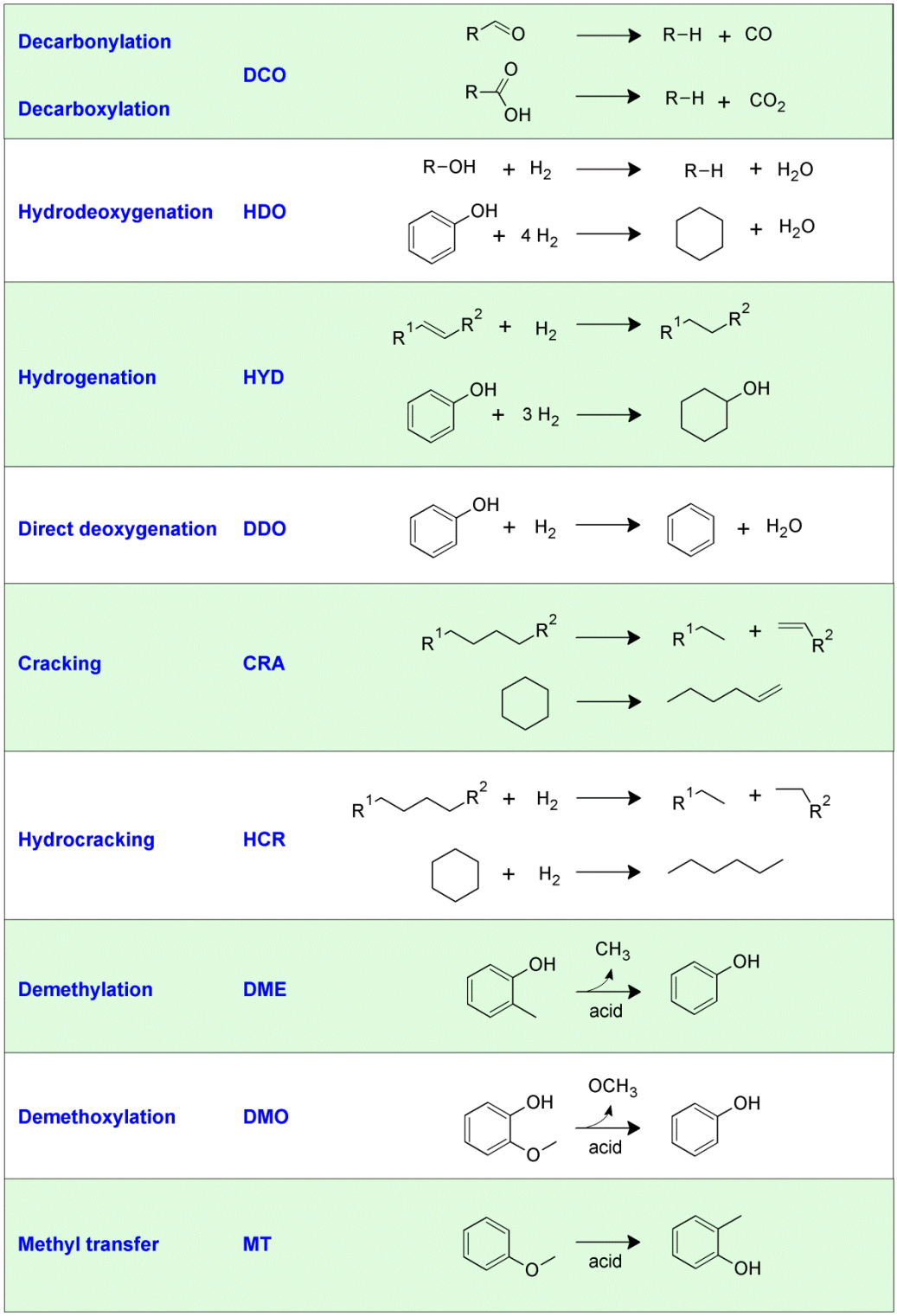

Figure 7 Reactions that may occur during HDO. R denotes H, CH_3, and aromatic/aliphatic groups present in bio-oil. Drawn on the basis of [20,130,182].

Due to the complex nature of the HDO reaction network, the HDO reactivity can be difficult to quantify. In a simple approach, it may be described as inversely related to the oxygen bond dissociation energy, which follows the trend Ar-OH > Ar-OR > R-OH > R-OR' (see Table 3) [168], with Ar representing aromatic species and R representing aliphatic species.

Table 3 Bond dissociation energies for breakage of C-O bonds between black carbon and red oxygen. Data from [168].

Bond type	Dissociation energy [kJ/mol]
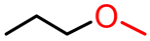	339
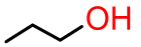	385
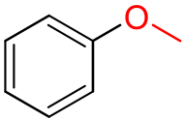	422
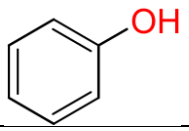	468

More detailed reactivity scales were presented by Elliott [166] (see Figure 8), Yin et al. [183] (see Figure 9), and Grange et al. [184] (see Table 4). Figure 8 and Figure 9 both give a reactivity ranking, which will depend on the catalyst identity and the thermodynamics. The iso-reactive temperature in Table 4 is the temperature required for deoxygenation to take place, and as seen from Table 4 it is much lower for simple oxygenates such as ketones and carboxylic acids (T_{iso} = 203 °C and 283 °C) compared to phenolic species (T_{iso} > 300 °C). The activation energy for deoxygenation follows the same trend (see Table 4).

Phenolic species, primarily derived from lignin, are very resistant to HDO owing to the strong Ar-O bond and the stabilizing nature of the aromatic ring. Hence, they have received great attention in the bio-oil upgrading literature as will be evident in the following sections. HDO of phenolics may (depending on the choice of catalyst) require hydrogenation of the aromatic ring to facilitate

deoxygenation by weakening the C-O bond, which in turn results in a high hydrogen demand. In fact, it has been questioned whether the DDO pathway is even feasible since it requires scission of a strong C-O bond [168,185]. Moreover, presence of other components in the bio-oil may hamper deoxygenation of phenolic compounds [186].

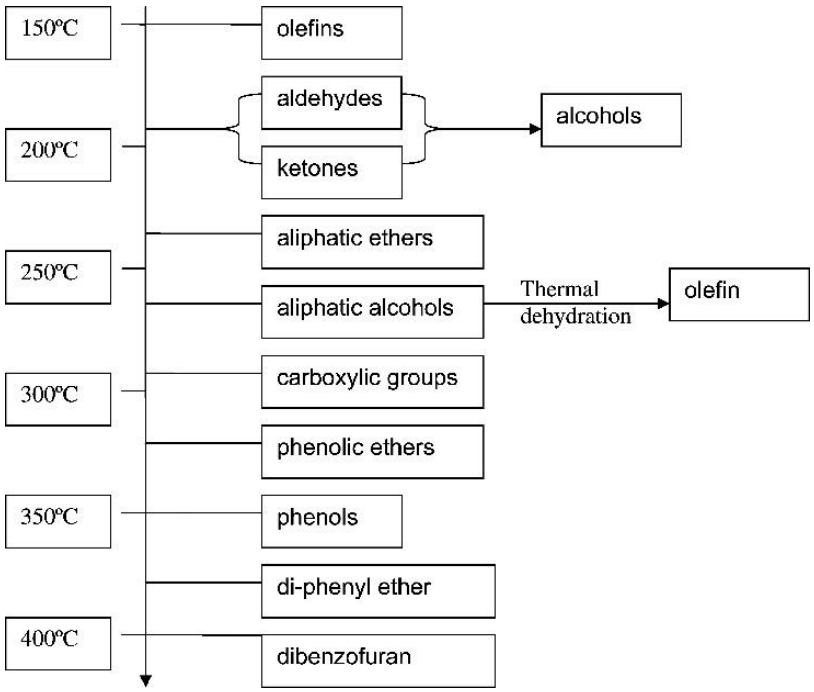

Figure 8 Reactivity of oxygenates under hydrotreating conditions. Reprinted with permission from [166] *(copyright 2007, American Chemical Society).*

Table 4 Activation energy (E_A), iso-reactive temperature (T_{iso}), and H_2 consumption for HDO of different reactants over Co-MoS_2/Al_2O_3. Reprinted from [184] *(copyright 1996) with permission from Elsevier.*

Reactant	**E_A [kJ/mol]**	**T_{iso} [°C]**	**Molar H_2 consumption [H_2/reactant]**
Ketone	50	203	2
Carboxylic acid	109	283	3
Methoxyphenol	113	301	≤ 6
4-methylphenol	141	340	≤ 4
2-ethylphenol	150	367	≤ 4
Dibenzofuran	143	417	≤ 8

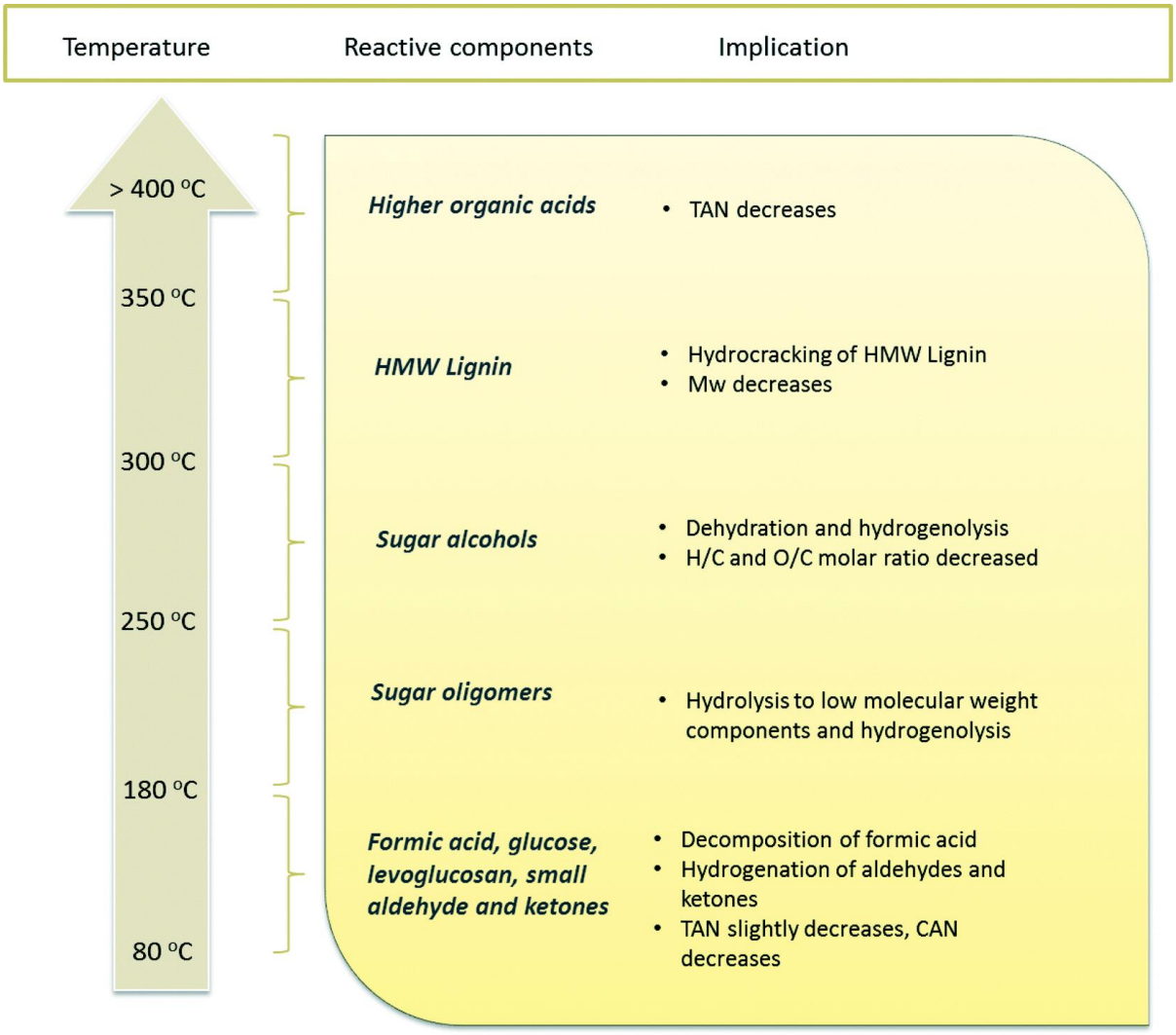

Figure 9 Reactivity of oxygenates including types of reactions, and implications on selected bio-oil properties [183] *including total acid number (TAN) and carbonyl number (CAN). Partly based on HDO of pine derived bio-oil over a Ni-Cu/SiO_2-ZrO_2 catalyst at up to 200 bar and 60-410 °C. Reproduced by permission of The Royal Society of Chemistry.*

Simple, cellulose derived oxygenates, on the other hand, are very reactive [166,183]. Aldehydes and ketones readily undergo polymerization and condensation reactions upon storage, while heating of bio-oil above around 80 °C may cause undesired coke formation [134,135,187]. Low temperature and high H_2 pressure is typically required to stabilize such reactive species [121,188]. Simple oxygenates have received little attention in HDO studies, probably due to their high reactivity. This

is in spite of their high concentration in bio-oil compared to aromatic species (see Figure 5) and them being reactive oxygenates responsible for several detrimental properties of bio-oil (e.g. instability and acidity, and coking of catalysts and reactor plugging). Stabilization and upgrading of simple oxygenates has instead been targeted through other approaches such as liquid phase ketonization and aldol condensation [189–191]. Cellulosic sugar (polyol) fragments such as levoglucosan and cellobiosan occur as intermediates during pyrolysis [105,122] and are among the most reactive bio-oil species owing to the high polymerization and coking tendency, which directly affects catalyst lifetime and operation stability [188].

Figure 10 shows the enthalpy of reaction and equilibrium constant for the HDO and DCO reactions of a range of the most abundant bio-oil compounds (see Table 2). The HDO reactions (Figure 10a, R1-R4) are highly exothermic, and full conversion of an oxygenate-rich feed is associated with a risk of thermal runaway; especially in batch and fixed bed reactor experiments. DCO reactions (Figure 10a, R5 and R6) are less troublesome in terms of heat development and may even be endothermic as is the case for 2-butenal decarbonylation. All reactions in Figure 10 (except for R1, see below) are spontaneous in the temperature range of 100-700 °C.

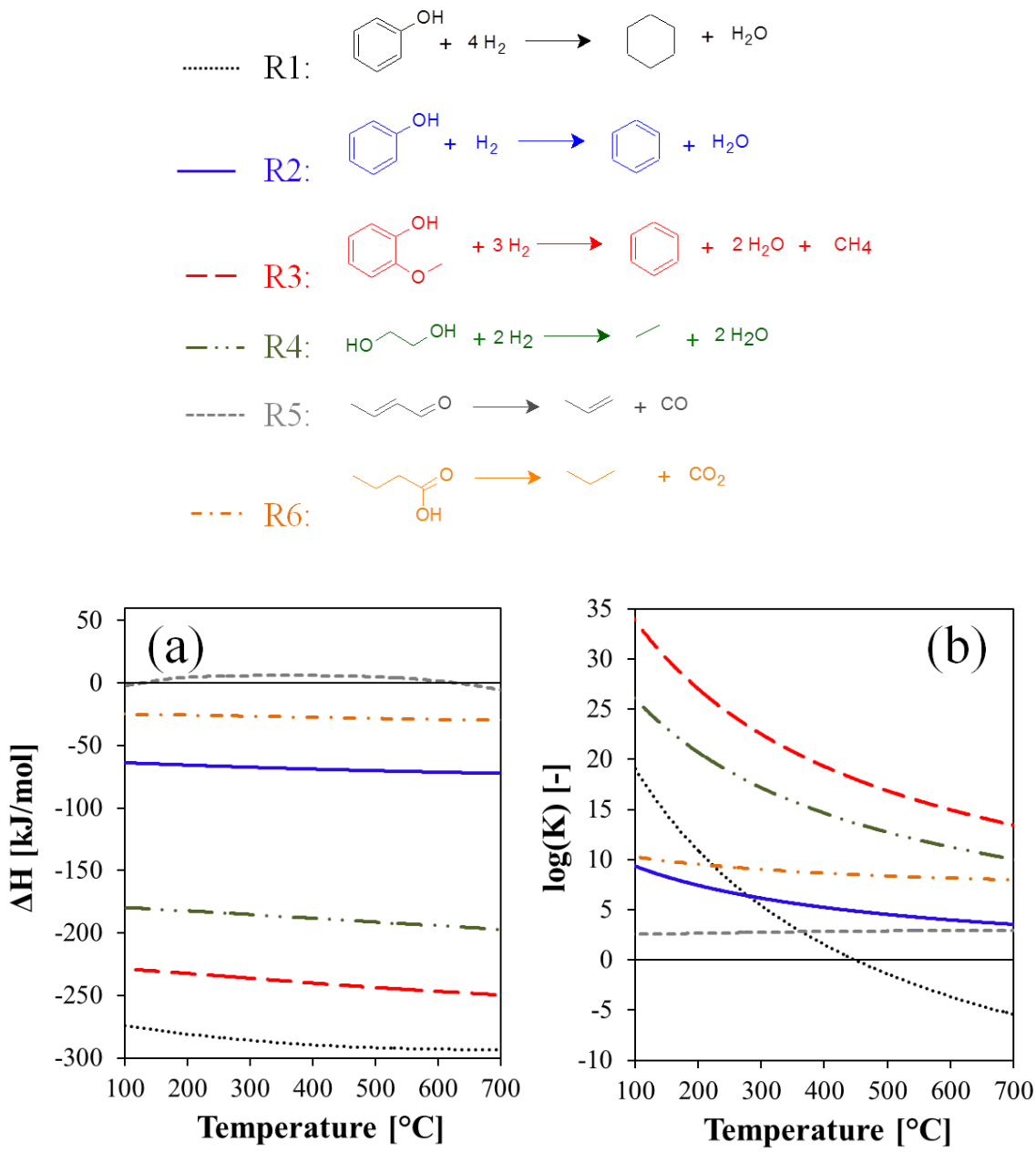

Figure 10 (a) Enthalpy of reaction (per mol oxygenate reacted). (b) Equilibrium constants for model HDO and DCO reactions. Calculated with the software package HSC Chemistry v.9.4.1.

The selectivity towards HYD or DDO products does not only depend on the choice of catalyst but to a high extent also on the reaction thermodynamics. The DDO route for phenol HDO (Figure 10, R2) becomes more favorable than the HYD route (Figure 10, R1) at temperatures above ~275 °C.

At ~450 °C, the equilibrium constant for R1 is <1; the Gibbs free energy is >0 kJ/mol, and hydrogenation of the aromatic ring is unfavorable. Similar results were obtained by Edelman et al. [192].

With the thermodynamics in mind, the consumption of hydrogen can be (partly) controlled through the choice of operating temperature and H_2 pressure. A thermodynamic calculation has shown that the conversion of phenol into cyclohexane (Figure 10, R1) in H_2 at 25 bar is ~100% at 200-300 °C (using the software package HSC Chemistry v.9.4.1). At >300 °C, the conversion drops reaching 90% at 475 °C, 60% at 590 °C, and 40% at 650 °C. A high temperature (>300 °C) and low H_2 pressure (e.g. atmospheric) will favor the DDO path and a low hydrogen consumption. Note that the DDO path for phenolic species will require a high temperature to activate the strong arylic C-O bond.

Dwiatmoko et al. [193] studied the effect of various carbohydrate derived compounds (sugars, carboxylic acids, furans, furfurals, and aldehydes) on the HDO of guaiacol over ruthenium catalysts in a batch reactor, which was pressurized with 40 bar H_2 and then heated to a reaction temperature of 270-300 °C. Among the tested compounds, only furfural and 5-hydroxymethylfurfural affected the guaiacol conversion. They observed that the conversion of guaiacol dropped from 98% to 28% when the molar furfural/guaiacol ratio was increased from 0.47 to 0.96 while the yield of fully deoxygenated products decreased from 50 to 14% over a Ru/C catalyst at 270 °C. Further increasing the furfural/guaiacol ratio led to even lower conversion and yields. Full conversion of furfural was obtained in all cases with nearly unchanged product selectivity. The inhibition of guaiacol conversion by furfural was explained by competitive adsorption, which was supported by density functional theory (DFT) calculations of the adsorption energy. A similar observation was made by

Ryymin et al. [194] for a Ni-MoS_2/Al_2O_3 catalyst, where methyl heptanoate was reported to suppress phenol conversion without the opposite being observed.

As reviewed by Furimsky [168], numerous mechanistic studies exist for the HDO of bio-oil model compounds and mainly for the conversion of phenolic species. Bui et al. [182] presented a general reaction scheme for guaiacol HDO over transition metal sulfides based on experiments with MoS_2 and Co-MoS_2 (bulk and Al_2O_3-supported) performed in a fixed bed reactor at 300 °C and 40 bar H_2 (see Figure 11). The Al_2O_3 support was associated with DME and MT reactions, while Co promotion was associated with DDO reactions. A more detailed reaction network was presented by Runnebaum et al. [175] based on a comprehensive experimental study on the conversion of guaiacol, anisole, cyclohexanone and 4-methylanisole in a fixed bed reactor over a Pt/Al_2O_3 catalyst at 300 °C and 1.4 bar (see Figure 12).

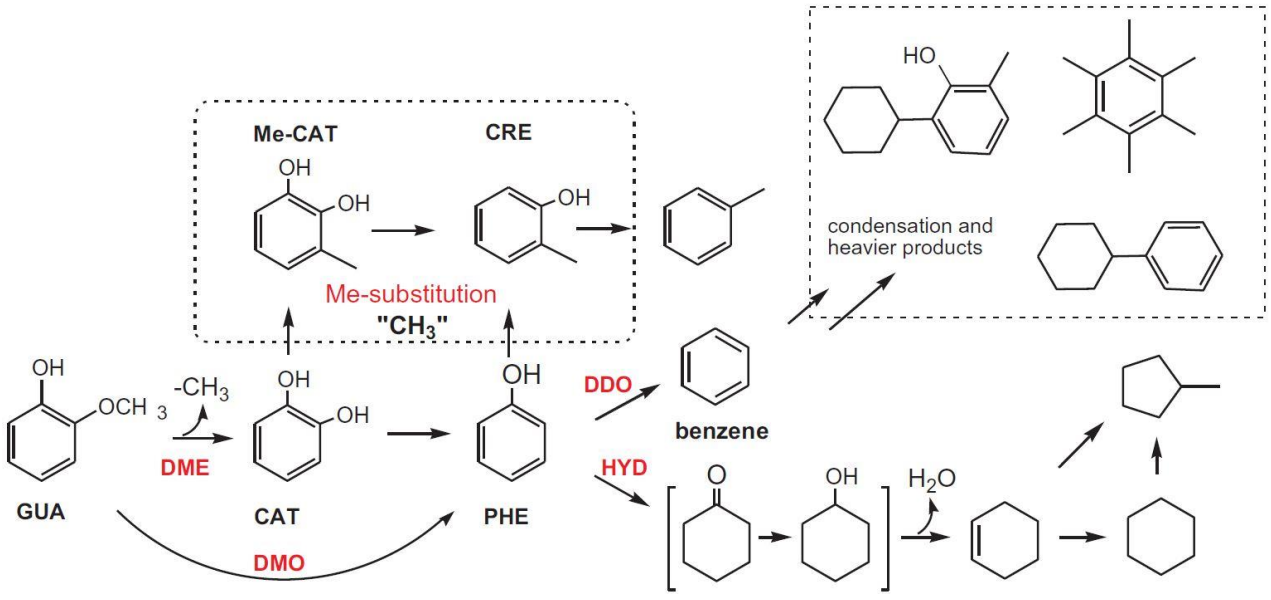

Figure 11 General reaction scheme for guaiacol conversion over transition metal sulfide catalysts under H_2 pressure. Me: methyl. Reprinted from [182] *(copyright 2010) with permission from Elsevier.*

As indicated by Figure 11 and Figure 12, the reaction mechanism for HDO of even a single bio-oil model compound is rather complex. The specific reaction mechanism will depend on the type of catalyst (including active phase particle size, promoters, and support), the operating conditions, and the presence of inhibitors or poisons. Therefore, a complete mechanistic and kinetic understanding of the HDO of real bio-oil will not be obtained in the near future. However, such a detailed understanding may not be necessary in order to develop an industrial scale process. This is the case for conventional hydrotreating, where global, lumped kinetic models are typically applied [163].

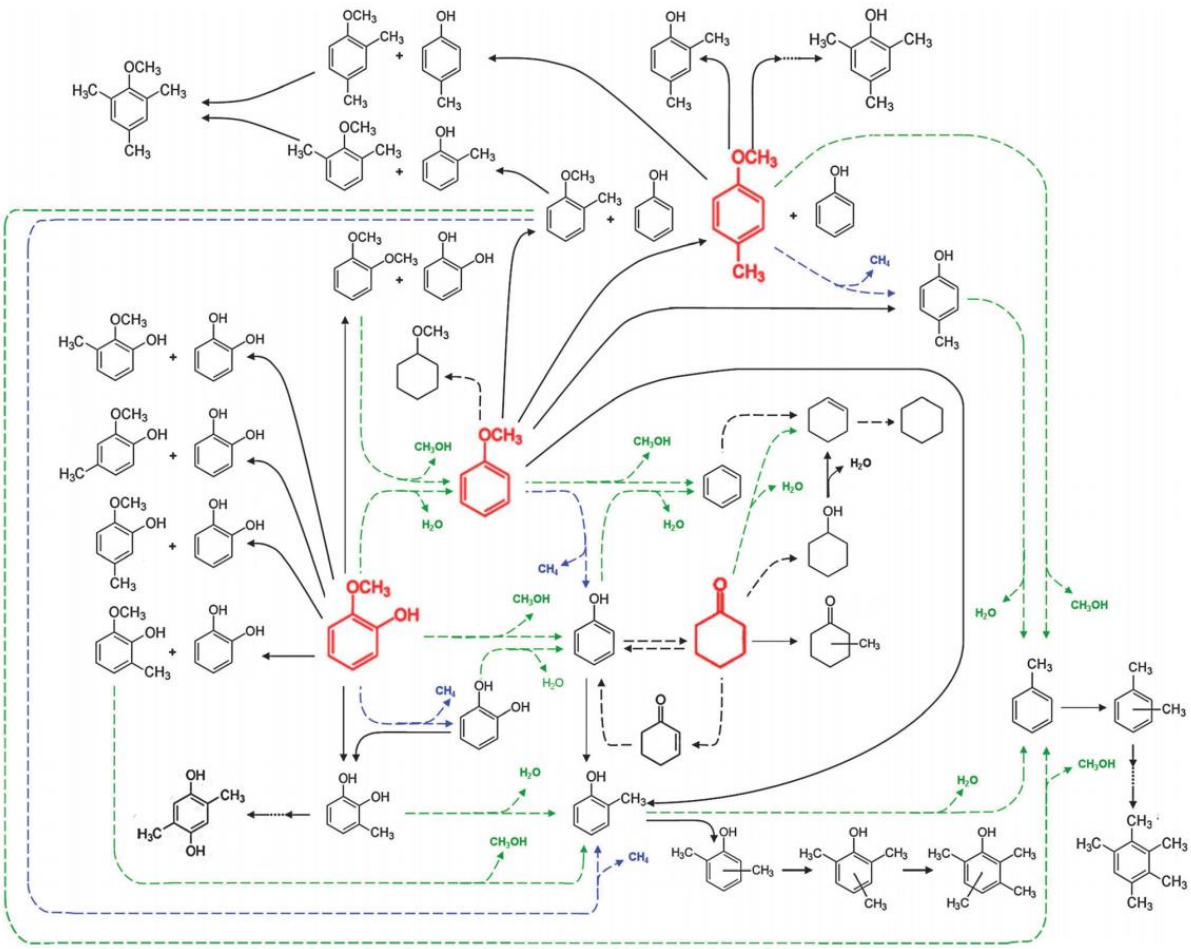

Figure 12 Simplified reaction network for HDO of lignin-derived representative model compounds. Red compounds: Reactants. Black compounds: Intermediates and products. Arrows represent reactions: HDO (dashed green), hydrogenolysis (dashed blue), hydrogenation or dehydrogenation (dashed black), transalkylation (solid black). Reprinted from [175] *with permission from The Royal Society of Chemistry.*

3.2. Bio-oil Upgrading

An overall simplified reaction for HDO of bio-oil may be written as [23]:

$$CH_{1.33}O_{0.43} + 0.77H_2 \rightarrow \text{“}CH_2\text{“} + 0.43\ H_2O \quad (2)$$

with “CH_2“ representing the fully deoxygenated hydrocarbon product. The reaction is exothermic with an overall heat of reaction of approximately 2.4 MJ/kg oil [195]. HDO with moderate to high degree of deoxygenation will result in two liquid phases, a low polarity upgraded oil phase and an aqueous phase. Three liquid phases may form if distinct organic phases with higher and lower density than water are formed. This was reported in the case of high degrees of deoxygenation [188,196]. Complete deoxygenation according to generalized equations, similar to equation (2), have been associated with an oil yield of 56-58wt% [197]. However, this remains a theoretical number due to the complex bio-oil composition and variety of reactions taking place (see Figure 7). A more realistic reaction was proposed by Venderbosch [188] for a specific experiment (gas phase not included):

$$CH_{1.47}O_{0.56} + 0.386H_2$$

$$\rightarrow 0.742CH_{1.47}O_{0.11\ \text{(oil fraction)}} + 0.192CH_{3.02}O_{1.09\ \text{(water fraction)}} + 0.285\ H_2O \quad (3)$$

The product consisted of two phases and the oxygen content in terms of O/C ratio was decreased from 0.56 (feed oil) to 0.11 (product oil fraction). Similarly, the oxygen content in the resulting water fraction was increased compared to that in the feed oil (from 0.56 to 1.09) [188]. Cracking and DCO reactions lead to the formation of CH_4, CO, CO_2, and light (C_2-C_4) hydrocarbons [188,198] which cannot be retrieved in the condensed oil. Depending on the catalyst, there could also be C_1 interconversion reactions such as steam reforming/methanation and water gas shift.

The efficiency of bio-oil upgrading processes can be evaluated (and compared) based on the bio-oil yield (Y_{oil}) and degree of deoxygenation (DOD):

$$Y_{oil} = \left(\frac{m_{oil}}{m_{feed}}\right) \cdot 100\% \quad (4)$$

$$DOD = \left(1 - \frac{O_{oil}}{O_{feed}}\right) \cdot 100\% \quad (5)$$

with *m* being the mass of feed and produced oil, and *O* being the content of oxygen in the produced oil and feed, respectively. Specifically for catalytic fast pyrolysis (also covering catalytic fast hydropyrolysis), Venderbosch [47] proposed to evaluate the degree of deoxygenation as the actual oxygen reduction, ξ_O, by comparing the oxygen content of the produced oil to that of the "thermal oil" produced by thermal deoxygenation in the corresponding uncatalyzed process:

$$\xi_O = \left(1 - \frac{O_{oil}}{O_{thermal\ oil}}\right) \cdot 100\% \quad (6)$$

Venderbosch [47] additionally pointed out the importance of considering the carbon recovery in the produced oil. The carbon recovery is affected by DCO reactions, cracking, and coking. The energy recovery of the upgraded oil compared to the feed is also a very important parameter, which is often overlooked (see equation (1)). Other parameters such as the resulting O/C and H/C ratios provide valuable information on the oil quality. Full deoxygenation (DOD = 100%) is not necessarily the ultimate goal in bio-oil upgrading. Methanol, ethanol, and dimethyl ether have high oxygen contents (35 and 50wt%, respectively) but are regarded as fuels of high value. Additionally, there is an inherent trade-off between the degree of deoxygenation and oil yield, in part due to the removal of oxygen. This can be seen from the representative example on yields of oil, water, and gas at varying degrees of deoxygenation from bio-oil HDO shown in Figure 13, which also shows how the energy content of the oil (HHV) increases as a function of increasing deoxygenation.

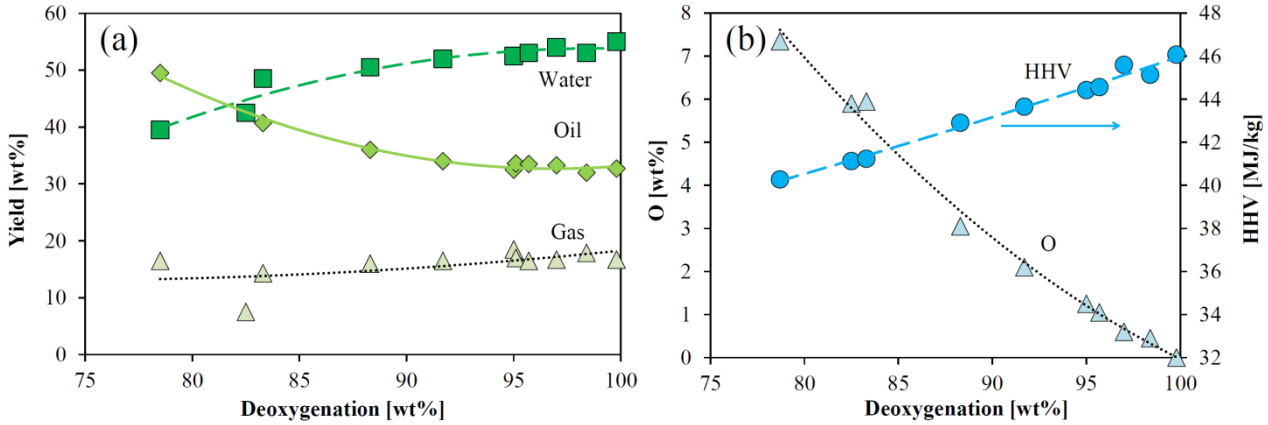

Figure 13 Results from upgrading of eucalyptus bio-oil via thermal hydrotreatment (slurry reactor, at deoxygenation < 83%) and catalytic hydrotreatment (fixed bed reactor, commercial Co-MoS_2 and Ni-MoS_2 catalysts, at deoxygenation > 83%). (a) Yields of oil, water from feed+reaction, and gas. (b) O content and energy content in the produced oil, calculated based on the assumption that C, H, and O sum to 100wt%. Based on data from Samolada et al. [198] *(copyright 1998) with permission from Elsevier.*

The exact composition of the produced gas and oil was not stated by Samolada et al. [198]. The gas phase, which was produced at yields of < 20%, was reported to consist of CO, CO_2 and hydrocarbons, and for the oil, only the weight based C/H ratio and the oxygen content was stated. The HHV in Figure 13 was calculated assuming that the content of C, H, and O in the upgraded oil sum to 100wt%, and by using the correlation fitted to liquid hydrocarbons and oxygenates by Lloyd and Davenport [199], neglecting contributions from N and S:

$$\text{HHV} = (0.3578 \cdot \text{wt\% C} + 1.1357 \cdot \text{wt\% H} - 0.0845 \cdot \text{wt\% O})\ \text{MJ/kg} \quad (7)$$

As the degree of deoxygenation was increased from below 80% to 100%, the HHV was improved from 40 to 46 MJ/kg, the molar H/C ratio was increased from 1.4 to 1.8, and the molar O/C ratio was decreased from 0.1 to zero. The product properties could thus be tuned to match those of fossil fuels by increasing the HDO severity.

As a minimum requirement, deoxygenation should be performed to a degree, which stabilizes the oil. This is not so much a matter of oxygen content as it is of oxygenate identity. For a typical bio-oil with 15-20wt% oxygen on dry basis, removal of the more reactive oxygenates corresponds to a

degree of deoxygenation of 30-50% (see Table 5). Further deoxygenation and incorporation of hydrogen could be targeted towards increasing the heating value (see Figure 13b) sufficiently to allow for using the produced oil directly as a fuel (alternatively as blend in), as a co-feed in petrochemical hydrotreating, or as a means of storing hydrogen in the oil.

Table 5 Calculation of required degree of deoxygenation to remove oxygen from reactive aliphatic acids and aldehydes. The moisture free content of oxygen, acetic acid, and hydroxyacetaldehyde for different fast pyrolysis oil was reported by Azeez et al. [32]. Acetic acid accounted for ≥ 90wt% of the detected acids. Hydroxyacetaldehyde accounted for ≥ 70wt % of the detected aldehydes.

Composition		**Beech**	**Spruce**	**Iroko**	**Albazia**	**Corn cob**
Acetic acid	[wt%]	8.0	2.5	6.1	6.8	8.5
Hydroxyacetaldehyde	[wt%]	7.9	9.8	7.0	6.7	5.1
O_{total}	[wt%]	20.7	19.8	8.5	14.9	7.7
$O_{acetic\ acid}$	[wt%]	4.3	1.3	3.3	3.6	4.5
$O_{hydroxyacetaldehyde}$	[wt%]	4.2	5.2	3.7	3.6	2.7
DOD required to remove $O_{acetic\ acid}$ + $O_{hydroxyacetaldehyde}$	[%]	41	33	82	48	94

An overview of different bio-oil upgrading studies is given in Table 6. More comprehensive reviews of HDO of both bio-oil and model compound studies are available in the literature [20,130,168,169].

Table 6 Updated overview of HDO studies for upgrading of bio-oil. Based on [20] *(copyright 2011) with permission from Elsevier.*

Catalyst	Bio-oil source	Setup	Time [h]	P [bar]	T [°C]	DOD [%]	O/C [molar]	H/C [molar]	Y_{oil} [wt%]	Ref.
Co-MoS_2/Al_2O_3	Beech	Batch	4	200	350	82	0.07	1.20	26	[196
Co-MoS_2/Al_2O_3	Beech	Batch	4	100	250	41	0.27	1.24	28	[196
Co-MoS_2[a]	Maple and oak	Continuous	4	≤300	370	99.9	0.00	1.82	33	[200
Ni-MoS_2[a]	Maple and oak	Continuous	-	≤300	370	97	0.00	1.79	34	[200
Ni-MoS_2/Al_2O_3	Beech	Batch	4	200	350	74	0.10	1.24	28	[196
Ni-MoS_2/Al_2O_3	Beech	Batch	4	100	250	37	0.31	1.48	31	[196
Ni-MoS_2/Al_2O_3	Pine	Continuous	-	87	400	28	-	-	84	[201
Ni-MoS_2/Al_2O_3	Pine[b]	Continuous	168-192[c]	96	330	100	0.00	1.18	-	[202
Ni-MoS_2/Al_2O_3	Wood	Continuous	6	100	300	100	-	2.1	-	[203
Ni-MoS_2[a]	Pine[d]	Continuous	13-16[e]	100	350	94	0.01[i]	1.06	64	[45]
Ni-MoS_2[a]	Pine[d]	Continuous	73-97[e]	138	300	60	0.07[i]	1.39	73	[45]
Ni-MoS_2[a]	Pine[d]	Continuous	117-132[e]	138	290	62	0.07[i]	1.37	82	[45]
Ni/SiO_2	Wheat straw	Batch	4	130-180	250	51	0.25	1.46	15	[120
Ni/ZrO_2	Wheat straw	Batch	4	130-180	250	41	0.21	1.36	13	[120
Fe_2O_3/SiO_2	Pine	Batch	5	>35[f]	300	31	0.30	1.05	33	[204
Co_3O_4/SiO_2	Pine	Batch	5	>35[f]	300	17	0.39	1.22	31	[204
Fe_2O_3-Co_3O_4/SiO_2	Pine	Batch	5	>35[f]	300	26	0.31	1.21	27	[204
NiP/AC[g]	Hardwood	Batch	3	110-170	300	65	0.11	1.29	63	[205
NiRuP/AC[g]	Hardwood	Batch	3	110-170	300	48	0.19	1.39	59	[205
CoP/AC[g]	Hardwood	Batch	3	110-170	300	62	0.12	1.26	60	[205
CoRuP/AC[g]	Hardwood	Batch	3	110-170	300	48	0.19	1.37	63	[205
Pd/C	Beech	Batch	4	200	350	85	0.06	1.26	65[h]	[196
Pd/C	Beech	Batch	4	100	250	56	0.19	1.30	44	[196
Pd/C	Mixed wood	Continuous	-	138	340	63	0.12	1.49	62	[206
Pt/Al_2O_3-SiO_2	Pine	Continuous	-	87	400	45	-	-	81	[201
Pt/C	Beech	Batch	4	200	350	76	0.11	1.36	27[h]	[196
Pt/C	Beech	Batch	4	100	250	35	0.32	1.60	57	[196
Pt-Pd/ACP[g]	Black poplar	Continuous	6	≤ 65	450	-	-	-	21	[207
Pt-Pd/FCC	Black poplar	Continuous	6	≤ 65	450	-	-	-	14	[207
Ru/Al_2O_3	Beech	Batch	4	200	350	78	0.04	1.10	36[h]	[196
Ru/Al_2O_3	Beech	Batch	4	100	250	37	0.39	1.70	23	[196
Ru/C	Forestry residues	Continuous	-	230	350-400	70	0.11	1.48	39	[188
Ru/C	Hardwood	Batch	3	110-170	300	42	0.22	1.43	64	[205
Ru/C	Beech	Batch	4	200	350	86	0.06	1.24	53[h]	[196
Ru/C	Beech	Batch	4	100	250	44	0.26	1.34	35	[196
Ru/TiO_2	Beech	Batch	4	200	350	77	0.09	1.32	67[h]	[196
Ru/TiO_2	Beech	Batch	4	100	250	50	0.23	1.56	37	[196

a) Commercial catalyst with unspecified support. b) From liquefaction in supercritical CO_2. c) Operating time at the noted conditions. Entire experiment run time: 240 h. d) From catalytic fast pyrolysis in a CFB reactor using a none-zeolite, alumina-based catalyst. e) The experiment from was run for 16 h at 100 bar and 350 °C, 103 h at 138 bar and 300 °C, and 365 h at 138 bar and 290 °C. Results are shown for the time ranges noted in the table. f) Pressure at room temperature, prior to heating. g) Activated carbon (AC) or phosphorus activated carbon (ACP). h) A heavy and light oil phase was obtained, results represent an average. i) Calculated based on the assumption that the content of C, H, and O sums to 100 wt%.

As seen from Table 6, several different catalytic systems are active in upgrading of bio-oil with the oil yield and properties depending on the catalyst system and applied operating conditions. Most of the studies in Table 6 were performed at pressures above 100 bar, and at moderate temperatures above 250 °C. There is a general trade-off between yield and degree of deoxygenation for the obtained oil as discussed previously. Cheng et al. [204] used non-conventional Fe_2O_3/SiO_2, Co_3O_4/SiO_2, and Fe_2O_3-Co_3O_4/SiO_2 catalysts for the HDO of pine bio-oil in a batch reactor operated at 300 °C. They achieved both a lower oil yield and DOD than in the remaining studies listed in Table 6, showing a limited potential for these catalyst systems. Most studies were made using batch reactors, which are not suited to study catalyst stability and long term product quality, and even for the continuous experiments the run time was much shorter than needed industrially. In fact, several experiments were terminated due to coking and reactor plugging [200,206,207]. In most of the studies, where reactor plugging was not observed, carbon deposition on the catalyst was mentioned as a main source of deactivation [45,120,196,201,202,204,205,207]. Sheu et al. [201] were not able to conduct an attempted experiment for HDO of pine bio-oil with a sulfided NiW/Al_2O_3 catalyst due to rapid reactor plugging. Wang et al. [202] reported 21.4wt% carbon deposited on a spent Ni-MoS_2/Al_2O_3 used for pine bio-oil HDO; it was however run for more than 200 h at varying operating conditions (280-350 °C and 34-97 bar H_2). During operation at 100 bar and 350 °C, Mante et al. [45] experienced reactor plugging and uncontrolled temperature increases in the conversion of a loblolly pine oil over a commercial Ni-MoS_2 catalyst operated in a fixed bed reactor setup. By increasing the operating pressure and decreasing the temperature, they were able to run for 365 h. They did, however, experience continuous deactivation, which resulted in a significant decrease in the DOD. At constant conditions of 138 bar and 290 ºC, the DOD had decreased from 97% to 45% during 325 h on stream. They reported carbon deposition, loss of sulfur from the catalyst active phase, and deactivation by water exposure as potential causes.

Mortensen [203] reported rapid catalyst deactivation over a commercial Ni-MoS_2/Al_2O_3 catalyst at 300 °C and 100 bar (see Figure 14). Initially, 100% deoxygenation was obtained with the produced oil being clear and colorless with an H/C ratio of 2.1, similar to crude oil. This initial product primarily consisted of naphthenes and linear/branched hydrocarbons. However, rapid catalyst deactivation was observed, and after 11 h the degree of deoxygenation was down to 69%, the H/C ratio had decreased to 1.9, and the produced oil looked more similar to the feed.

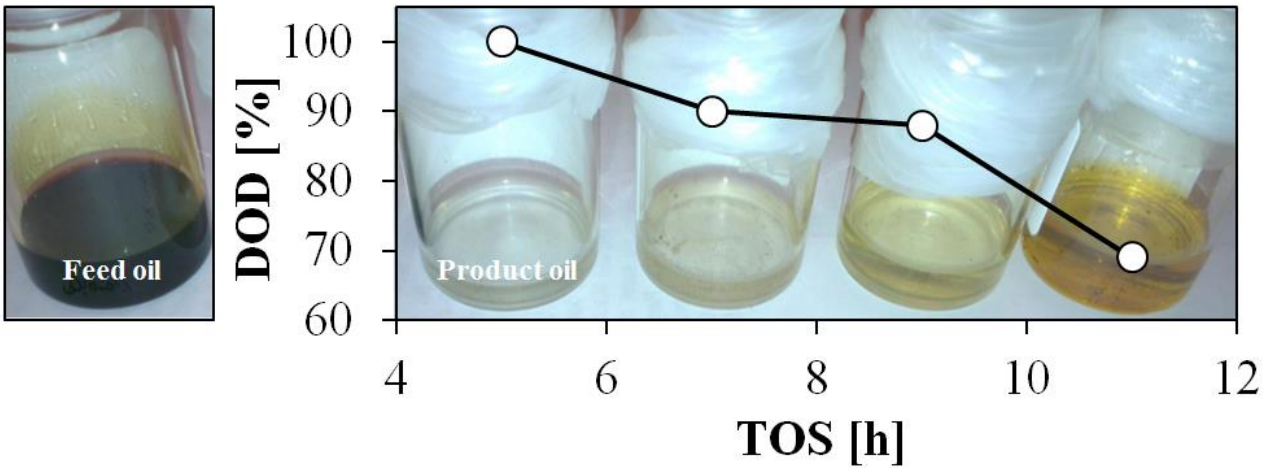

Figure 14 Feed wood-derived bio-oil and deoxygenated product oil including DOD as a function of TOS. HDO performed in a fixed bed reactor using a commercial Ni-MoS_2/Al_2O_3 catalyst at 300 °C and 100 bar. DOD data from [203] *is averaged over 2 hours.*

Mante et al. [45] were able to obtain both a high oil yield of 64-82% and a high DOD of 60-94% by hydrotreating a loblolly pine oil. Note that they used a bio-oil obtained from catalytic fast pyrolysis rather than fast pyrolysis. Catalytic fast pyrolysis typically gives a low oil yield, due to the higher degree of coke formation, decarboxylation, and cracking to light gasses. This was addressed by Venderbosch [47], who compared the results from various catalytic and non-catalytic pyrolysis studies and showed, that the carbon yield in the produced oil was in the range of 5-25% for catalytic fast pyrolysis and above 50% for fast pyrolysis. Catalytic fast pyrolysis can additionally be used to

remove the most reactive species and produce a more stable bio-oil, which is easier to upgrade by HDO. This makes it difficult to compare HDO results on bio-oils from fast pyrolysis and catalytic fast pyrolysis. Mante et al. [208] have reported a carbon yield of 10% from their catalytic pyrolysis process. In this work, 18% carbon was lost to an aqueous phase, 50% was lost to char (8% as solid char and 42% as CO and CO_2 from char combustion), 7% was lost to pyrolysis gasses, and 15% was unaccounted for. In contrast to the work of Mante et al. [45,208], information on the pyrolysis oil yield, whether being from a catalytic process or not, is often not reported in upgrading studies, possible because this information has not been available when acquiring the bio-oil from external suppliers. It is our opinion that the oil yield, the energy content, and the degree of deoxygenation obtained in bio-oil upgrading studies should also be presented and discussed on the basis of the feed biomass, and we encourage researchers to do so to in future work. This will allow for better comparison of the process efficiency and thereby also the industrial potential between different studies.

3.3. Catalysts

As mentioned above and summarized in Table 6 several catalytic systems have been applied for the HDO of bio-oil. This section reviews the most widely applied catalysts for HDO, namely sulfides, oxides, reduced transition metals, and phosphides. A brief description of other catalysts is also given.

3.3.1. Sulfides

As biomass and bio-oils contain sulfur, it is important to consider a sulfur tolerant catalyst for HDO, and the MoS_2 based systems are thus a good choice. Co- and Ni-MoS_2 catalysts (also referred to as Co-/NiMoS or sulfided Co-/NiMo catalysts) have received significant attention in upgrading of bio-

oil by HDO [171,178,182,194,196,200–202,209–223] based on their well-known activity in conventional hydrotreating [163]. Studies also exist on noble metal sulfides such as ReS_2 [224–226] and RuS_2 [227], but their much higher price most likely would prohibit commercial use if the current stability issues are not solved.

Ni and Co are used as promoters as they significantly enhance the catalytic activity and stability compared to unpromoted MoS_2. Several theories have been proposed for the role of promotion as reviewed by Topsøe et al. [163]. It is now widely accepted that the role of promotion is the formation of highly active CoMoS and NiMoS phases, in which Ni or Co substitutes Mo at the edges of MoS_2 slabs [163,228,229]. For Co-MoS_2, it has been shown that Co has a preference for promoting the S-edge of the hexagonal Co-MoS_2 structure, whereas both a hexagonal and a less systematic distorted hexagonal structure has been reported for Ni-MoS_2 [228–230]. The slabs are stacked with the S-edge in alternating direction as shown in Figure 15. The size and shape of the individual particles (composed of mono- and multilayer polygonal slabs) is determined by a complex interplay between catalyst composition (e.g. identity of promoter), and sulfidation conditions [229,231–234].

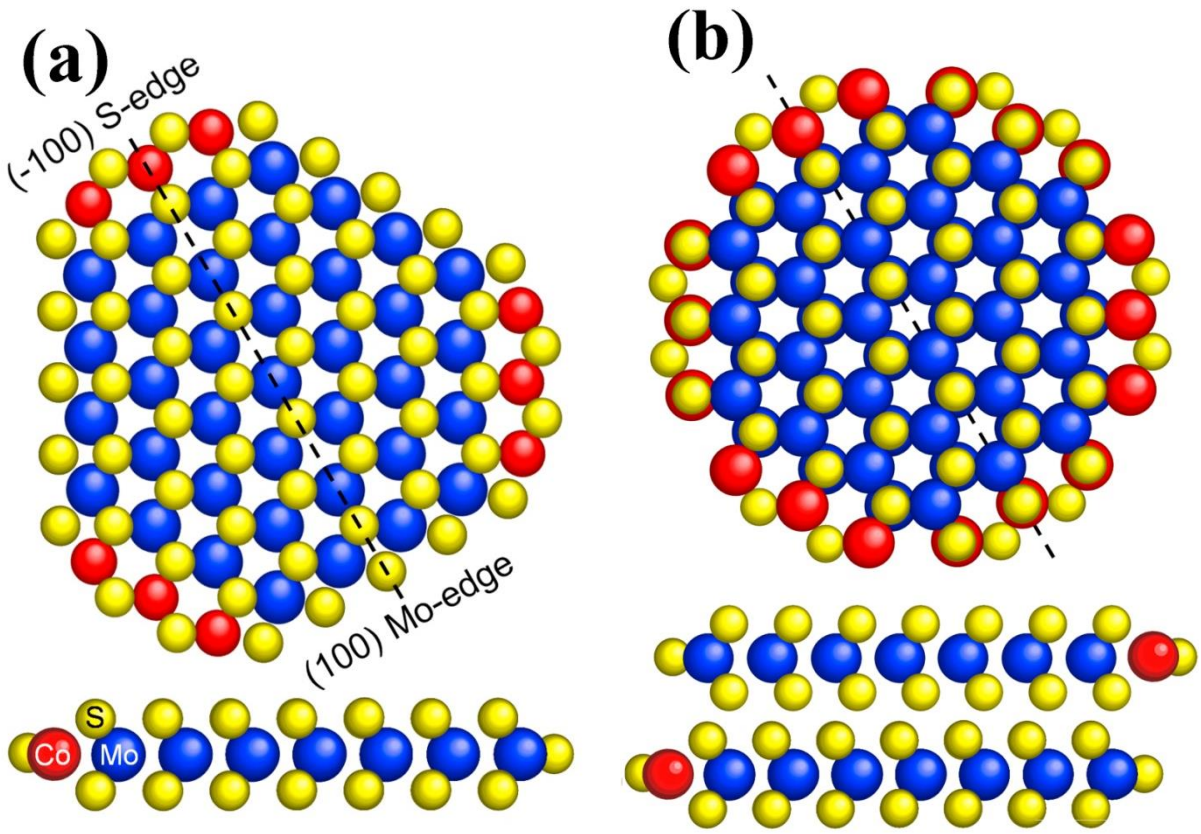

Figure 15 Ball-models for the hexagonal CoMoS structure of Co promoted MoS_2 in top view and side view. Blue: Mo, yellow: S, red: Co. (a) Single slab structure. (b) Double slab structure. Reprinted from [228] *(copyright 2015) with permission from Elsevier.*

The active sites for C-O (in HDO) and C-S (in HDS) scission is widely accepted to be coordinatively unsaturated sites (CUS) of sulfur at the promoted (or unpromoted) MoS_2 edge [194,235–237]. CUS can be present either as sulfur vacancies or as unsaturated sites at the sulfur terminated edge, where more sulfur (or oxygen from oxygenates) can adsorb, and this adsorption of a heteroatom may be correlated with a restructuring of the S atoms at the surface.

Romero et al. [172] studied HDO of 2-ethyl phenol over MoS_2 based catalysts and proposed the reaction mechanism shown in Figure 16. The target oxygen atom chemisorbs to a sulfur vacancy, which is created at a MoS_2 slab edge by reduction with H_2. SH groups generated from feed H_2 are present at the MoS_2 edges [236,237]. They enable proton donation from S to the attached molecule,

which forms a carbocation that can undergo direct C-O bond cleavage to give the deoxygenated compound [216,236–238]. The active site is regenerated when the deoxygenated product and water are desorbed. Another mechanism was proposed for HDO of aromatic oxygenates, with initial saturation of the aromatic ring [172]. In this mechanism, two adjacent vacancies are needed in order to facilitate adsorption through a sterically more constrained flat adsorption mode, which facilitates ring hydrogenation (see Figure 17). As opposed to the mechanism proposed by Romero et al. [172], a DFT study from Moses et al. [235] on HDS of thiophene showed that C-S scission could take place on CUS on a CoMoS edge without formation of sulfur vacancies.

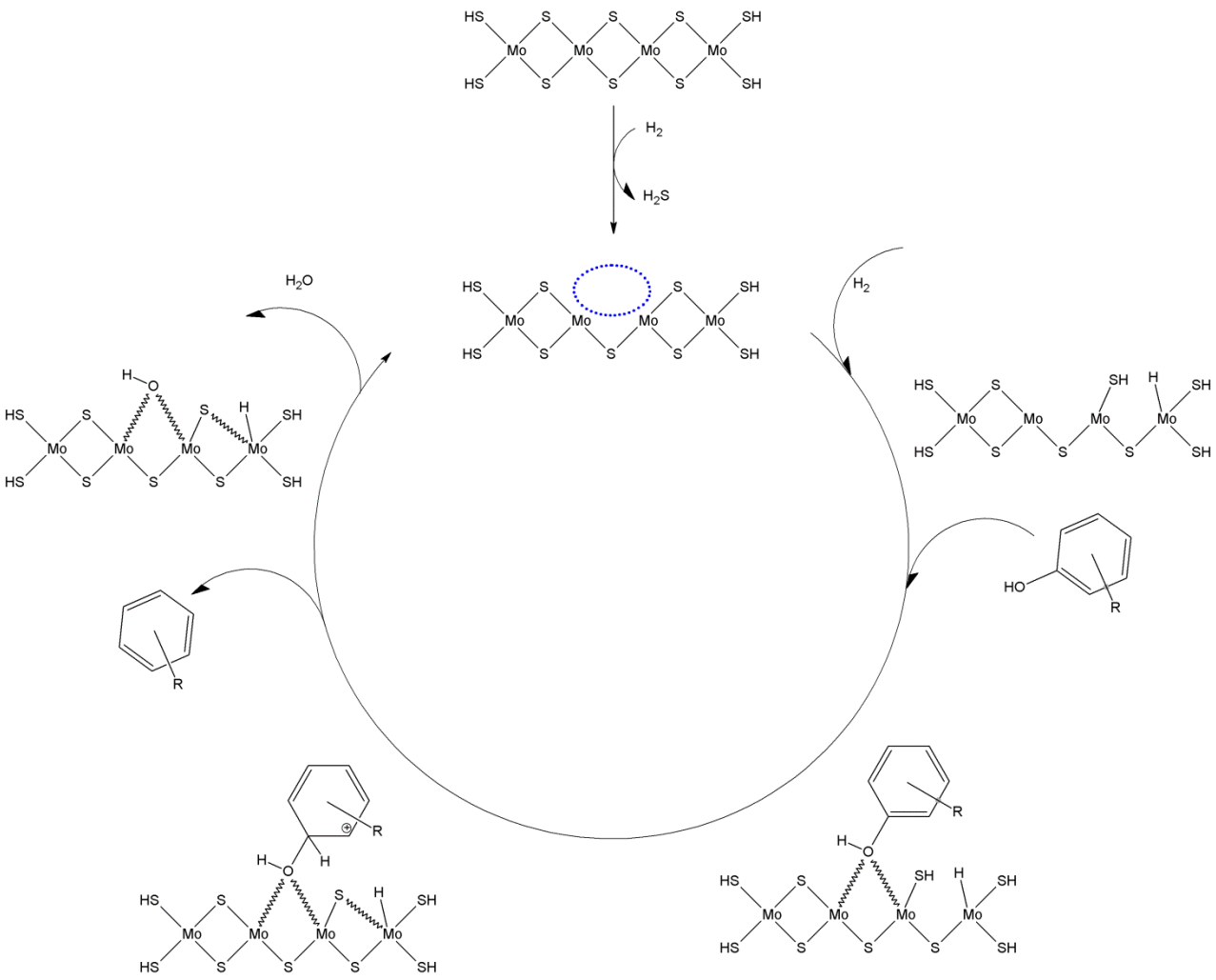

Figure 16 Proposed HDO mechanism of alkyl substituted phenol over MoS_2 with sulfur vacancy as active site (R denotes alkyl group). Drawn on the basis of [20] and [172].

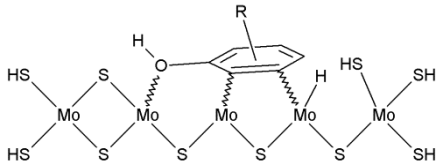

Figure 17 Flat ring adsorption of alkyl substituted phenol onto MoS_2 (R denotes alkyl group). Drawn on the basis of [172].

Based on DFT and experimental studies with thiophene, Lauritsen et al. [230,239,240] found that fully sulfided brim sites at edges of both NiMoS and CoMoS structures exhibit catalytic activity for adsorption and hydrogenation of thiophene. These so-called brim sites have been visualized at atomic resolution as bright brims along the MoS_2 edges using scanning tunneling microscopy (STM) (see Figure 18). They are located at the edge of the top basal plane of a multi-slab particle and exhibit metallic character due to their electronic properties The mechanisms of HDO and HDS therefore seem to be governed by an interaction of two different active sites controlling the degree of hydrogenation (over brim sites) and desulfurization/deoxygenation (via CUS) [241]. Furthermore, it has been proposed that different types of active sites come into play in the HDO of different oxygenate functional groups [215]. The identity and nature of active sites as well as particle morphology and the exact location of promoter atoms in Co- and Ni-MoS_2 catalysts is still debated, which can partly be traced back to the highly dynamic nature of these catalyst systems.

There is some dissimilarity between HDO and HDS. One example is the comparison between sulfur and oxygen analogues such as thiophene and furan as they interact differently with sulfur vacancies due to steric constraints [242].

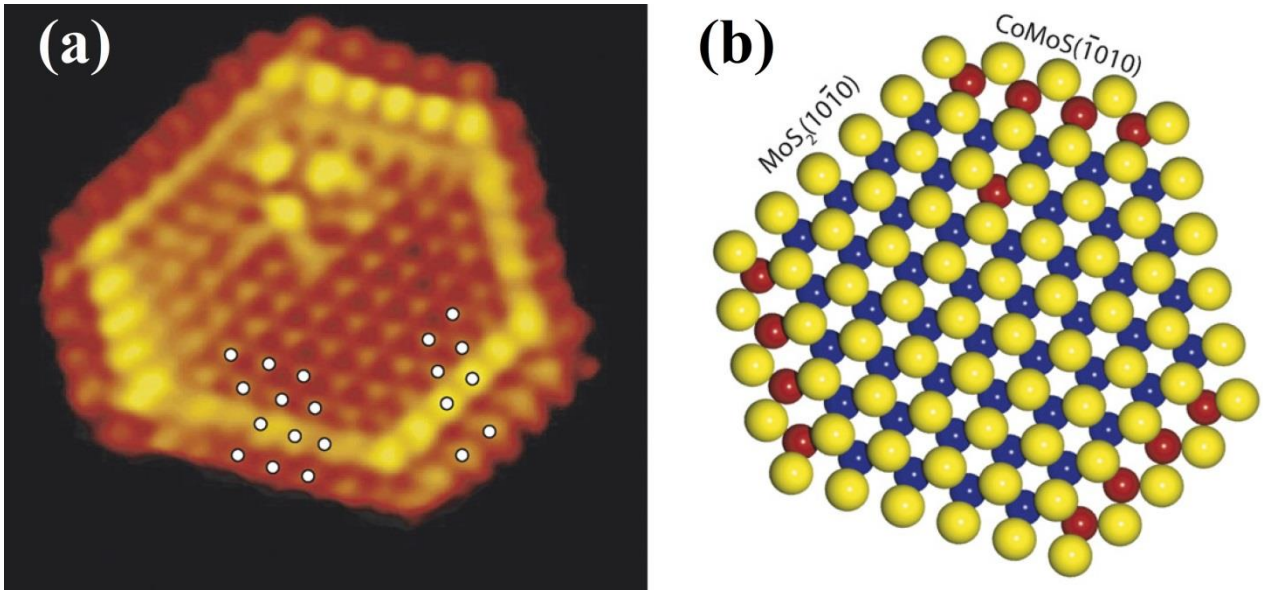

Figure 18 (a) Atom-resolved STM image of a CoMoS slab on an Au(111) surface. (b) Ball-model of the slab. Blue: Mo, yellow: S, red: Co. Reprinted from [230] *(copyright 2007) with permission from Elsevier.*

It is necessary to co-feed H_2S in order to the enhance activity [209,213,243] and avoid oxidation by keeping the sulfide catalyst systems in the active sulfided form during HDO [168,203,213,242]. Gutierrez et al. [219] proposed that H_2S co-fed in the HDO of a broad variety of model compounds is responsible for creating and retaining nucleophilic SH-groups at the sulfided catalyst surface and that these groups can activate oxygenates at the catalyst surface. However, H_2S can also be a reaction inhibitor [214–216], but the inhibiting effect depends on the oxygenate functionality and reaction mechanism [216,217].

A concern that has been raised is that the use of sulfide catalysts for HDO results in incorporation of sulfur into the product, which contradicts the increasingly strict legislation on sulfur in fuels [117,118,244] and contaminates the otherwise sulfur scant bio-oil. It has been shown that sulfur from the catalyst surface - regardless of whether H_2S is fed to the system - can be integrated into the deoxygenated compounds and thereby end up in the product oil [216,217,245,246]. However,

sulfide catalysts are used industrially in HDS to remove sulfur from oil down to a few parts per million (ppm) [163]. Mortensen et al. [137] investigated the HDO of phenol in 1-octanol (50 g/L) over a Ni-MoS_2/ZrO_2 catalyst in a fixed bed reactor at 280 °C and 100 bar and found that sulfur incorporation into the product could be avoided, as long as the conversion was kept high (≥90%). This was obtained by keeping the residence time high at a low weight hourly space velocity (WHSV) below 0.5 h^{-1}.

3.3.1.1. Role of Promotion

MoS_2 is typically promoted with Co or Ni, which weakens the surface metal-sulfur bond energy [247,248] and facilitates CUS formation. Co or Ni promotion is used to enhance the overall catalyst performance; both in terms of providing better hydrogenation activity [209,220,230,239,240] and in terms of a better stability towards deactivation [209,213,242].

The activity and selectivity of Ni-MoS_2/Al_2O_3 and Co-MoS_2/Al_2O_3 in HDO are comparable according to a study of Laurent and Delmon [215], who investigated the conversion of 4-methylacetophenone, diethyldecanedioate and guaiacol in a batch reactor at 260-300 °C and 10 bar H_2. However, promotion with Ni caused a higher decarboxylation activity as opposed to Co [215]. For phenolic species, it is commonly accepted that Co promotes DDO routes while Ni promotes HYD routes [182,216,217,219,220,246,249,250]. In line with this observation, Co-MoS_2/Al_2O_3 seems to have a higher activity for HDO of aromatic species compared to Ni-MoS_2/Al_2O_3, while the opposite is the case for aliphatic species [216,217,243,246]. The choice of Co or Ni promotion could therefore take into consideration the feed composition (aromatic/aliphatic), but also whether the reaction gas contains CO, which has been reported to inhibit Co-MoS_2, but not Ni-MoS_2 [220]. However, the choice of temperature affects this conclusion, as thermodynamics determine whether aromatic ring hydrogenation is favorable or not (see Figure 10).

Bouvier et al. [220] studied the HDO of 2-ethylphenol over Al_2O_3 supported MoS_2, Ni-MoS_2, and Co-MoS_2 in a fixed bed reactor at 340 °C and 70 bar (≈ 60 bar H_2) with varying H_2S concentration in the feed (0.1-0.5 bar corresponding to ~1430-7145 ppm). Their results are shown in Figure 19. The HYD and ACI activity for all three catalysts increased with increasing H_2S concentration. At the same time the DDO pathway, which primarily occurred with Co promotion, was strongly inhibited by H_2S. It was proposed that the inhibiting effect observed for Co-MoS_2 was caused by CUS saturation inhibiting oxygenate adsorption. On the contrary, Laurent and Delmon [215] did not report any significant influence of H_2S on the HDO of guaiacol. For aliphatic oxygenates such as ethylene glycol [209], 1-octanol [203], diethyldecanedioate [215], methyl heptanoate [217], and heptanoic acid [217], H_2S has been reported to have a promoting effect on the conversion over Ni-MoS_2 and Co-MoS_2 catalysts, even at very high concentrations of up to 2.4% [217].

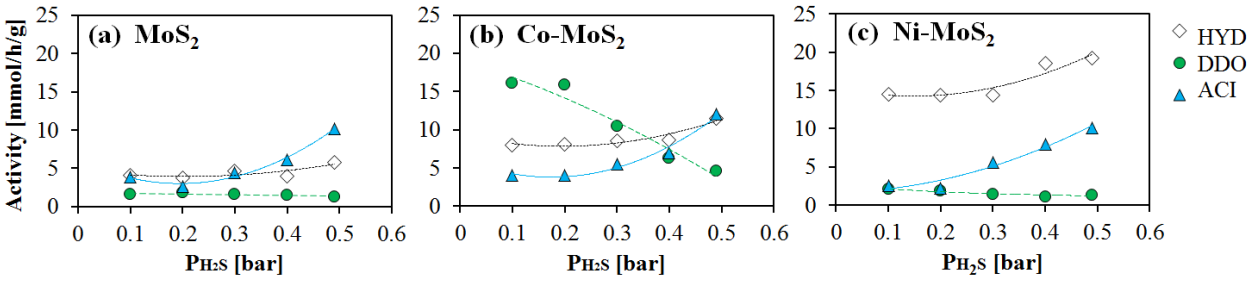

Figure 19 HYD, DDO, and ACI activity from HDO of 2-ethylphenol at 340 °C and 70 bar (fixed bed reactor) over promoted and unpromoted MoS_2 catalysts. The activity in mmol/h/g is the conversion of 2-ethylphenol into HYD, DDO, and ACI products per gram of catalyst. Drawn on the basis of data from [220].

The role of Ni promotion in unsupported MoS_2 was investigated by Ruinart de Brimont et al. [171] who found that the selectivity towards DCO of ethyl heptanoate at 250 °C and 15 bar (14.4 bar H_2) increased with increasing degree of Ni promotion, while HDO selectivity followed the opposite trend. The DCO selectivity was reported to follow the trend:

Ni_3S_2 > Ni-$MoS_{2(0.43)*}$ > Ni-$MoS_{2\ (0.2)*}$ > Ni-$MoS_{2\ (0.1)*}$ >MoS_2 * Ni/Mo molar ratio (8)

In the same study, the HDO reaction rates of heptanal had the following trend with DCO reaction rates being insignificant for all catalysts:

Ni-$MoS_{2\ (0.43)*}$ >> Ni-$MoS_{2\ (0.2)*}$ > Ni-$MoS_{2\ (0.1)*}$ > Ni_3S_2 ≈ MoS_2 * Ni/Mo molar ratio (9)

The reactivity was found to be more complex for heptanoic acid and ethyl heptanoate, due to competition between HDO and DCO reactions. Dupont et al. [251] used DFT calculations to study the interaction and HDO pathways of methyl propionate, propionic acid, propanal, and propanol with MoS_2 and Ni-MoS_2. They found that promotion with Ni facilitated a bidentate adsorption of propanal, which lowered the activation energy for the hydrogenation of propanal into propanol. The reaction of propanol to propane was proposed to occur via the formation of an intermediate thiol at the catalyst surface. The rate limiting step in propanal HDO to propane was the C-O cleavage in propanol, for which the activation energy was found to be lower over Ni-MoS_2 compared to MoS_2.

Based on DFT calculations, Badawi et al. [213,242] found that a H_2S/H_2O partial pressure ratio >0.025 is necessary to avoid S-O exchanges at the S-edge of MoS_2, which is similar to our recent results [209]. Badawi et al. [213] reported promotion by Co to enhance stability towards water with no S-O exchange at 100% Co promotion at the S-edge in the partial pressure range of H_2S/H_2O of 10^{-5}-10^{2} at 350 °C. This stabilizing effect was supported by transmission electron microscopy (TEM) studies showing that exposure of MoS_2 to water led to a decrease in slab length and stacking height, which was explained by S-O exchange. Exposure of Co-MoS_2 to water resulted in insignificant crystallite changes. The conversion of 2-ethylphenol was studied by Badawi et al. [213] over Co-MoS_2/Al_2O_3 and MoS_2/Al_2O_3 in a fixed bed reactor at 340 °C and 70 bar with a H_2S/H_2O ratio of 0.04-0.12. Deactivation of both catalysts with decreasing H_2S/H_2O ratio by addition of water

was seen, but for the Co promoted sample, the deactivation was mainly reversible, as $\geq$ 90% of the initial activity could be recovered by returning to the initial water free reaction conditions. Badawi et al. [214] also used DFT calculations to assess the Gibbs free energy of adsorption of known inhibitors at 350 °C for a 50% promoted Co-MoS_2 edge, which indicated that the inhibition strength followed a trend of CO > H_2O ≈ H_2S. We recently performed an *in-situ* quick extended X-ray absorption fine structure (Q-EXAFS) study [209], in which promoted and un-promoted $MoS_2/MgAl_2O_4$ catalysts were exposed to varying ratios of H_2S/H_2O in hydrogen at 400-450 °C. There was hardly any bulk transformation of the Mo sulfide phase to Mo oxide, and only negligible changes in the active phase were observed. More surface sensitive techniques should be used in future.

Bui et al. [182] investigated the role of Co promotion in bulk and Al_2O_3 supported MoS_2 for the HDO of guaiacol in a fixed bed reactor operated at 40 bar H_2 and 300 °C. They found that promotion with Co enhanced overall reaction rates and the selectivity towards DDO of intermediate phenol into benzene. DME reactions were observed for unpromoted MoS_2 while Co-MoS_2 also exhibited DMO activity.

3.3.2. Oxides

Oxides of Mo, Ni, W, V and other metals have HDO activity [179,252–259]. It has been proposed that the HDO reaction mechanism for reducible oxide catalysts follows a reverse Mars-van Krevelen mechanism [252,253] (see Figure 20), similar to the mechanism for sulfides proposed by Romero et al. [172] (see Figure 16). This implies that low H_2 pressures are necessary to avoid reduction of the active phase into inactive species [252,254,255]. Low H_2 pressures are favored from an economical perspective but may pose difficulties from an upgrading perspective, where higher H_2 pressures can mitigate catalyst deactivation by coking. In this mechanism (see Figure 20), an O-

vacancy (acting as a Lewis acid site) is created by elimination of water (reduction with hydrogen) and facilitates adsorption of an oxygenate at the vacancy. The C-O bond in the oxygenate is cleaved through electron donation from Mo, the deoxygenated product is desorbed and the active site is regenerated by reaction with H_2.

No hydrogenation activity, enabling saturation of double bonds, has been detected for MoO_3 [252,256]. A revised HDO mechanism has been presented for supported MoO_3 suggesting that the support enables dispersion of MoO_x clusters with ZrO_2 and TiO_2 being capable of efficiently stabilizing Mo in the redox active intermediate Mo^{+3} and Mo^{+5} states [256].

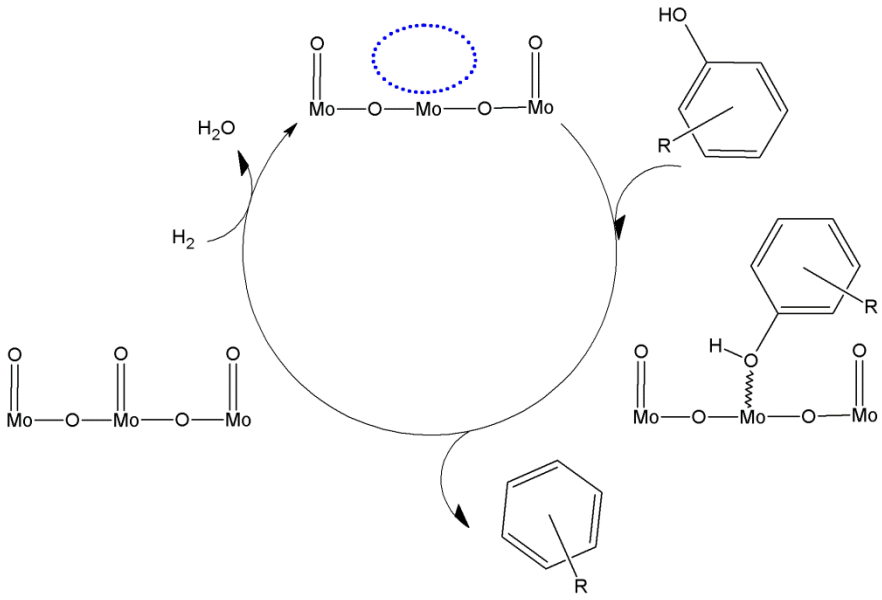

Figure 20 Proposed reverse Mars-van Krevelen mechanism for HDO of alkyl substituted phenol over MoO_3 (R denotes alkyl group). Drawn on the basis of [252,256].

The activity of oxides in HDO relies on the presence and strength of acid sites. The Lewis acidity affects the initial chemisorption step, where the oxygen lone pair of the target oxygenate is

chemisorbed at a vacancy. Brønsted acidity influences hydrogen availability at the catalyst surface in terms of the presence of hydroxyl groups. Auroux and Gervasini [260] have reported the Lewis acidity, based on NH_3 adsorption, of a broad range of oxides to follow the trends:

Concentration of sites: $Cr_2O_3 >> MoO_3 > ZrO_2 \approx WO_3 > Nb_2O_5 > TiO_2 > Al_2O_3 > V_2O_5$ (10)

Strength of sites: $Cr_2O_3 >> ZrO_2 \approx WO_3 > Nb_2O_5 > TiO_2 > Al_2O_3 > MoO_3 \approx V_2O_5$ (11)

The contribution from Brønsted acid sites was assumed negligible. ZrO_2, TiO_2, and Al_2O_3 are amphoteric and have been reported to have basic character as well [260]. Li and Dixon [261] reported another relative Lewis acid strength scale based on DFT calculations:

$WO_3 > MoO_3 > Cr_2O_3$ (12)

The Brønsted acid strength in terms of relative hydroxyl acidity was investigated by Busca et al. [262], who found:

$WO_3 > MoO_3 > V_2O_5 > Nb_2O_5 > Al_2O_3 > TiO_2 > ZrO_2$ (13)

Furthermore, the metal-oxygen bond strength should be weak enough to facilitate vacancy formation but strong enough to enable oxygenate chemisorption and C-O bond breaking. The catalytic HDO activity of MoO_3 has been ascribed to the formation of oxycarbide and oxycarbohydride phases ($MoO_xC_yH_z$) [254,255] as well as the formation of hydrogen molybdenum bronzes (H_xMoO_3, x = 0-2) [253].

Prasomsri et al. [252] have reported HDO activity of various oxides tested for acetone conversion in a fixed bed reactor at 400 °C and < 1 bar H_2. They reported the acetone consumption rate to follow the trend $MoO_3 > V_2O_5 > Fe_2O_3 > CuO \approx WO_3$ with a selectivity towards deoxygenated

hydrocarbon (mainly propene – due to the insignificant hydrogenation activity) above 88% for all oxides. Reactivation of spent MoO_3 was possible through calcination in O_2 at 400 °C [255,256].

Whiffen and Smith [254] compared the HDO of 4-methylphenol in a batch autoclave at 41-48 bar and 325-375 °C using MoO_3, MoO_2, MoS_2, and MoP. They reported the turn over frequency (TOF) to decrease in the order MoP > MoS_2 > MoO_2 > MoO_3. MoO_3 was reduced to MoO_2 during the reaction and based on the findings of Prasomsri et al. [252,255,256] it can be concluded that the partial pressure of H_2 of 41-48 bar was too high to retain the MoO_3 in the active phase.

The activity of partially reduced W and Ni-W oxides supported on active carbon was investigated by Echeandia et al. [179] in a fixed bed reactor operated at 150-300 °C and 15 bar. All catalysts were proven active for HDO of phenol with the Ni-W oxide catalysts showing a significantly higher conversion compared to the W oxides. It was shown that W was fully reduced after 6 hours on stream, whereas partial reduction of Ni was achieved.

As described above, the working principle behind oxide and sulfide catalysts is a vacancy or CUS based mechanism, which means that inhibition is possible if continuous regeneration of the active site is not ensured. Water formed during HDO can oxidize the active edge of sulfides [168,203,213,242] and inhibit further reaction (see section 3.3.1). The H_2 required for HDO can over-reduce and thereby deactivate oxide catalysts, and sulfur is a potential poison due to its strong adsorption [263,264]. As a result, the active phase of both oxide and sulfide catalysts could change during operation, and catalyst preparation and reaction conditions should be chosen to push the active phase towards the desired composition.

3.3.3. Reduced Transition Metals

Reduced transition metal catalysts such as Ni, Pt, Pd, Ru, and Rh are active in HYD and HDO reactions [120,185,188,196,201,206,265–267]. The reaction rate increases with increasing H_2 pressure (as opposed to oxides, see section 3.3.2) and these catalysts do not require a feed of H_2S to remain active (as opposed to sulfides, see section 3.3.1). As a down-side, most reduced transition metals are highly sensitive to sulfur poisoning, which means that sulfur in bio-oil must be removed upstream of catalytic HDO [137]. This would however require either a sulfur selective adsorbent or hydrotreating over Ni/Co-MoS_2 catalysts which, as discussed above, are also HDO catalysts.

Mortensen et al. [20] proposed that HDO over transition metals relies on a bifunctionality combining the ability of oxygenate adsorption (referred to as oxygenate activation) with hydrogenation activity. It was proposed that oxygenate adsorption takes place at the metal-support interface, while hydrogen donation is facilitated by the reduced transition metal particles [20].

A DDO reaction mechanism, in which phenol is converted into benzene by direct C-O scission, is challenged by a high bond dissociation energy (see Table 3), as shown by DFT calculations for HDO of phenol over Rh [268]. Instead two other mechanisms have been proposed for the DDO mechanism, in which the C-O bond is weakened prior to scission (see Figure 21). Instead of a direct C-O bond cleavage (mechanism A in Figure 21), it has been proposed that an initial hydrogenation step at the ortho position weakens the C-O bond and that subsequent acid-catalyzed dehydration then leads to the desired DDO product (mechanism B in Figure 21) [269,270]. This mechanism would require a bifunctional catalyst comprising both hydrogenation activity and acid sites.

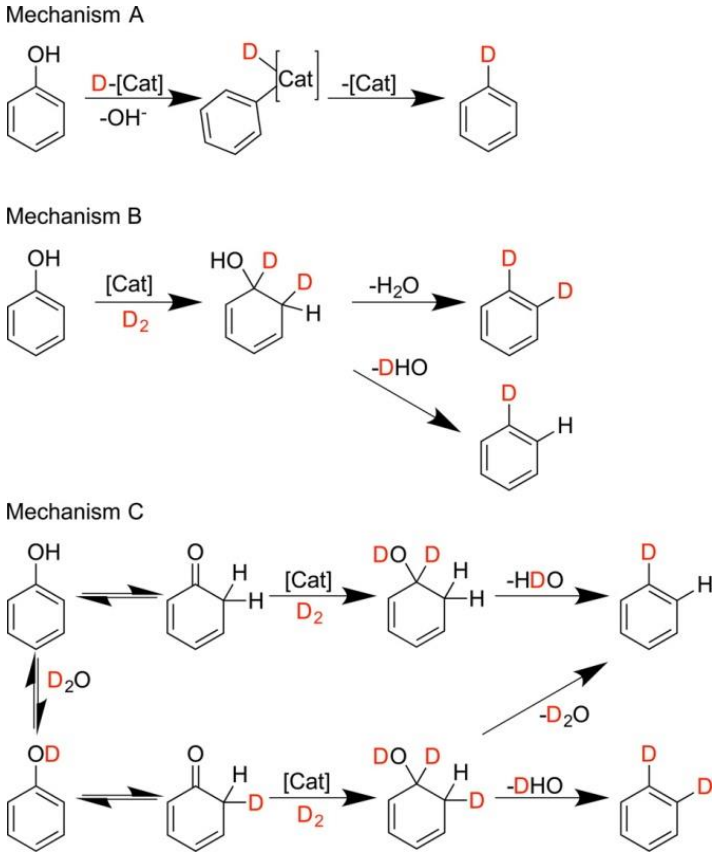

Figure 21 Three proposed reaction mechanisms for DDO of phenol. Isotopic labelling indicates predicted products when using D_2 as reductant. Mechanism A) Based on direct C-O cleavage. Mechanism B) Based on initial hydrogenation followed by dehydrogenation. Mechanism C) Based on initial tautomerization followed by hydrogenation and dehydration. Reprinted with permission from [174] *(copyright 2015, American Chemical Society).*

Resasco et al. [185,271–274] have recently presented a mechanism (mechanism C in Figure 21), which is initialized by a tautomerization step, i.e. the interconversion between the enol and keto form of phenol. This proposed tautomerization step was recently supported by Griffin et al. [275] who compared the conversion of m-cresol over Pt supported on C and TiO_2. Resasco et al. [185,271–274] have reported that the mechanism depends on the support acidity and oxophilicity. While acid sites catalyze dehydration, oxophilic sites have been proposed to facilitate interaction with the carbonyl (C=O) group present in the tautomer keto form of phenol. This interaction promotes hydrogenation of the C=O bond on metal particles at the metal-support interface. Nelson et al. [174]

have recently presented a thorough experimental and theoretical study of the conversion of phenol over Ru/TiO_2, which partly supports the work of Resasco et al. [185,271–274]. Using isotopic labelling (as indicated in Figure 21), they confirmed the presence of phenol tautomerization. They were however not able to confirm the subsequent hydrogenation/dehydration steps as proposed by Resasco et al. (see mechanism C in Figure 21). Instead they proposed that the amphoteric character of the TiO_2 support plays a crucial role in activating H_2O as a co-catalyst with the ability to donate and accept electrons and to lower the C-O scission barrier by donating a proton to the abstraction of the phenolic OH group [174].

As it can be inferred, there is a consensus that the mechanism of HDO over reduced transition metals depends on a bifunctionality based on the interplay between the support and active material. The reaction mechanism is however still under debate. To some extent this may be ascribed to the complexity introduced by the bifunctionality, namely the dependence of choice of catalyst active phase and support. Also, as previously pointed out, the thermodynamics determine whether ring hydrogenation is favorable or not; an important restriction, which is often overlooked.

3.3.3.1. Noble Metals

Noble metals such as Pt [175,196,201,271,276–282], Pd [185,196,206,274,275,281,283–286], and Ru [188,193,196,271,278,287] have received significant attention in the HDO literature. Oh et al. [278] studied the HDO of *miscanthus sinensis* bio-oil over carbon supported noble metals in a batch reactor pressurized to 30 bar at room temperature with H_2, and reached a 78.2% degree of deoxygenation over Pt/C at 350 °C. The HHV of the bio-oil was increased by 61% during HDO and unstable sugar fragments (acetic acid, furfural, vanillin, and levoglucosan) were reported to be converted into stable compounds.

de Souza et al. [185] converted phenol (in vapor phase) over Pd/SiO_2, Pd/Al_2O_3, and Pd/ZrO_2 at 300 °C and atmospheric pressure in a fixed bed reactor. They reported the density of acid sites (Brønsted

and Lewis) to follow the trend: $Pd/Al_2O_3 > Pd/ZrO_2 > Pd/SiO_2$. Compared to the other catalysts, Pd/ZrO_2 was reported to have a two times higher activity (determined as TOF), and a three times higher selectivity towards benzene. A physical mixture of Pd/SiO_2 and ZrO_2 showed similar activity to the Pd/SiO_2 catalyst, and it was therefore proposed that the higher activity of Pd/ZrO_2 was caused by interactions at the metal-support interface, which are governed by the oxophilic nature of ZrO_2. The positive support effect from ZrO_2 was confirmed for a Ni/ZrO_2 catalyst [185] in agreement with the work of Mortensen et al. [265]. Another approach is to use bimetallic catalysts, in which an oxophilic metal like Fe is combined with a hydrogenation active metal such as Pd [283,284] or Ni [273].

Different conclusions have been made when comparing the HDO activity of noble metals compared to conventional hydrotreating catalysts. Gutierrez et al. [281] investigated the conversion of guaiacol over various catalysts in a batch reactor at 100 °C and 80 bar, where the guaiacol conversion followed the trend:

$$Rh/ZrO_2 >> Co\text{-}MoS_2/Al_2O_3 \approx Pd/ZrO_2 > Pt/ZrO_2 \quad (14)$$

Gutierrez et al. [281] reported that the activity of the noble metal catalysts was too high for comparison of the tested catalysts at 300 °C. However, HDO was primarily observed in experiments conducted at 300 °C, whereas hydrogenation reactions were dominant at 100 °C [281], which might be explained by 100 °C being too low to facilitate C-O bond breaking.

Results from Wildschut et al. [196] are shown in Figure 22 (see also Table 6). They investigated the HDO of beech wood bio-oil in a batch reactor operated at mild (250 °C and 100 bar) and severe (350 °C and 200 bar) conditions over 4 h. Mild conditions only led to a DOD of 35-56%, while severe conditions resulted in a degree of deoxygenation of 74-86%. Especially Ru/C and Pd/C seemed promising with an oil yield of $\geq$ 53% and a deoxygenation degree $\geq$ 85%. As it can be seen,

the sulfided Co-MoS_2 and Ni-MoS_2 catalysts were among the poorest performing catalysts at both mild and severe conditions with lower oil yields and DOD. However, no sulfiding agent was introduced to the batch reactor to keep these catalysts in their active sulfide form.

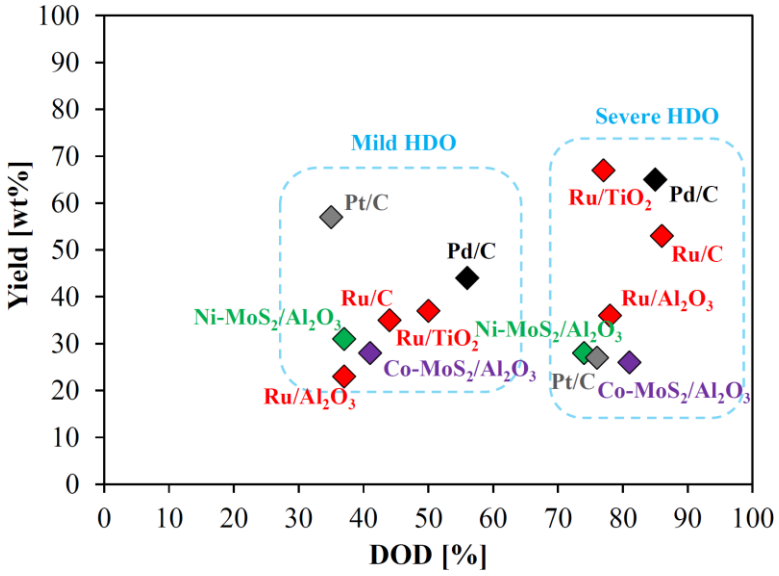

Figure 22 Comparison of DOD and oil yield in HDO of beech wood bio-oil with various catalysts [196]. *Experiments were performed in a batch reactor at mild (250 °C and 100 bar) and severe (350 °C and 200 bar) conditions over 4 h. All oil obtained at severe conditions (except for Ni-MoS_2/Al_2O_3 and Co-MoS_2/Al_2O_3) consisted of a heavy and a light oil fraction and hence, this data is represented as an average of both phases.*

Even though noble metals are active in HDO reactions, they are commercially unattractive due to their high price and limited availability [288]. In addition, they are highly sensitive towards sulfur [263], which is present in biomass and bio-oil (see Table 1).

3.3.3.2. Non-noble Metals

A cheaper alternative to noble metals is e.g. Ni, which is the most widely applied non-noble reduced transition metal for HDO [120,138,183,285,289–295]. Mortensen et al. [292] studied the HDO of phenol over Ni/SiO_2 in a batch reactor operated at 275 °C and 100 bar. They reported both hydrogenation and deoxygenation reactions to be dependent on the Ni particle size as shown in Figure 23 and related the TOF to particle size as well as theoretical distribution of different metal sites (steps, corners, facets). The rate of deoxygenation of cyclohexanol to cyclohexane increased

linearly with increasing dispersion (decreasing particle size), and a correlation with the fraction of exposed Ni step sites was proposed. On the other hand, the decreasing rate of hydrogenation of phenol to cyclohexanol with increasing dispersion could not be linked to the exposure of a specific type of site possibly because of the interplay with oxygen vacancies in the support as discussed above.

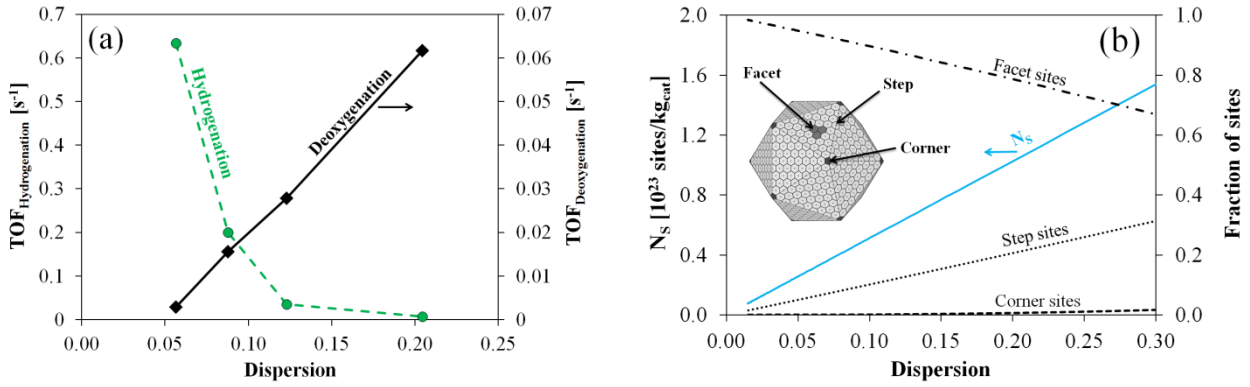

Figure 23 (a) TOF of hydrogenation and deoxygenation of phenol over Ni/SiO_2 in a batch reactor operated at 275 °C and 100 bar. (b) Calculated number of sites (N_S) and fraction of different sites (facet, step, corner) on Ni icosahedron crystal. Adapted from Mortensen et al. [292] *(copyright 2015) with permission from Elsevier.*

Boscagli et al. [120] reported that Ni supported on active carbon and various oxides (Al_2O_3, TiO_2, SiO_2, ZrO_2) had deoxygenation activities comparable to that of a Ru/C benchmark. The experiments were performed in a pressurized batch autoclave (80 bar at room temperature) operated at 250 °C using a wheat straw bio-oil. The O/C ratio was reduced from around 0.6 to less than 0.3 for all catalysts. The Ru/C catalyst possessed better hydrogenation activity resulting in an H/C ratio around 1.7, whereas those from the Ni catalysts were in the range of 1.3-1.5.

Yakovlev et al. have investigated the activity of Ni and bimetallic Ni-Cu catalysts for the HDO of anisole [290,291] and real bio-oil [183,294]. Anisole conversion experiments in a fixed bed reactor operated at 10 bar and 300 °C showed that complete deoxygenation was achieved with Ni-Cu supported on Al_2O_3 and CeO_2 with the following degree of HDO obtained [290]:

$Ni\text{-}Cu/CeO_2 > Ni\text{-}Cu/Al_2O_3 > Ni/Al_2O_3 > Ni/ZrO_2 > Ni\text{-}Cu/ZrO_2 > Ni/SiO_2$ (15)

In a thorough study on the HDO of pine bio-oil over a $Ni\text{-}Cu/SiO_2\text{-}ZrO_2$ catalyst, Yin and Yakovlev et al. [183] performed experiments at up to 200 bar and varying temperatures (60-410 °C) in both a batch reactor and a three stage fixed bed reactor setup. They focused on the varying reactivity of cellulose and lignin derived oxygenates (see Figure 9), and showed how the O/C and H/C ratio in the upgraded oil depended on the reaction temperature (see Figure 24). The deoxygenation was continuously improved with increasing temperature while the H/C ratio showed an optimum at intermediate temperatures. This was explained by different reactions dominating at different temperatures; i.e. aldehyde and ketone hydrogenation at low temperature, condensation and elimination reactions at medium temperatures, and hydrogenation and deoxygenation of aromatics at high temperature. The poorer H/C ratios obtained in the continuous setup compared to the batch reactor was explained by mass transfer limitations and shows the importance of considering the influence of the experimental design (reactor dimension, space velocities, catalyst pellet size, and dilution) in fixed bed catalyst activity studies. The critical parameter in batch reactors is the mixing, which is determined by the stirrer speed and the dimensions of the impeller and autoclave.

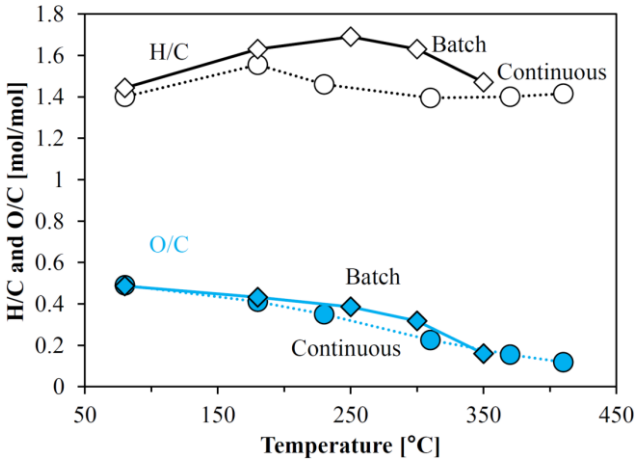

Figure 24 H/C and O/C ratio in upgraded pine bio-oil converted over a Ni-Cu/SiO_2-ZrO_2 catalyst at up to 200 bar and varying temperatures in a batch reactor and a continuous three stage fixed bed reactor setup. Data from [183].

Bimetallic Ni-Fe catalysts have also been studied [204,273,296]. Nie et al. [273] studied bimetallic catalysts and reported that the hydrogenation activity of a Ni/SiO_2 catalyst could be modified by adding oxophilic Fe, which facilitated hydrogenation of the carbonyl group in the tautomerized keto form of phenolic species, which could then be deoxygenated by dehydration.

3.3.4. Phosphides

As discussed in section 3.3.2, Whiffen and Smith [254] reported that an unsupported MoP had higher activity for HDO of 4-methylphenol compared to the corresponding sulfides and oxides at the given reaction conditions. Metal phosphides (especially Ni_2P) have shown promising activity and stability in HDO reactions [297–302]. Additionally, there are studies on sulfided [173] and non-sulfided [299] NiMoP systems used for HDO of furans and aromatic oxygenates. Oyama et al. [297,303] investigated the HDO activity of several phosphides (based on Ni, Co, Fe, W, and Mo) supported on SiO_2. For the conversion of 2-methyltetrahydrofuran in a fixed bed reactor at 300 °C and atmospheric pressure [303], MoP and WP showed the highest selectivity towards HDO products while the overall TOF decreased according to:

$Ni_2P > WP > MoP > CoP > FeP$ (16)

All catalysts were more active than a Pd/Al_2O_3 reference; an improvement compared to previous results [297]. Guo et al. [205] used Ni, Co, and Ru phosphide catalysts supported on activated carbon for HDO of hardwood bio-oil in a batch reactor at 300 °C and 110-170 bar and compared the performance with that of a benchmark Ru/C catalyst (see also Table 6). Similar oil yields of 59-64wt% was obtained for Ru/C, NiRuP/AC, CoRuP/AC, and the best performing monometallic NiP/AC and CoP/AC catalysts. However, the degree of deoxygenation was markedly improved with the monometallic phosphides (DOD = 62-65%) as compared to the bimetallic phosphides and the ruthenium benchmark (DOD = 42-48%).

Moon et al. [298] investigated the conversion of guaiacol over Ni_2P/SiO_2 at 1 and 8.1 bar of H_2 in a fixed bed reactor operated at 300 °C during 30 hours on stream. A conversion of ~80% was achieved at 1 bar while 100% conversion was achieved at 8.1 bar. Furthermore, the conversion was reported to follow a DDO route at low H_2 pressure and a HYD route at high H_2 pressure. At 1 bar, the main product formed was benzene (~60% selectivity), while it was cyclohexane (~90% selectivity) at 8.1 bar. Slight oxidation of the active phase in the spent catalyst exposed to 1 bar was evidenced by X-ray absorption spectroscopy (XAS), particularly EXAFS [298].

3.3.5. Alternative Catalysts

A range of other catalysts have also been investigated for the HDO of bio-oil. Transition metal carbides and nitrides (typically based on molybdenum or tungsten) have received increasing attention within the last decade [130,304–308]. Their potential lies in their low cost, similar hydrotreating (HDN, HDS) properties as conventional sulfides [309] as well as properties, which bear some similarity to noble metals [310]. Ruddy et al. [130] have presented a detailed overview of model compound HDO studies over a broad range of traditional and alternative catalysts including carbides and nitrides. While studies on nitrides remain scarce it is clear that carbides are

less attractive as they are sensitive to water [306,311], which is inevitable in HDO. There are also examples of other reaction conditions and catalyst systems in the HDO literature. These include HDO in a sub- or super-critical liquid phase [312–314], aqueous phase HDO where a mineral acid is used to promote hydrolysis reactions [204,270,315], use of boride catalysts [316], co-feeding a hydrogen donor such as methanol [41], and more.

3.4. Role of Support

Investigations of the influence of catalyst support in HDO have been scattered over different catalytic systems and model compounds. The role of the support depends on the catalyst system (e.g. reduced transition metals or sulfides) and on the identity of oxygenates subject to HDO (i.e. reaction mechanism).

In conventional hydrotreating, γ-Al_2O_3 is the prevailing support [163]. In HDO, however, Al_2O_3 has a number of undesired properties. The high concentrations of water present in bio-oil, and formed during HDO, can convert γ-Al_2O_3 into Boehmite (AlOOH) [188,317]. This decreases the activity as the transformation into Boehmite can trap crystals of the catalytically active material in the support lattice [317]. Furthermore, the high acidity of Al_2O_3 results in high coke formation propensity. Popov et al. [177] linked the acidity of Al_2O_3 with a high carbon formation affinity through saturation studies using a phenol/argon flow where 2/3 of Al_2O_3 was covered with phenolic species at 400 °C.

The acidity of various supported Ni catalysts was measured by Mortensen et al. [265] by NH_3 chemisorption and was seen to follow a decreasing trend as follows:

$$Ni/Al_2O_3 \geq Ni/ZrO_2 \geq Ni/CeO_2 > Ni\text{-}V_2O_5/ZrO_2 > Ni/MgAl_2O_4 > Ni/CeO_2\text{-}ZrO_2 >> Ni\text{-}V_2O_5/SiO_2 > Ni/SiO_2 > Ni/C \quad (17)$$

The HDO of phenol at 275 °C and 100 bar H_2 revealed no clear relation between catalyst acidity and HDO activity. Instead, Mortensen et al. [265] found a correlation between the oxide support metal-oxygen (M-O) bond strength and the catalyst hydrogenation activity (see Figure 25). This was explained by the formation of O-vacancies that act as Lewis acid sites [318,319] at the perimeter of the Ni nanoparticle where phenol is adsorbed and hydrogenated to cyclohexanol. Deoxygenation of the formed cyclohexanol was concluded to take place on the Ni metal sites and therefore be independent on O-vacancy formation.

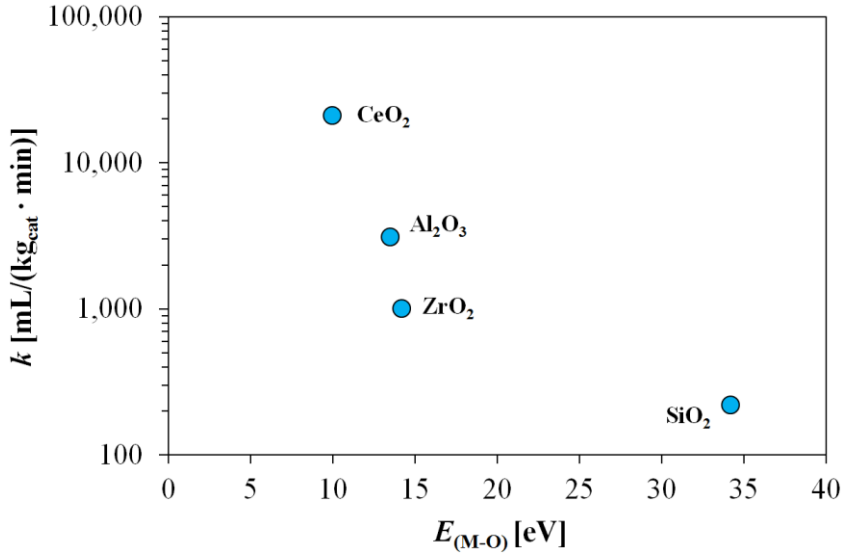

Figure 25 Hydrogenation activity (rate constant, k) of supported Ni catalysts as a function of metal-oxygen bond strength, $E_{(M-O)}$, of the support material. Hydrogenation activity: phenol conversion in autoclave at 275 °C and 100 bar H_2 from [265]. *$E_{(M-O)}$ data from* [318]. *Adapted with permission from* [265] *(copyright 2013, American Chemical Society).*

Contrarily, Lee et al. [269] reported that the catalyst acidity and HDO activity for guaiacol conversion in a batch autoclave at 250 °C and >40 bar H_2 followed the same trend for a noble rhodium catalyst, where NAC refers to nitric acid treated carbon black:

$$Rh/SiO_2\text{-}Al_2O_3 > Rh/Al_2O_3 > Rh/NAC > Rh/ZrO_2 \quad (18)$$

Carbon has been proposed as a promising support [178–180,196] due to its low acidity and thereby low coke formation tendency [178–180]. The correlation between low acidity and low coke affinity has also been reported for SiO_2 [297], where Popov et al. [177] showed that the concentration of adsorbed phenol on SiO_2 only was 12% relative to the concentration on Al_2O_3 at 400 °C. While phenolic species were concluded to only interact with SiO_2 via hydrogen bonds, dissociated species were strongly adsorbed on Al_2O_3 acid sites [177,320]. Another study concluded that both Ni/Al_2O_3 and Ni/AC caused a lower degree of deoxygenation compared to Ni/SiO_2 due to a respectively too strong and too weak interaction between support and anisole at 180-220 °C and 5-30 bar H_2 [289]. High acidity micro- and mesoporous materials such as hierarchical zeolites and alumina doped silicates have been applied as HDO catalyst support [321–323]. As mentioned, zeolites, which are commercially used in the FCC process [158], typically have a high cracking activity, which may limit the oil yield.

ZrO_2, CeO_2, and ZrO_2-CeO_2 mixtures have received attention as promising support materials [185,218,265,274,277,281,290,300,324–327]. These oxophilic carriers can potentially activate molecules for HDO on the catalyst surface [185,290,327]. CeO_2 is additionally known to be a versatile support with redox sites (oxygen storage and exchange) and acid-base sites [328]. Recent studies on ZrO_2 have proposed that the monoclinic crystal phase (*m*-ZrO_2) has a higher propensity of forming catalytically active O-vacancies than the tetragonal phase (*t*-ZrO_2) [329]. It was however pointed out by de Souza et al. [272] that the reaction rate of the deoxygenation step considered by Foraita et al. [329] was independent on ZrO_2 morphology. In their studies [272], they found that the *t*-ZrO_2 had more oxophilic sites compared to *m*-ZrO_2, which promoted deoxygenation.

SiO_2, ZrO_2, and TiO_2 carriers have been shown to promote an HDO reaction route for phenols, which involves a tautomerization step (see section 3.3.3) and it has been proposed that the HDO activity can be tuned through the support oxophilicity [174,185,271–273,275]. For MoO_3, which is

active in HDO at low H_2 pressures, it was shown that the support plays an important role in stabilizing redox-reactive Mo oxidation states [256] (see section 3.3.2).

Wu et al. [300] investigated the conversion of guaiacol in a fixed bed reactor at 300 °C and atmospheric pressure over Ni_2P supported on Al_2O_3, ZrO_2, and SiO_2. The activity declined in the order Ni_2P/ZrO_2 > Ni_2P/Al_2O_3 > Ni_2P/SiO_2. The adverse properties of SiO_2 were elaborated by Moon and Lee [301], who performed a combined activity and *in-situ* EXAFS study on the HDO of guaiacol over supported Ni_2P. Experiments conducted in a batch reactor at 30 bar and 300 °C showed that while AC and ZrO_2 supported catalysts had a stable conversion over time, Ni_2P/SiO_2 experienced significant deactivation. EXAFS studies revealed that SiO_2 was very sensitive to water and via its hydrophilic character facilitated oxidation of the active phase to nickel phosphate [301].

Bui et al. [218] investigated the conversion of guaiacol over MoS_2 and Co-MoS_2 supported on ZrO_2, TiO_2, and Al_2O_3 in a fixed bed reactor operated at 300 °C and 40 bar H_2. Al_2O_3 catalyzed demethylation and methyl substitution reactions at a rate 7 times higher than for the other supports. The HDO activity of Co-MoS_2/ZrO_2 per Mo atom was four times higher than that of Co-MoS_2/TiO_2 and Co-MoS_2/Al_2O_3, while MoS_2 on both ZrO_2 and TiO_2 had an activity two times that of MoS_2/Al_2O_3. Co-MoS_2 on ZrO_2 and TiO_2 was stable for >60 h operation while a constant deactivation was seen for Co-MoS_2/Al_2O_3. The adverse effects of Al_2O_3 were ascribed to its high acidity, which was expected to enhance coke formation on the catalyst surface.

It is crucial to acknowledge that the choice of support material affects the activity and selectivity of HDO catalysts and to include it in the catalyst design. Three aspects are important concerning choice and evaluation of support in HDO catalyst design:

- Propensity of carbon formation. This generally increases with increasing acidity resulting in undesired coke formation.

- The interaction between the support and bio-oil oxygenates. Adsorption of HDO reactants through oxygen vacancies/oxophilic sites in the support is possible.
- Stability against water and possibility for regeneration, e.g. by burning off coke at high temperatures (>400 °C).

The evaluation of catalytic HDO activity using different supports must include considerations on fundamental properties such as active phase dispersion (or particle size), surface area, and pore volume/size distribution in order to allow proper comparison of different catalysts. Ideally, catalyst activities should be reported as TOF. This requires determination of the concentration of active sites, which relies on identifying the active site based on suitable characterization techniques (e.g. chemisorption, spectroscopy, scattering, or electron microscopy), potentially coupled with DFT.

3.5. Choice and Influence of Operating Conditions

Reaction conditions for HDO should be chosen to facilitate high catalyst activity over prolonged periods of time with minimum deactivation. In this regard, different requirements will arise depending on the feedstock and catalyst identity.

3.5.1. Temperature

HDO is typically carried out in the range of 250-400 °C (see Table 6), which should favor full HDO from a thermodynamic perspective [20], see also Figure 10. The process should be operated below ~450 °C, if both deoxygenation and hydrogenation of aromatics is targeted. At higher temperatures, hydrogenation becomes unfavorable, and the exothermic nature of HDO reactions could furthermore limit the choice of temperature in a batch or fixed bed reactor as full deoxygenation could lead to generating hot spots. Additionally, coking increases with temperature, especially above 450 °C [181].

Elliott et al. [206] investigated the influence of temperature in the HDO of wood derived bio-oil over a Pd/C catalyst in a fixed bed reactor operated at 140 bar. Increasing the temperature from 310 °C to 340 °C increased the degree of deoxygenation from 65% to 70% but above 340 °C cracking reactions became dominant. Increasing the temperature from 310 °C to 360 °C had a negative effect on both the oil yield, which decreased from 75% to 56%, and on the degree of deoxygenation which decreased from 65% to 52%. At the same time, the gas yield increased by a factor of three.

The change in reactivity with temperature is dependent on the bio-oil composition and reactivity of individual species with the more reactive oxygenates coming from cellulose and hemicellulose and the more refractory oxygenates from lignin (see section 3.1). The catalytic upgrading can be performed in a dual stage continuous process to achieve high degrees of deoxygenation with limited formation of gas and coke (e.g. by cracking reactions). In dual stage HDO, the first reactor is operated at mild conditions below 250-350 °C to stabilize the most reactive species, while the second reactor is operated at higher temperatures, to facilitate complete deoxygenation of refractory phenolic species [121]. Dual stage reactor setups are thus targeted at minimizing coke formation from reactive compounds, while enabling HDO of all types of oxygenates. An early review of dual stage studies can be found in the work of Elliott et al. from 2007 [166], while a more recent brief review was provided by Wang et al. [121] in 2013. Some more recent studies are mentioned in the following.

Elliott et al. [330] used a single reactor with separate heating zones in the hydroprocessing of a softwood bio-oil at ≈135 bar over a Co-MoS_2/Al_2O_3 catalyst. The temperature was set to 240-250 °C in the first zone and 380-390 °C in the second, but the exothermal reactions caused the measured temperature to be up to 60 °C higher. The setup was operated continuously for up to 95 h. The degree of deoxygenation reported was 98-99% with a decent oil yield of 55-58wt% db. Catalyst deactivation was reported, and plugging due to carbon residues was reported for one experiment,

which was started in succession of a former experiment without cleaning the spent catalyst with acetone. The composition of the spent catalyst was not reported. Elliott et al. [331] later showed similarly promising results for a dual stage setup operated with a sulfided Ru/C catalyst in the first stage and a Co-MoS_2/Al_2O_3 catalyst in the second stage. The carbon deposition on the spent CoMo catalyst was around 10wt%. In this work, they investigated hot vapor filtration of the bio-oil feed and showed that the content of Ca, Na, and K could be significantly reduced for switchgrass bio-oil. Further dual stage HDO studies from Elliott et al. can be found in [166,332,333].

In the previously mentioned work of Yin et al. [183], both a batch reactor and a three stage HDO setup was employed in the conversion of pine bio-oil at up to 200 bar. They followed the influence of temperature on the composition of the produced oils by GC×GC, gel permeation chromatography (GPC), ^{1}H-NMR spectroscopy, thermogravimetric analysis (TGA), the total acid number (TAN), the carbonyl number (CAN), and more. Based on these analyses, they presented the reactivity scale in Figure 9, starting at a low temperature of 80-180 °C, at which the small and most reactive oxygenates (formic acid, glucose, levoglucosan, aldehydes, and ketones) would decompose and be hydrogenated.

A clear advantage of the dual (or multiple) stage HDO processes is the immediate possibility to stabilize the bio-oil in steps while it is re-heated. The different compound classes can be targeted at separate temperatures using different catalysts types. Severe catalyst deactivation as well as coking and reactor plugging has however also been observed in dual stage HDO studies. For example, Routray et al. [129] used Ru/C at 130 °C followed by Pt/ZrP at 300-400 °C to upgrade oak bio-oil in a dual stage setup and reported that reactor plugging occurred after 55-71 h for all their experiments. Since thermally induced re-polymerization reactions may occur at <200 °C [188], it is recommended to operate the first stage in a dual (or triple) stage HDO setup at lower temperatures to reduce carbon deposition leading to plugging and/or catalyst deactivation.

3.5.2. Residence Time

A fairly low liquid hourly space velocity (LHSV) of 0.1-1.5 h^{-1} (corresponding to a high residence time) is generally applied in HDO processes to obtain high degrees of deoxygenation [30,137,334]. For example, Elliott et al. [206] investigated the HDO of bio-oil over a Pd/C catalyst at 140 bar and 340 °C and observed that the oxygen content in the product oil decreased from 21 to 10wt% when the LHSV was decreased from 0.70 h^{-1} to 0.25 h^{-1}. For sulfided catalysts, a low LHSV also helps to prevent incorporation of sulfur into the produced oil [137]. There are, however, cases of a slight negative effect of a lower LHSV due to enhanced cracking and coke formation [201].

3.5.3. Hydrogen Pressure

A high H_2 pressure of 100-300 bar has traditionally been applied in HDO processing of bio-oil (see Table 6). It is generally favorable in order to saturate unstable species, suppress coke formation, and ensure a high solubility of hydrogen in the oil leading to an increased availability of hydrogen at the catalyst surface [188,210]. Nevertheless, many recent studies have been concentrated on the HDO of model compounds at near atmospheric pressure, which allows for a simpler process [185,252,255,256,298,303].

It has been reported how different reactions (i.e. DDO/DCO or HYD) can be controlled through the H_2 pressure [202,286,298], which is in agreement with the thermodynamics. The thermodynamic restrictions (see Figure 10) should always be kept in mind, as the equilibrium will determine which reaction pathways are favorable. Mortensen et al. [20] looked into the hydrogen consumption in the HDO of bio-oil, which was studied by Venderbosch et al. [188] (see Figure 26). The slope of hydrogen consumption increases as a function of the degree of deoxygenation, which can be related to the difference in reactivity and hydrogen consumption of different oil constituents (see section 3.1). For HDO of the least reactive phenolic species, a high hydrogen consumption is required (see

Table 4) as it proceeds through the HYD path, which results in a hydrogen consumption surpassing the stoichiometric demand for oxygen removal at high deoxygenation degrees. The H/C ratio of the produced oil increases when hydrogenation (saturation of double bonds) occurs. As a result, the heating value of the oil increases and it has been reported that the HHV of upgraded oil is proportional to the hydrogen consumption with an increase of 1 MJ/kg for every mol H_2 consumed per kg feed [335].

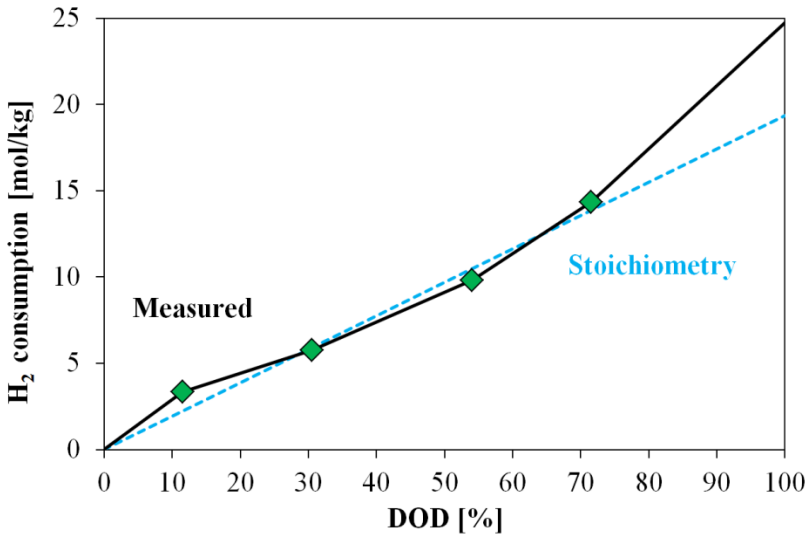

Figure 26 Measured H_2 consumption as a function of degree of deoxygenation for the HDO of forestry residue bio-oil over a Ru/C catalyst operated in a fixed bed reactor at 175-400 °C and 200-250 bar including proposed extrapolation until 100% DOD [188]. *Comparison with stoichiometric requirement re-calculated with 31wt% organic bound oxygen and a H_2:O requirement of 1 (based on [20]). Adapted from [20] (copyright 2011) with permission from Elsevier.*

3.6. Catalyst Deactivation

Catalyst deactivation is a key bottleneck in the development of industrially robust HDO processes. Deactivation generally occurs from exposure to water and due to coking, sintering of the active phase, poisoning by nitrogen, sulfur (except for sulfides) or chlorine species, and metal deposition (especially alkali metals) [137,138,186,188,195,203,336,337]. Catalyst type and operating conditions influence the nature and severity of deactivation, but deactivation from carbon deposition and water is generally dominant in HDO catalysis.

Mortensen et al. [138] studied the influence of sulfur, chlorine, and potassium on a Ni/ZrO_2 catalyst tested for HDO of guaiacol in 1-octanol at 250 °C and 100 bar. The results are shown in Figure 27. Sulfur (added as 1-octanethiol) caused rapid deactivation of the catalyst due to the sulfidation of Ni particles into NiS_x. Both potassium (added as KNO_3 and KCl) and chlorine (added as chloro-octane) deactivated the catalyst. For chlorine, the deactivation was shown to be reversible, as the activity could be regained after removal of chlorine from the feed. With all tested poisons being strong, it was concluded that sources of sulfur and alkali metals must be removed from the feed upstream of any HDO unit operating with reduced Ni based catalysts. Mortensen et al. [137] also found that a $Ni\text{-}MoS_2/ZrO_2$ deactivated in the presence of alkali and chlorine, so it seems these species are general poisons to HDO catalysts. Alkali metals can potentially be removed with the ash rich char formed during pyrolysis (by filtering the pyrolysis vapors before condensation), but the gaseous sulfur compounds are more difficult to remove. Therefore, sulfur tolerant catalysts, mainly sulfides, show promise as they need sulfur in the gas to stay active.

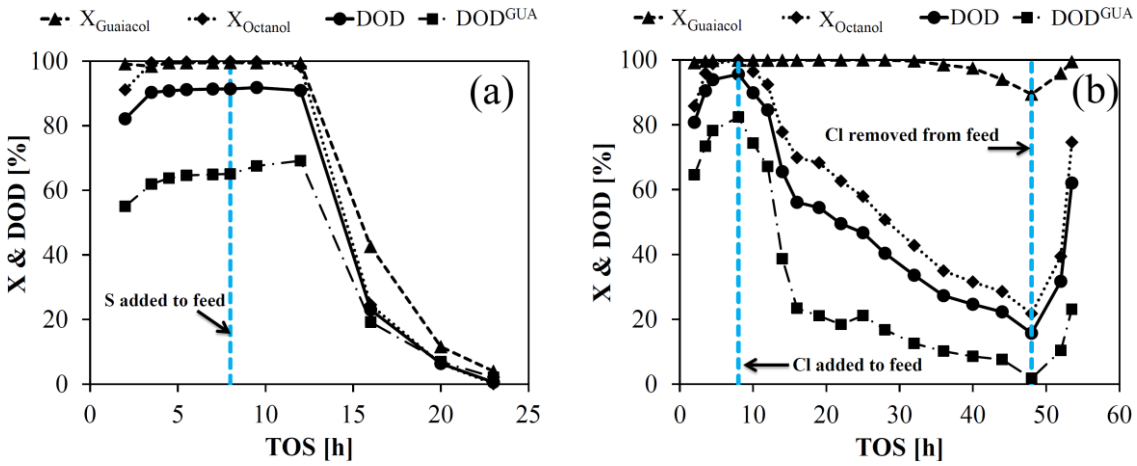

Figure 27 Conversion (X) and DOD of guaiacol (GUA) and 1-octanol over a Ni/ZrO_2 catalyst tested at 250 °C and 100 bar in a fixed bed reactor. The guaiacol in 1-octanol feed was doped with 1-octanethiol (S addition) and chloro-octane (Cl addition) during the run to test deactivation induced by sulfur and chlorine, respectively. Adapted from [138] *with permission from the Royal Society of Chemistry.*

3.6.1. Water

Water is a known catalyst poison to many catalyst systems, where it can either interact with the active phase and inhibit the target reactions or degrade the support material, e.g. by accelerating sintering processes or in the case of γ-Al_2O_3 by conversion into Boehmite (AlOOH) [188,317]. Water formed during pyrolysis of biomass is mixed into the bio-oil, and additional water is formed during the subsequent HDO due to the high concentration of oxygen in the feed. It is therefore important to develop water tolerant catalysts; an important aspect, which is often overlooked in HDO research.

For sulfide catalysts, there is a risk that water may saturate active sites (CUS) through chemisorption, which limits oxygenate adsorption and thereby inhibits HDO. As mentioned in section 3.3.1.1, Badawi et al. [213,242] performed DFT calculations showing that a partial pressure ratio of $H_2S/H_2O > 0.025$ is needed to avoid S-O exchanges at the S-edges of MoS_2, while 100% Co promotion at the S-edge inhibited S-O exchange in the H_2S/H_2O range of 10^{-5}-10^{2} at 350 °C [213]. However, as mentioned by Şenol et al. [243], contradictory conclusions on the effect of water have been presented in the literature. In order to understand the influence of water on HDO, it is important to apply both theoretical and analytical tools (as in [213] and [174]) as well as being able to distinguish between the influence of water from those of other parameters such as operating conditions (e.g. H_2, H_2S, temperature), feed identity and catalyst support.

Looking into the other catalyst classes, phosphides operated at low H_2 pressures are oxidized by water and lose their activity [298]. Carbides have also been reported to deactivate as a function of water induced oxidation [203]. Oxide catalysts may be subject to active site saturation in a similar manner as sulfides with the difference that oxides cannot be treated with H_2S to remove water from the active phase. For MoO_3, it has been indicated that deactivation by water can be mitigated by controlling the ratio of H_2/H_2O [252,253]. However, this ratio must be carefully controlled, as oxides

can only be exposed to a low (near or sub atmospheric) H_2 pressure in order to avoid reduction [254,255].

3.6.2. Carbon Deposition

Carbon formation occurs through polymerization condensation reactions at the catalytic surface. The resulting polyaromatic (potentially also polyaliphatic) species adsorb strongly to the catalyst surface and block active sites and fill up the pore volume, which in turn reduces reaction rates, especially during initial operation [336]. Fonseca et al. [338,339] reported that carbon deposition in a Co-MoS_2/Al_2O_3 catalyst used for hydrotreating of a fossil feed mainly occurred during an initial deposition stage, which led to occupation of about one third of the total pore volume by carbon. The carbon deposition after this initial deposition was limited. A more severe carbon deposition is expected for bio-oil, which has a high polymerization and coking propensity compared to fossil oils.

The reaction rates of carbon formation depend strongly on the feed, but process conditions can be controlled to reduce carbon formation; i.e. by lowering the temperature, increasing the hydrogen pressure, and decreasing the space velocity of the feed bio-oil. Unsaturated hydrocarbons such as aromatics and alkenes have a high affinity for carbon formation as they have a significantly stronger interaction with the catalyst surface compared to saturated analogues [336]. For oxygenates, the propensity of coking is increased for compounds with more than one oxygen atom in its structure [336,340] while carbonyls (i.e. ketones) may polymerize through aldol condensation [341].

Carbon formation increases with increasing catalyst acidity; Lewis acidity is responsible for chemisorbing compounds to the catalyst surface, and Brønsted acidity is responsible for forming polymerization active carbocations through proton donation [336]. For HDO catalysts where the reaction mechanism involves acid sites, coke formation on these sites is critical. Additionally, organic acids (e.g. acetic acid) in the feed can catalyze thermal degradation of bio-oil constituents increasing the affinity for carbon deposition [287].

In terms of mitigating coke formation during HDO, elevated temperatures should be avoided. The rate of dehydration increases at higher temperatures leading to increased carbon formation [336]. Furthermore, H_2 can be used to stabilize reactive coke precursors. For a Co-MoS_2/Al_2O_3 catalyst, H_2 has been shown to effectively decrease carbon formation by saturating adsorbed species such as alkenes [336].

A simple model for the loss of HDS and HDO activity over a Co-MoS_2/Al_2O_3 catalyst due to coking was proposed by Yamamoto et al. [342]:

$$k = k_0(1 - \Theta_c) \quad (19)$$

Here, k is the apparent rate constant during deactivation, k_0 is the rate constant over the fresh catalyst, and Θ_c is the fraction of active sites covered by coke. The model proposes an apparent proportional correlation between the extent of carbon deposition on the catalytic surface and the resulting degree of catalyst deactivation [336].

Weber et al. [341] proposed that coking during processing of bio-oil is dominated by gelation reactions, forming 2-D and 3-D polymers by thermally induced polymerization and aldol condensation as opposed to linear chain growth. Using gelation kinetics, they successfully modeled the increased pressure drop from carbon deposition in a dual bed setup consisting of a sulfided Ru/C catalyst operated at ~180 °C followed by a promoted MoS_2 catalyst operated at ~400 °C [341].

3.6.3. Regeneration and Activity Control

Only a few detailed studies on regeneration of HDO catalysts have been published. However, the need for catalyst regeneration must be assessed in the development of HDO processes. If a catalyst based on cheap and abundant materials is applied, it may simply be replaced when necessary, although too frequent regeneration or replacement may be impractical.

In industrial naphtha-reforming, the commonly applied Pt-Re/Al_2O_3 catalyst deactivates over time due to coke deposition, contamination with impurities from the feed, and loss of chlorine, which is used as a promoter for the acid function of Al_2O_3 [343]. The regeneration process includes coke burn-off followed by an oxo-chlorination step, which re-introduces chlorine into the catalyst structure and re-disperses the metal phase, which sinters during the coke burn-off [343]. A similar regeneration process may be possible for noble metal based HDO catalysts.

In FCC units, continuous regeneration is ensured by letting spent catalyst run through a coke-burnoff unit upon recycling into the reactor. This could be favorable for oxide catalysts [255,256]. Prasomsri et al. [255] investigated for the HDO of various phenolic compounds over a bulk MoO_3 catalyst. The catalyst lost 50% of its activity within the 24 h test, despite the low reactant concentration of 1.5 vol.%, due to a combination of reduction of the oxide phase and carbon deposition, but could be regenerated by oxidation in pure O_2 (atmospheric pressure) for 3 h at 400 °C (see Figure 28). Deactivation rates at such scale may require the reaction to take place in a circulating fluid bed reactor or a moving bed reactor, or to have several parallel reactors in swing operation.

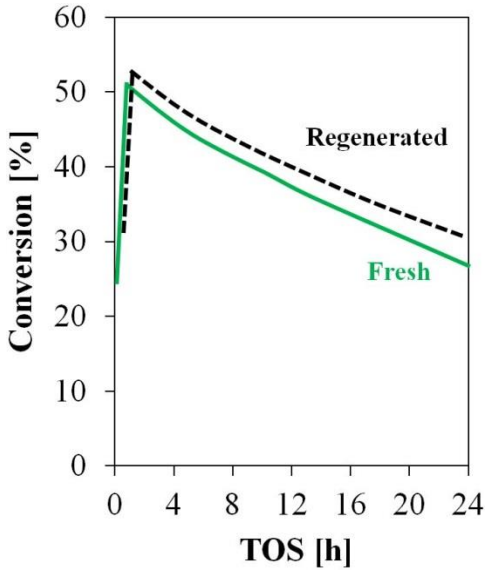

Figure 28 Conversion of m-cresol over bulk MoO_3 in a fixed bed reactor at 320 °C and atmospheric pressure (0.015 bar feed, balance H_2). Regeneration by calcination at 24h. Data from [255].

If coke burn-off is used to regenerate sulfides, a separate sulfidation step is needed to reactivate the active phase, which is oxidized during the coke burn-off. Sulfidation could also be used to regenerate a catalyst deactivated by water, if this is not circumvented by adjustment of the H_2S/H_2O ratio during operation. Badawi et al. [213] exposed a Co-MoS_2/Al_2O_3 sample to water at 350 °C. This decreased the uptake of CO (a measure for sulfide active sites) measured by infrared (IR) spectroscopy at a frequency of 2072 and 2055 cm^{-1} by 28%. It was concluded that the catalyst could be regenerated by resulfidation as the CO uptake on the resulfided sample was similar to that of the initial sample.

Industrial hydrotreating catalysts are regenerated by *ex-situ* combustion to remove coke deposits [344]. Deactivation occurs throughout the entire catalyst lifetime of several years, and thus, the operating conditions are used to control the catalyst activity until regeneration becomes the last option to regain activity. This deactivation occurs in stages, initially mainly by coking and in the end predominantly by pore blockage (see Figure 29a) [336], and the overall activity can be maintained by increasing the temperature. It is important to increase the temperature stepwise according to the deactivation. If the temperature increase is introduced before sufficient deactivation has occurred, it may result in accelerated coking (see Figure 29b) [181].

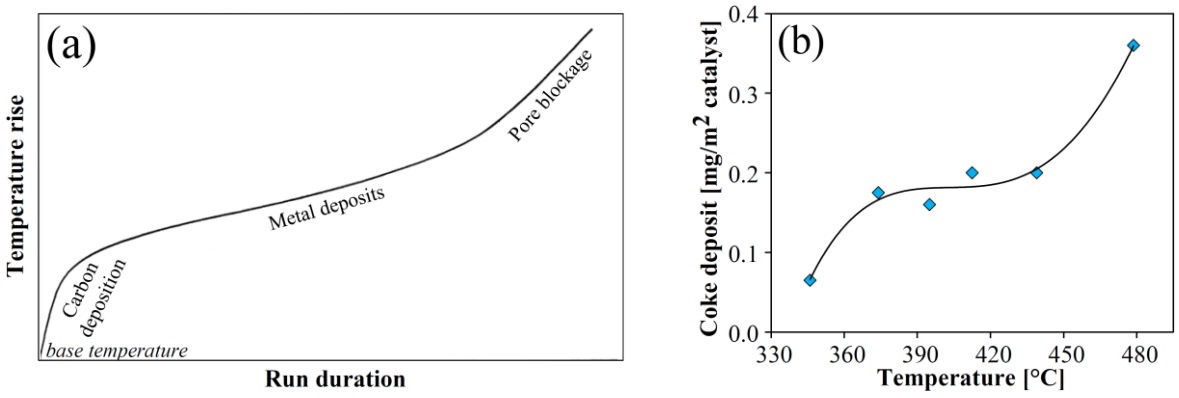

Figure 29 (a) Typical temperature rise in hydrotreater as a function of run time to account for continuous deactivation, based on [336] *(copyright 1999) with permission from Elsevier. (b) Temperature dependent carbon deposition on a Co-MoS_2/Al_2O_3 catalyst used for fossil feed hydrotreating, based on* [181] *(copyright 1979), with permission from Elsevier.*

The stability of sulfides used for HDO of bio-oil is challenged by the large fraction of water present compared to traditional hydrotreating. As described above, adjustment of the H_2S level in the feed gas should be used to keep the catalyst in the active sulfided form, so stable operation can be obtained by increasing the temperature throughout the run. This should be done until catalyst deactivation is so severe that a stable activity cannot be maintained through further temperature increase. At this time, the catalyst should be regenerated or renewed. For bio-oil, this strategy may however have the pitfall that increased temperature can lead to excessive coking of the reactor upstream of where the catalyst is active.

3.7. Kinetic Models

A comprehensive review on kinetic studies on the HDO of both petrochemical and biomass derived model oxygenates was provided by Furimsky [168]. Several more recent studies also provide kinetic models for the HDO of model compounds, but only a few kinetic studies of HDO of bio-oil have been performed. In this case, lumped kinetic expressions have been developed due to the complexity of the feed.

Sheu et al. [201] investigated the HDO of pine wood bio-oil over supported Pt/Al_2O_3-SiO_2, Ni-MoS_2/Al_2O_3, and Co-MoS_2/Al_2O_3 in a fixed bed reactor at ~350-400 °C and 45-105 bar with a WHSV of 0.5-3.0 h^{-1}. The kinetics were evaluated based on the expression:

$$-\frac{dw_O}{dZ} = k \cdot w_O^m \cdot P^n \qquad (20)$$

Here, w_O is gram of oxygen in the hydrotreated oil divided by gram of oxygen in the raw bio-oil, Z (cm) is the axial position in the reactor, k is the rate constant defined by an Arrhenius expression, P (kPa) is the total pressure (mainly H_2), m is the reaction order for oxygen in the hydrotreated bio-oil, and n is the reaction order for the total pressure. Sheu et al. [201] assumed a first order

dependency on oxygen (i.e. m = 1) for all three catalysts. It was possible to fit the pressure dependency and activation energy to the data as summarized in Table 7. With n in the range of 0.3-1.0, increased hydrogen pressure had a positive effect on the rate of deoxygenation as expected. The activation energies were found to be in the range of 45.5 to 71.4 kJ/mol with that for the platinum catalyst being the lowest. The dependency on oxygen mass fractions and axial reactor position limits the model to the specific experimental setup and feed.

Table 7 Parameters from the kinetic expression in equation (20) for different catalysts. Experiments were performed in a fixed bed reactor at ~350-400 °C, 45-105 bar with pine wood bio-oil as feed [201].

Catalyst	***m*** **[-]**	***n*** **[-]**	E_A **[kJ/mol]**
Pt/Al_2O_3-SiO_2	1.0	1.0	45.5±3.2
Co-MoS_2/Al_2O_3	1.0	0.3	71.4±14.6
Ni-MoS_2/Al_2O_3	1.0	0.5	61.7±7.1

A similar kinetic model was presented by Su-Ping et al. [211] who investigated the HDO of bio-oil (feedstock not stated) using a Co-MoS_2/Al_2O_3 catalyst in a batch reactor operated at 360-390 °C. The resulting kinetic expression was:

$$-\frac{dC_O}{dt} = k \cdot C_O^{2.3} \qquad (21)$$

where C_O is the total concentration of oxygen in the oil, k is the reaction rate constant, and t is the time. A dependency on H_2 partial pressure was omitted due to a low dependency observed in the range of 15-30 bar H_2. The oxygenate reaction order of 2.3 is higher than the assumed first order dependency of Sheu et al. [201]. Su-Ping et al. [211] found an activation energy of 91.4 kJ/mol, which is also higher than the values reported by Sheu et al. [201]. Nevertheless, the complexity and diversity of bio-oil feeds as well as differences in reactor setup, choice of catalyst, and process conditions makes it difficult to compare kinetic models across various studies. For the model presented by Su-Ping et al. [211], the high oxygenate reaction order could be explained by a high

initial reaction rate caused by very reactive species. As these react and disappear, a rapid decrease in the rate will be observed.

Massoth et al. [221] developed a Langmuir-Hinshelwood type kinetic model for the HDO of methyl substituted phenols over Co-MoS_2/Al_2O_3 in a fixed bed reactor at 28.5 bar and 300 °C:

$$-\frac{dx}{d\tau} = \frac{k_1 \cdot K_A \cdot x + k_2 \cdot K_A \cdot x}{(1 + C_0 \cdot K_A \cdot x)^2} \quad (22)$$

Here, x denotes mole fraction of phenol, whereas C_0 denotes the feed concentration. K_A (m^3/mol) is the equilibrium constant for the adsorption of phenol onto the catalyst, τ ((kg·h)/m^3) is the space time, and k_1 and k_2 (mol/kg/h) are reaction rate constants for DDO and HYD of phenol, respectively. Nie et al. [277] presented a more complex Langmuir-Hinshelwood kinetic model for the HDO of m-cresol over a Pt/SiO_2 catalyst operated at 300 °C and atmospheric pressure in a fixed bed reactor. Their model took into account the partial pressures of m-cresol, 3-methyl-cyclohexanone, 3-methyl-cyclohexanol, toluene, methylcyclohexane, and 3-methyl-1-cyclohexene. Direct deoxygenation of the arylic C-O bond was considered through a tautomerization/secondary hydrogenation pathway as opposed to hydrogenolysis. Mortensen et al. [265] took a simpler approach for the screening of a broad range of catalysts and their activity in the conversion of phenol in a batch reactor at 275 °C and 100 bar. They used a set of global reaction rate expressions of the type:

$$r_i = k_i' \cdot C_y \quad (23)$$

Here, r_i refers to the rate of hydrogenation of phenol to cyclohexanol (i = 1) and the deoxygenation of cyclohexanol to cyclohexane (i = 2), respectively. k' (mL/kg/min) is the lumped rate constant (assuming constant hydrogen pressure) and C_y represents the concentration of phenol (y = 1) and cyclohexanol (y = 2) in the liquid.

Clearly, working with HDO of model compounds allows for a more detailed investigation of reaction pathways and enables a more comprehensive understanding of the reaction mechanisms and kinetics over different catalysts. Setting up detailed kinetic models for HDO of real bio-oil including all possible reaction pathways is challenging due to the high complexity of the feed, as apparent from the still highly simplified network in Figure 12.

General applications of kinetic models for HDO of model compounds are obviously limited, but they can be used for screening of catalyst activity, by comparing the value of the determined reaction rate constants, as shown by Mortensen et al. [265]. Kinetic expressions developed for the HDO of real bio-oil feeds describe the deoxygenation on an overall level, but are highly dependent on the conditions applied (e.g. feed identity, reactor configuration, and operating conditions). On the other hand, detailed mechanistic expressions developed for model compound HDO are limited to the specific model compound(s) of choice, and expanding this type of model for all bio-oil components is very complex. These compromises on accuracy and applicability of kinetic models are well-known from conventional hydrotreating, where it has been shown that simple and generalized models (similar to equations (20) and (21)) are useful tools in the development and optimization of catalysts and reaction conditions [163].

3.8. Perspectives of HDO as Upgrading Technique for Condensed Bio-oil

Catalytic HDO studies have focused either on upgrading condensed bio-oil or selected model compounds. Studies on HDO of condensed bio-oil involves the complexity of working with real feeds. They enable application at industrially relevant operating conditions and they use a diverse multi-compound feed, which means that the experiments are subject to adverse phenomena such as inhibition and coking, which must also be dealt with at large scale. On the other hand, model compound studies allow for catalyst development at a more fundamental stage. This is necessary in

order to understand and optimize the catalyst formulation and operating conditions, for example via detailed investigations of reaction networks, thermodynamics, kinetics, and catalyst deactivation.

In short, both real feed and model compound studies are needed to develop and optimize industrially relevant processes that combine fast pyrolysis and catalytic HDO, with the latter potentially performed on the pyrolysis vapors before condensation of the oil. Based on the findings presented throughout this section, sulfided catalysts currently seem to provide the most flexible operating window for the HDO of bio-oil. They have a high HDO activity and they are sulfur tolerant, water tolerant (when co-feeding H_2S and using a different support than γ-Al_2O_3), stable against high H_2 pressure (which is necessary to minimize coking), moderately priced, and regenerable. Depending on the exact process, operating conditions, and bio-oil composition targeted, most of the catalyst types reviewed above could be possible HDO candidates, although it seems that especially noble metals struggle with high price, low abundance, and risk of deactivation by bio-oil contaminants.

In section 2.4 it was concluded that bio-oil cannot be used as an engine fuel, partly because of its instability. This issue also limits the potential for single stage HDO as a feasible upgrading technique for condensed bio-oil. The reactive oxygenates, which originate from cellulose and hemicellulose [166,168,183,187], cause severe coking and polymerization resulting in fixed bed reactor plugging and catalyst deactivation [188], which strongly challenges the development of a continuous process. While it seems that multiple stage HDO could overcome these issues, it is advised to assess the stability of the feed oil during storage and mild heating. This should be done in order to ensure that feeding and heating of the oil to the first stage is possible, even for long times of continuous operation, which may require that the operating temperature is increased upon catalyst deactivation as discussed in section 3.6.3. If instead HDO is performed in vapor phase, prior to condensation of the produced oil, reactive intermediates can be hydrogenated and stabilized immediately when formed. Processes combining fast pyrolysis and HDO are reviewed in section 4.

4. Combined Biomass Fast Pyrolysis and Catalytic Product Upgrading

As reviewed by Resende [345], it has been considered to perform combined fast pyrolysis and catalytic upgrading as a method for obtaining a stabilized, higher quality bio-oil, either with a catalyst in the pyrolysis reactor and/or with a downstream reactor for upgrading pyrolysis vapors before oil condensation. An overview of the possible reactor configurations is given in Figure 30. The background for this is the adverse properties of fast pyrolysis bio-oil and the difficulties in upgrading by subsequent HDO as outlined in the preceding sections. Catalytic fast pyrolysis is typically performed in fluid bed reactors, where the bed material acts as both heat transfer material and catalyst. Reactors for downstream vapor upgrading are typically fixed bed reactors.

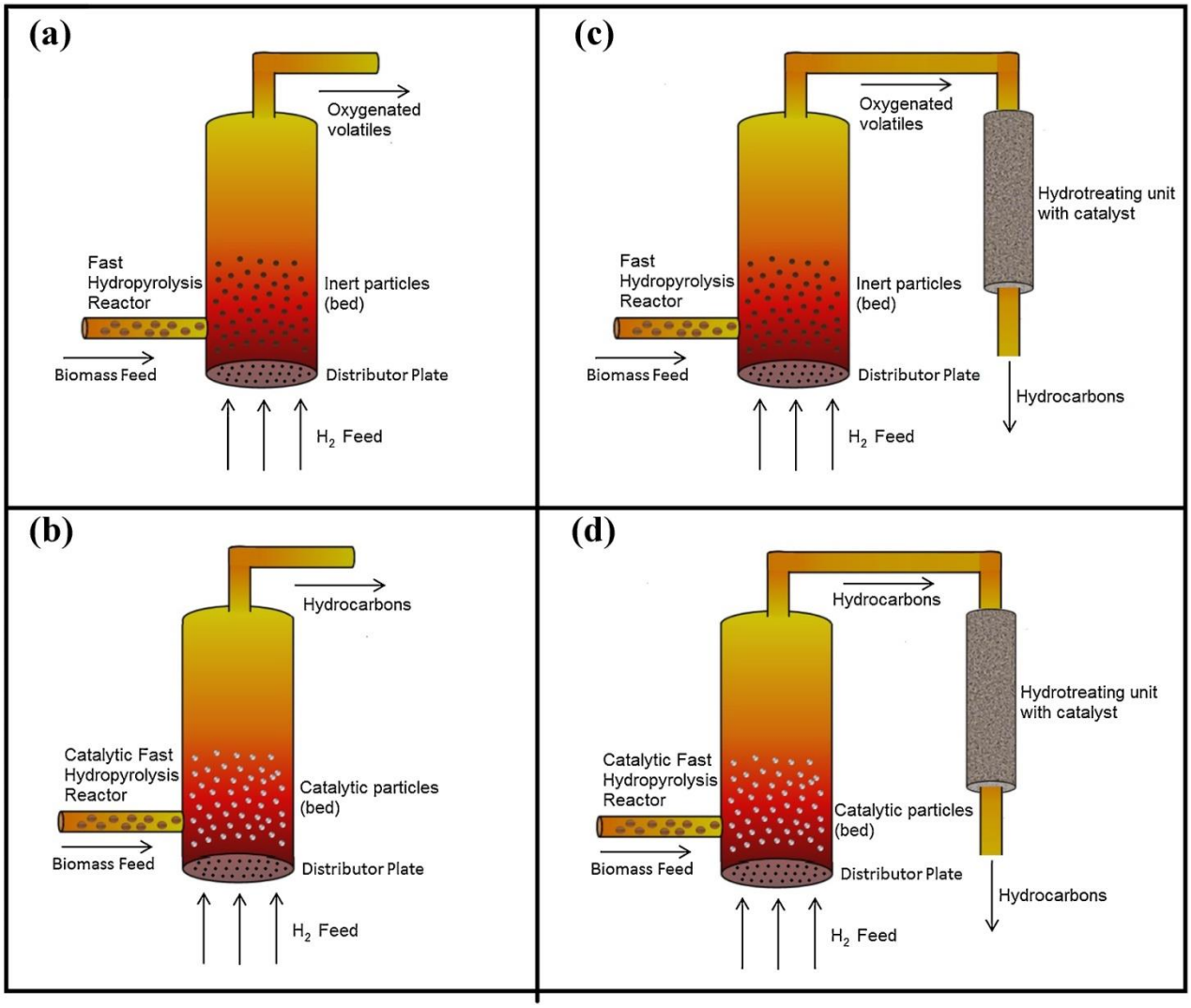

Figure 30 Overview of different reactor configurations for continuous production of bio-oil via fast pyrolysis in a fluid bed reactor: (a) Fast hydropyrolysis, (b) Catalytic fast hydropyrolysis, (c) Fast hydropyrolysis and downstream catalytic HDO (fixed bed) on pyrolysis vapors, (d) Catalytic fast hydropyrolysis and downstream catalytic HDO (fixed bed) on pyrolysis vapors. Reprinted from [345] *(copyright 2016) with permission from Elsevier.*

Catalytic fast pyrolysis at atmospheric pressure and without hydrogen addition has been intensively investigated using zeolite catalysts for cracking the bio-oil to achieve lower oxygen content (around 24wt%) and higher aromatic content compared to standard fast pyrolysis [47]. Such a bio-oil is easier to upgrade by HDO. However, as discussed by Venderbosch [47], the product of catalytic fast pyrolysis is either a low yield of bio-oil and high yield of char, with low energy recovery in the oil, or a bio-oil resembling non-catalytic fast pyrolysis bio-oil.

Another method, which is aimed at achieving both deoxygenation and fast pyrolysis in one step, is fast hydropyrolysis, in which the gas is changed from an inert to H_2 or partial H_2 (scenario a in Figure 30). If an HDO catalyst is present in the reactor it is called catalytic fast hydropyrolysis (scenario b in Figure 30). Catalytic fast hydropyrolysis is often performed at elevated pressure to increase the driving force for HDO. This approach has been more successful in achieving both high energy recovery and bio-oil with low oxygen content [47]. Both non-catalytic and catalytic fast hydropyrolysis can be coupled with downstream HDO, performed in a fixed bed reactor, for vapor phase product upgrading (scenario c and d in Figure 30).

The different concepts in Figure 30 each have their advantages and disadvantages. An advantage of not having a catalyst in the pyrolysis reactor (scenario a and c) is that the optimal temperature of ~500 °C for fast pyrolysis (see Figure 4) can be applied without having to also consider what might be optimal for the catalytic HDO reactions. Note, however, that without the HDO catalyst, the H_2 used in fast hydropyrolysis typically does not enable significant HDO [346–349]. Therefore, the advantage of *in-situ* HDO is not obtained here, and it becomes crucial to have a short residence time before the downstream HDO reactor to avoid secondary reactions such as polymerization [105]. For concepts with a catalyst in the fluid bed (scenario b and d), the choice of catalyst becomes crucial; a too reactive catalyst may crack all species to light gases, and no oil phase is formed. This was observed by Dayton et al. [350] using a commercial hydrotreating catalyst (pre-reduced). Initially, mostly gaseous products were obtained, but due to catalyst deactivation a liquid product was obtained after ~20 hours on stream.

4.1. Lab-scale Tests

Milligram scale pyrolysis-GC setups allow for fast pyrolysis of biomass and immediate product analysis [125,351–356]. Catalytic fast hydropyrolysis is achieved by mixing the biomass with a catalyst and applying a flow of H_2.

Investigations by Melligan et al. [351,352] using a pyrolysis-GC setup (the CDS Analytical Pyroprobe) have shown different bio-oil product distributions between non-catalytic fast pyrolysis using He and H_2 [351,352], particularly an increase in alkanes and oxygen free aromatics was observed with increasing H_2 pressure [352]. The oxygen content in the product was further decreased by adding a downstream HDO reactor using a Ni based catalyst [351,352].

Using a similar Pyrolysis-GC setup, Gamliel et al. [353,354] found that catalytic fast hydropyrolysis at 31 bar and 600 °C using M-ZSM-5 (M = Ni, Pd, Ru) as catalysts most resulted in increased CH_4 (M = Ni and Ru) or CO (M = Pd) yields, and decreased char and aromatics yield compared to H-ZSM-5. Marchand et al. [355] found that Pd-ZSM-5 increased the aromatics yield compared to H-ZSM-5 in catalytic fast hydropyrolysis of lignin at 17 bar and 650 °C. However, they used larger catalyst to biomass ratios compared to Gamliel et al. (20/1 and 10/1 in ref. [355] vs. 5/1 in refs. [353,354]). Performing non-catalytic fast hydropyrolysis at 650 °C and employing a downstream HDO reactor loaded with the Pd-ZSM-5 and operated at 300 or 400 °C increased the yield of cycloalkanes due to the hydrogenation of aromatics.

Fast pyrolysis investigations by Thangalazhy-Gopakumar et al. [356] showed minor differences between He and H_2 atmospheres, also for catalytic fast pyrolysis, however the H-ZSM-5 catalyst employed had no hydrogenation activity. Using H-ZSM-5 impregnated with Co, Ni, Mo, or Pt as catalysts for catalytic fast hydropyrolysis of pinewood at 27.6 bar improved the hydrocarbon yield compared to using the H-ZSM-5 catalyst [125]. This was attributed to the hydrogenation activity of the metal impregnated catalysts.

4.2 Pilot Scale Fluid Bed and Cyclone Reactors

Fast pyrolysis of rice husks in a fluid bed reactor using sand as the bed material reported by Meesuk et al. [346–348] showed that changing the atmosphere from N_2 to H_2 only had a minor influence on bio-oil oxygen content and heating value. However, in combination with an active catalyst (i.e.

performed as catalytic fast hydropyrolysis) the oxygen content was significantly reduced and the heating value was increased. Fluid bed fast pyrolysis of biomass in N_2, CO_2, CO, CH_4 and H_2 at atmospheric pressure reported by Zhang et al. [349] showed only minor product differences as function of gas atmosphere.

Pilot scale studies of fluid bed fast hydropyrolysis of loblolly pine performed by Dayton et al. [350] showed almost no deoxygenation at 400 °C when using inert SiC as the bed material and a low partial pressure of H_2 (0.5-3.0 bar). The oil product of fast hydropyrolysis contained 35-39wt% oxygen compared to 38-40wt% oxygen after fast pyrolysis in N_2. When changing the bed material from inert SiC to a pre-reduced commercial hydrotreating catalyst, a high degree of deoxygenation was achieved at 375 °C and 3.0 bar H_2 (4.2wt% oxygen in the oil compared to 43.5wt% in the feed). However, the oil yield was only about 10wt% after ~20 h on stream. The catalyst formulation was not published, but the oil yield improved as the catalyst deactivated with a stable oxygen content in the produced oil of 2 to 5wt% [350]. The same group later performed catalytic fast hydropyrolysis of loblolly pine in a smaller fluid bed reactor using a NiMo hydrotreating catalyst at 375 to 475 °C and 20.7 bar of 20-40% H_2 [357]. The catalyst was activated by reduction rather than sulfidation, and the state of the catalyst was not investigated, but it is likely to be Ni metal on MoO_x/Al_2O_3, where x = 2 to 3. The carbon efficiency was 36 to 42% while the organic liquid yield was around 23wt% (including C_{4+} gasses). The typical oxygen content in the organic liquid was 3 to 5wt%, indicating high yields and good oxygen removal efficiency. The time on stream was 90 min for these experiments.

A process referred to as H_2Bioil (see Figure 31) involving fast hydropyrolysis at elevated pressure and downstream HDO of pyrolysis vapors was published by Agrawal and Singh et al. [358–360]. The process combines fast hydropyrolysis with vapor upgrading to produce a bio-oil compatible with the current transportation fuel infrastructure. The pyrolysis gas may be recycled to the pyrolysis

reactor or utilized in a gas turbine and the char is combusted or gasified to provide heat and/or H_2 for the process [358,359]. In another process, it was suggested that the pyrolysis gas may be steam reformed to produce H_2 for the process [361]. Additional H_2 for the process may be obtained from electrolysis of water or biomass/coal gasification [358,359]. An economic analysis based on estimated yields indicated that the process compared very favorably to second generation bio-ethanol production and biomass gasification combined with Fisher-Tropsch fuel synthesis [359,360].

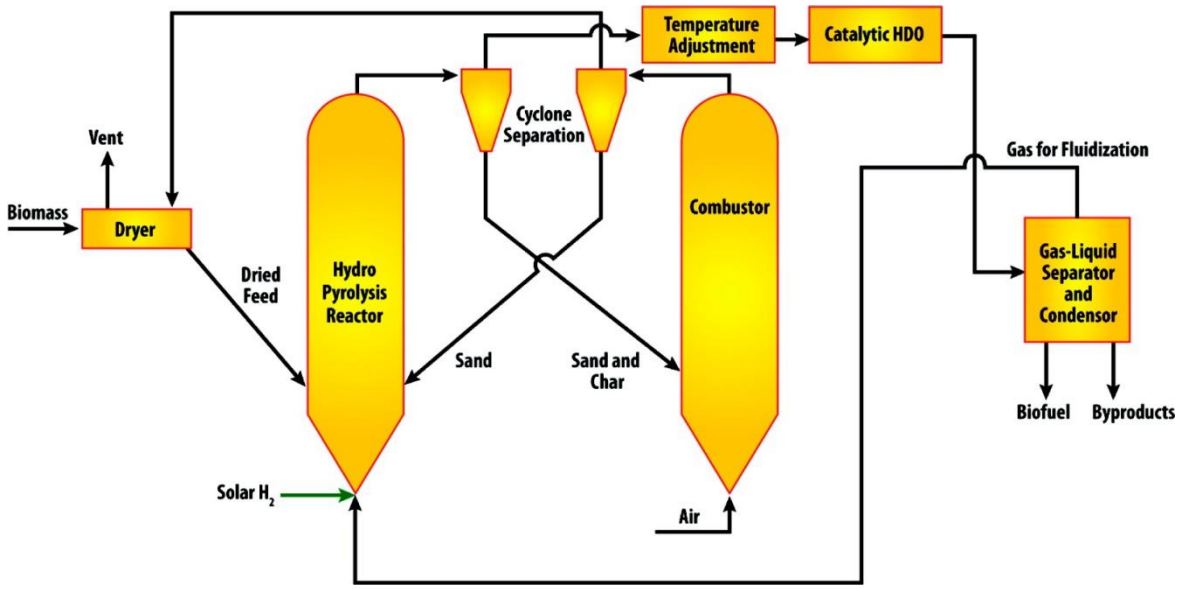

Figure 31 Proposed process diagram for the H_2Bioil concept: fast hydropyrolysis and downstream catalytic HDO (scenario c in Figure 30). Reprinted with permission from [359] *(copyright 2010, American Chemical Society).*

The H_2Bioil concept was partly verified by an experimental investigation using pure cellulose as biomass, an inverted cyclone fast hydropyrolysis reactor operated at 550 °C and a fixed bed HDO reactor with Al_2O_3, Pt/Al_2O_3, or Ru/Al_2O_3 as catalysts operated at 375 °C with 9 bar H_2 partial pressure and 27 bar total pressure [362]. The degree of deoxygenation obtained in those experiments was only 14-27%. In a follow-up study the HDO catalyst was improved by using Pt–Mo supported on multiwalled carbon nanotubes. The residence time in the HDO reactor was more than doubled

and the conditions adjusted to 480 °C in the pyrolysis reactor, 300 °C in the HDO reactor and 25 bar H_2 pressure, resulting in close to 100% deoxygenation using both cellulose and poplar wood as biomass [361]. No liquid oil was recovered, only an aqueous phase, so the bio-oil composition and yield was only based on GC analysis of the gas phase.

A similar concept called IH^2® (see Figure 32) was developed by the Gas Technology Institute (GTI) [363,364]. This process consists of a fluid bed catalytic fast hydropyrolysis reactor at moderate pressure (20-25 bar) and temperature (335-470 °C) and downstream HDO (345-400 °C) in a fixed bed reactor (i.e. configuration d in Figure 30) using unpublished, proprietary catalysts. The bio-oil can be integrated in the current infrastructure and the gas should be steam reformed to produce H_2 for the process [21]. A proof of principle experimental investigation of the hydropyrolysis and HDO steps of the process showed that fast hydropyrolysis was possible with several different types of biomass feedstock with a time on stream of 2-3 h [363]. Typical oxygen contents in the bio-oil were <0.5wt%, and with 26 to 30wt% bio-oil yield the energy recovery in the oil relative to the biomass feed was approximately 65%. Operation without the downstream HDO reactor resulted in 0.5-2.5wt% oxygen in the bio-oil; an oil which is likely to be stable enough and miscible with petroleum for co-feeding in a refinery hydrotreater.

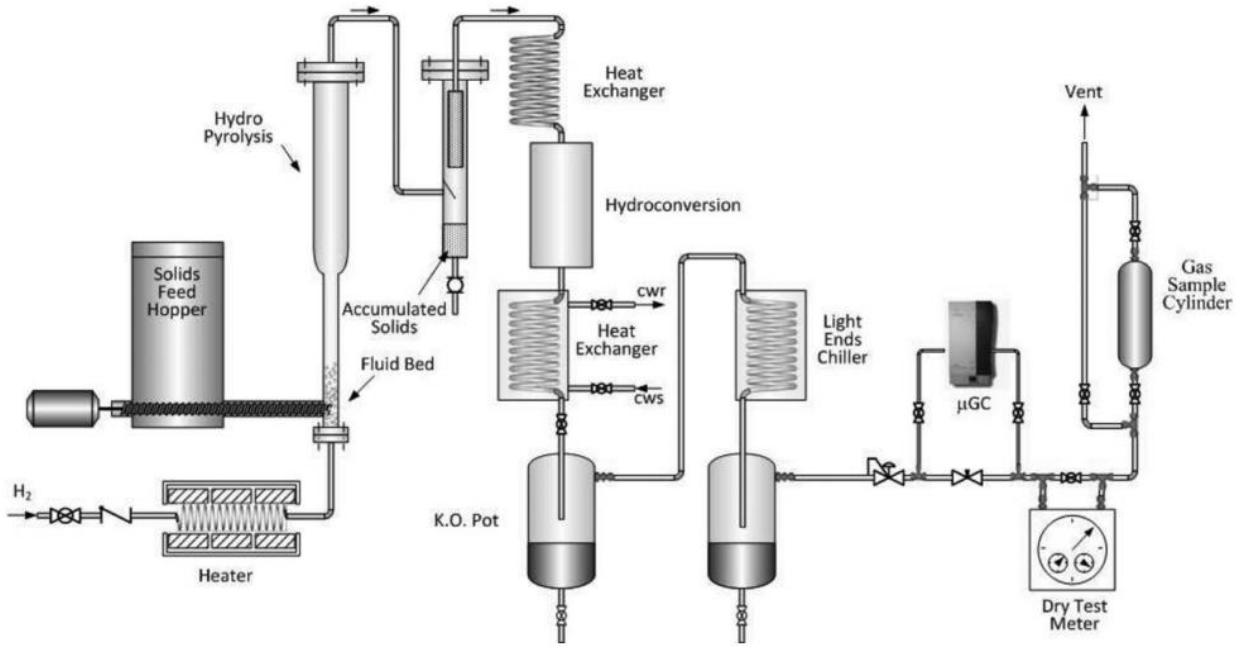

Figure 32 Process diagram for the IH²® process: catalytic fast hydropyrolysis and downstream catalytic HDO (scenario d in Figure 30). Reprinted from [363] *with permission (copyright 2011, American Institute of Chemical Engineers).*

The lab-scale process was scaled up to a 50 kg/day pilot facility where the same oil yield and oxygen contents were achieved over 750 h continuous operation using maple and pine wood [364]. Also, a life cycle assessment (LCA) and a techno-economic analysis of an industrial size process was published [365,366] showing 90 to 96% GHG savings of IH²® bio-fuels from bagasse, forest residue or corn stover compared to fossil fuels and an minimum fuel selling price of 1.64 US$/gal (2007 values, excluding taxes, distribution, blending, and marketing), which is favorable compared to other biomass to fuel processes. This compares well with US gasoline prices, which in 2011 were 2.8-3.3 US$/gal and in 2016 were 1.4-2.1 US$/gal (range covers several grades, excluding taxes) [367]. With the fluctuating oil prices [4,7] and reported uncertainties in the LCA [365,366], the resulting bio-fuel price indicates a promising potential, but should otherwise be used with caution.

Recently Zhang et al. [368] at Philips 66 performed fast hydropyrolysis of red oak wood in a fluid bed reactor with inert sand as the bed material followed by vapor phase HDO in a second fluid bed

reactor using a proprietary hydrotreating catalyst. Using 19 bar hydrogen pressure, a pyrolysis temperature of 425 °C and an HDO temperature of 350-425 °C, they could adjust the oxygen content in the bio-oil to between 17 and 2wt%. Below 6wt% oxygen in the bio-oil, the most reactive oxygenates were removed. The TAN along with the storage and thermal stability were similar to fossil diesel and better than soybean oil used for bio-diesel, indicating that these bio-oil products could blend into refinery streams. The carbon atom yield for the low oxygen bio-oils was 35 to 44%, which is similar to the results achieved with pressurized catalytic fast hydropyrolysis by Marker et al. [363,364] and Dayton et al. [357]. In a follow up NMR study of their bio-oils they showed that alkylation and/or transalkylation reactions on aromatic compounds took place in the HDO reactor with increasing significance at higher temperatures (particularly at 425 °C) where the degree of deoxygenation increases [369].

Similar results have also been obtained by the authors of this review, as we have recently performed catalytic fast hydropyrolysis of beech wood in a fluid bed reactor containing a sulfided $CoMo/MgAl_2O_4$ catalyst with and without a downstream fixed bed reactor containing a sulfided $NiMo/Al_2O_3$ catalyst [370]. At varying pressures of 16-36 bar and temperatures of 365-510 °C, the yield of condensed and condensable C_{4+} organics was 17-22wt% daf. The oil was essentially oxygen free when applying both reactors and the energy recovery in this oil product was 40-53%. Extensive oil characterization was performed showing that most hydrocarbons were naphthenes and aromatics, with minor amounts of paraffins, in the gasoline and diesel boiling point range. When using only the fluid bed reactor the oxygen content was 1.8wt%. Interestingly, the downstream fixed bed reactor both increased the carbon yield and decreased the oxygen content, indicating that alkylation reactions with olefins on aromatic compounds occurred over the $NiMo/Al_2O_3$ HDO catalyst, as also reported by the group at Philips 66 [369].

4.3. Perspectives of Fast Pyrolysis with *Ex-situ* and *In-situ* Hydrodeoxygenation

Overall, it appears that to realize biomass to hydrocarbon fuels using a fast pyrolysis based process, fast hydropyrolysis at elevated pressure using a high partial pressure of H_2 is a possible method. Most likely, it is advantageous if the pyrolysis step is catalytic, and downstream vapor HDO will be necessary to achieve a product with low oxygen content. Alternatively, oil condensed after catalytic fast hydropyrolysis may be co-processed in a refinery hydrotreater. There are a number of technical challenges to overcome in the scale-up e.g. feeding solid biomass to a pressurized fluid bed reactor. The catalyst formulation is highly important and questions about poisoning and mechanical degradation in the fluid bed as well as possible regeneration have yet to be answered.

Fast pyrolysis of lignocellulosic biomass produces oil with an increased volumetric heating value compared to its parent biomass (see section 2). In fact, the bulk energy density can be increased by a factor of >6 through fast pyrolysis [153,371]. There is however limited direct application for this bio-oil due to the high content of oxygen which is responsible for a wide range of detrimental properties. Upgrading of this bio-oil is necessary through catalytic HDO carried out at conditions similar to conventional hydrotreating or even at lower temperatures and pressures. As reviewed in section 3, several studies on catalytic HDO show promising results for this technique. However, as the vast amount of research studies have shown (see section 3 and 4), it seems advantageous to couple fast pyrolysis and HDO into catalytic fast hydropyrolysis in order to develop a technology which can continuously convert solid biomass into liquid fuel. Coke formation could be minimized by maintaining a high hydrogen pressure during catalytic fast hydropyrolysis. If instead HDO is performed on condensed oil in a separate step, coke formation should be limited by multiple stage processing (see section 3.5.1). Here, the reactive cellulose and hemicellulose derived oxygenates are hydrogenated in the first part of the HDO reactor at low temperature (from below 80 °C to 180 °C), and the final part of the HDO reactor cracks and deoxygenates the refractory lignin derived

oxygenates at high temperatures (>300 °C) [183]. A decrease in temperature in the outlet part of HDO reactor could be employed, if hydrogenation of aromatics is desired (according to the thermodynamic constraint). Regarding the more traditional one stage HDO with a single reactor operated at 250-400 °C (see Table 6), coking during heating of the oil will be so severe that catalyst deactivation, low energy recovery of the oil, and plugging make the process infeasible.

It has been proposed that fast pyrolysis of biomass into bio-oil can be implemented at delocalized sites to increase the energy density and make transportation economically feasible [20,371]. Mortensen et al. [20] presented a flow sheet for this process based on the work of Jones et al. [372] (see Figure 33) where raw bio-oil is produced at delocalized sites and subsequent upgrading is performed at a centralized plant. Here, HDO is used to upgrade the oil with a downstream recovery section similar to that applied in hydrotreating processes [158,163].

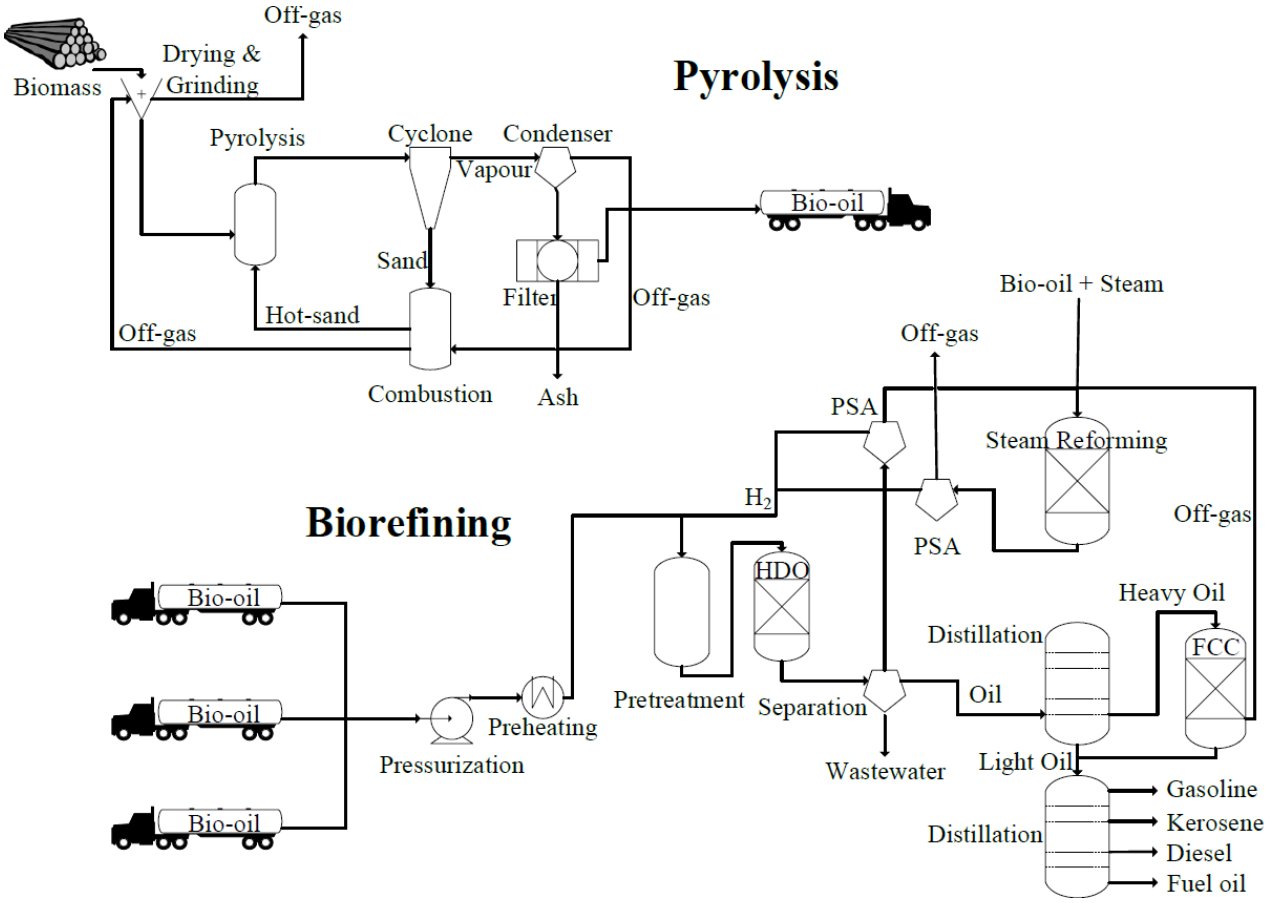

Figure 33 Overall flow sheet for a proposed production of bio-fuels on the basis of catalytic upgrading of bio-oil. PSA = pressure swing adsorption. Reprinted from [20] (copyright 2011) with permission from Elsevier.

Even with a seemingly promising process economy [372], implementation of delocalized pyrolysis plants is challenged by the instability of bio-oil, which cannot be reheated as required for subsequent HDO without severe coking and polymerization. This hurdle can potentially be overcome either by applying multiple stage HDO to achieve bio-oil stabilization during heat-up, or by performing the pyrolysis as catalytic fast hydropyrolysis. Catalytic fast hydropyrolysis could either be performed at delocalized or more centralized plants, since transportation of wood pellets across country boarders (and even continents) for combustion in combined heat and power plants is already feasible [152]. The produced bio-oil will most likely need further upgrading to achieve a fuel grade oil,

which could be realized at existing oil refineries by co-processing with fossil feeds. This would eliminate the need for construction and commissioning of new plants.

Centralized plants are more favorable in terms of the H_2 requirement, which is significant for both catalytic fast hydropyrolysis and catalytic HDO, and it is clear that the hydrogen consumption should be addressed in the development of a commercially attractive process. One option is to reform the light gasses produced in the fast hydropyrolysis (C_{1-3} hydrocarbons) into CO_2 and H_2 which can then be fed to the pyrolysis reactor. Additional H_2 could potentially be produced sustainably from electrolysis of water using electricity from wind and solar power. H_2 could potentially also be produced from the gasification of char. Another utilization strategy for the light gasses could be conversion into synthetic natural gas (SNG) by methanation.

Techno-economic analyses or LCAs can be used to evaluate whether a process is economically viable and allows for comparison of different processes. Such analyses have been performed for various fast pyrolysis and catalytic upgrading processes, for example stating that transportation of solid biomass is viable within a radius of <170 km [153]. As these analyses are based on a complex network of data and assumptions (i.e. agricultural yields, energy prices, process efficiencies, and yields), it is recommended to interpret the results with caution, especially if an uncertainty and sensitivity analysis is left out.

It must be considered what type of product the combined fast pyrolysis and bio-oil upgrading should produce. Table 8 gives an overview of the oil properties achieved by different methods. Even though HDO of condensed bio-oil produces an oil with a low oxygen content and high energy content, the instability of condensed bio-oil is a critical drawback. Instead, catalytic fast hydropyrolysis produces an oil similar to the HDO oil [363] but with the possibility to operate the process continuously for several hundred hours [373]. If the catalytic fast hydropyrolysis is coupled with downstream HDO,

the produced oil is further upgraded; the oxygen content is markedly decreased while the contents of carbon and hydrogen are increased. An important parameter, which is missing in Table 8, is the carbon based yield of the produced oil relative to the dry, solid biomass feed. As mentioned in section 3.2, the carbon based yield or data, which can be used to calculate this, is most often not reported in bio-oil upgrading studies. This makes it difficult to assess the overall process efficiency, and it is strongly recommended to include the carbon recovery in the produced oil in all future studies.

Table 8 Comparison of bio-oil properties from fast pyrolysis of wood and HDO of condensed fast pyrolysis oil with oils obtained from catalytic fast hydropyrolysis.

Property		**Fast pyrolysis oil**	**HDO oil**	**Catalytic fast hydropyrolysis oil**	
			(from condensed bio-oil)	**no HDO**	**downstream HDO**
Scenario (Figure 30)		-	-	b	d
Refs.		[22–24,115,119]	[188,196,200,206]	[363,370]	[363,370]
Carbon	[wt%]	44-58	76-87	77-90	85-89
Hydrogen	[wt%]	5.5-7.2	9.7-13	9.6-12	11-13
Nitrogen	[wt%]	0-0.2	<0.6	0.04-0.1	0.04-0.06
Oxygen	[wt%]	35-50	0.02-14.2	0.5-14	0.0-2.2
Sulfur	[wt ppm]	<400	<700	300-3,000	100-7,000
Viscosity (40-50 °C)	[cSt]	13-100	1	-	-
Density (15-40 °C)	[kg/L]	1.1-1.3	0.83-0.93	0.82-1.0	0.78-0.86
HHV	[MJ/kg]	16-21	41-46	-	-
H/C	[molar]	1.3-1.9	1.48-1.82	1.36-1.81	1.47-1.76
O/C	[molar]	0.4-0.8	<0.12	<0.14	<0.02

In catalytic fast hydropyrolysis, biomass particles are in direct contact with the catalyst, which also acts as heat carrier. There is a risk that this enables a detrimental transfer of poisons such as alkali metals from the biomass or char particles to the surface of the catalyst [48]. It is therefore crucial to investigate this potential (and likely) deactivation, ideally as a function of time or at least the composition of fresh and spent catalysts should be analyzed to assess the severity of any deposition of catalyst poisons. If fast pyrolysis is applied instead, hot vapor filtering can be used to remove

contaminants upstream of the HDO upgrading, but a negative influence on the oil yield has been reported in this configuration [331].

The boiling point of oxygenates is higher than for fuel type hydrocarbons with equivalent carbon numbers [157]. Thus, the oxygen content should preferentially be tuned to fit the target product, which could be a range of boiling point fractions. Fuel compositions are complex [374], and it is necessary to look at the specifications for the target fuel as well as what can be achieved from the biomass and process of choice. A common goal in the literature is to go all the way from solid biomass to a high-quality liquid fuel – preferably in one step. Complete deoxygenation of bio-oil is, however, often only achieved using severe operating conditions (see e.g. Figure 22 and Table 6), which limit the oil yield. Furthermore, as discussed above, re-heating of condensed bio-oil can cause severe process issues due to coking, polymerization, and reactor plugging. Therefore, catalytic fast hydropyrolysis seems promising as reactive oxygenates can be stabilized *in-situ* when formed. It may be of interest to target a less deoxygenated product to be used as a fuel additive (similar to ethanol or methanol) or to be co-processed in already functioning hydrotreating plants.

The investigation of coupled fast pyrolysis and catalytic HDO, such as catalytic fast hydropyrolysis, is still at an early stage and the technology needs to mature before more concrete considerations, for example based on LCAs, can be made regarding the process economy and sustainability, and application of the product oil. Furthermore, the requirements for (fluid bed) hydropyrolysis catalysts differ from those of commonly applied HDO catalysts. Firstly, they must have a high mechanical strength in order to ensure attrition resistance during fluidization. Secondly, a moderate or even low activity could be preferential in order to avoid extensive cracking or potential generation of hot spots (in fixed bed reactors). Thirdly, they must be tolerant against contaminants present in the feed. If fast pyrolysis is instead performed without a catalyst, this first stage is simplified, but the carrier gas

would most likely still be hydrogen, which is needed for downstream HDO. The catalysts and temperatures selected for downstream HDO must furthermore be carefully selected to avoid polymerization and coking related issues.

5. Conclusions and Outlook

The global society is facing challenges with global warming, depleting fossil resources, an increasing population, and a corresponding increase in energy demand. Our lifestyle depends on energy and there is a need for sustainable carbon based fuels. Lignocellulosic biomass such as wood, energy crops, straw, and agricultural waste is a renewable carbon based material that does not compete directly with food; note, however, that considerations on usage of agricultural land must be included. Fast pyrolysis is a simple and efficient way to convert solid biomass into a liquid with an increased volumetric energy density. The significant oxygen content (35-50wt% compared to <0.1wt% in heavy fuel oil) results in a heating value less than half that of conventional fossil fuels. Furthermore, as much of the oxygen is present as carboxylic acids, ketones, and aldehydes, bio-oil is acidic and unstable upon storage and heating.

Catalytic HDO is a promising technique for upgrading bio-oil, and much research has been devoted to developing and understanding catalyst systems as well as reaction and deactivation mechanisms. Particularly deactivation is a major issue in HDO, where coke deposition and exposure to high water concentrations pose a severe problem for many catalysts and influence both catalytic activity and selectivity. Due to the thermal instability of bio-oil, catalytic fast hydropyrolysis with immediate product stabilization seems an alternative, promising approach compared to sequential non-catalytic fast pyrolysis and single stage HDO of the condensed oil. Catalytic fast hydropyrolysis can be coupled with downstream HDO of the pyrolysis vapor for further product upgrade, prior to condensation of the produced oil. Another option is to couple non-catalytic fast pyrolysis with

downstream HDO of the pyrolysis vapor. However, for all three options (catalytic fast hydropyrolysis with and without downstream HDO, and fast pyrolysis with downstream HDO), several tasks remain, such as:

- Catalyst development for both (fluid bed) catalytic fast hydropyrolysis and downstream fixed bed HDO to optimize liquid yields: Investigation and optimization of known formulations as well as novel catalyst materials in combination with advanced experimental and theoretical tools such as DFT, TEM, STM, XAS, and tomographic techniques. Catalysts operated in fluid bed hydropyrolysis reactors and fixed bed HDO reactors must meet different specifications. In a fluid bed, the catalyst must be mechanically strong to avoid attrition and entrainment. Also, the catalyst should not be too active at 400-600 °C, which is the temperature range for maximum oil yields, since this would lead to an undesired loss of carbon from the biomass to cracking products such as CO, CO_2, CH_4, and C_{2-4} hydrocarbons. Finally, the coke formation on the catalyst surface should be minimized to limit the need for catalyst replenishment in the fluid bed during operation. In a down-stream fixed bed, there is greater flexibility in the choice of catalyst and operating conditions, since it is decoupled from the pyrolysis, and these choices should be based on the pyrolysis gas composition and the target oil composition.
- Better understanding of the kinetics of HDO occurring during catalytic fast hydropyrolysis including influence of impurities (e.g. alkali metals) on secondary reactions (e.g. cracking), which affect the selectivity towards HDO. Model compound studies using multi compound feeds should be employed in order to investigate how the HDO kinetics of various oxygenates are influenced by the presence of other compounds (e.g. through competitive adsorption). Developing a better generic understanding of the influence of the biomass and

pyrolysis vapor composition on the HDO kinetics and selectivity should support the realistic scenario that a biomass to bio-oil unit should be able to run efficiently with different feeds.

- Comprehensive investigation of catalyst deactivation (such as attrition, coking, phase change) and poisoning by elements abundant in biomass (such as alkali metals, chlorine, nitrogen, water, and sulfur) for different catalyst types in order to optimize catalyst performance. Catalyst deactivation should be mitigated and/or efficient regeneration methods should be developed.
- Investigation of catalytic fast hydropyrolysis of solid biomass directed at minimizing coke formation and cracking, and stabilizing reactive oxygenates. The influence of varying operating conditions for catalytic fast hydropyrolysis (temperature, H_2 partial pressure, space velocity, gas flows, etc.) should be investigated to optimize oil yield, deoxygenation, and energy yield in the produced oil.
- Development of new processes and reactor configurations for continuous processes including: fast pyrolysis with downstream HDO, catalytic fast hydropyrolysis, and catalytic fast hydropyrolysis with downstream catalytic HDO. This development should cover feeding of solid biomass into a pressurized reactor, catalyst regeneration and/or replacement, and integrated utilization of by-products (such as char, light gasses, product water, system heat). Long-term tests should eventually be performed to test the stability and robustness of the process.
- Assessment of target product(s). The operating conditions and catalyst type(s) should aim at the desired product composition (e.g. oxygen content in produced bio-oil) and yields (gas vs. bio-oil). The product could e.g. be a moderately oxygenated fuel additive or refinery blend-in, or an oxygen free ready-to-use fuel. A very important parameter to keep in mind

when studying and comparing the efficiency of these processes, is the carbon yield and energy yield in the produced oil compared to the feed biomass.

With all the work already performed on fast pyrolysis of biomass and on catalytic HDO of the condensed bio-oil and model compounds, the task at hand is to apply this knowledge in the further research, development, and demonstration of combined fast pyrolysis and HDO processes. This development is in its infancy, but several proof of concept studies already exist. Thus, what remains is a directed scientific and commercial effort within an appropriate political frame to ensure the development of an efficient route for renewable liquid fuels from biomass, which can be included in the future energy supply system.

Acknowledgements

This work is part of the research conducted at the CHEC research center at The Department of Chemical and Biochemical Engineering at the Technical University of Denmark (DTU). This work was supported by Innovation Fund Denmark (formerly The Danish Council for Strategic Research, The Programme Commission on Sustainable Energy and Environment) [Project 1305-00015B]. The project is carried out by a consortium of partners involving DTU, Karlsruhe Institute of Technology, Stanford University, and Haldor Topsøe A/S.

Conflicts of interest: None

References

[1] United Nations. Sustainable development goals 2016. http://www.un.org/sustainabledevelopment/energy/ (accessed April 21, 2016).

[2] United Nations - Department of Economic and Social Affairs Population Division. Population 2015. http://www.un.org/en/development/desa/population/ (accessed April 25, 2016).

[3] Independent Statistics & Analysis - U.S. Energy Information Administration. Forecasts 2014. https://www.eia.gov/forecasts/ (accessed April 25, 2016).

[4] Independent Statistics & Analysis - U.S. Energy Information Administration. International energy outlook 2016 - DOE/EIA-0484. 2016.

[5] Core Writing Team, Pachauri RK, Meyers LA. Climate change 2014: Synthesis report. IPCC, Geneva: 2014.

[6] The World Bank. 2013 Environment 3.13: World development indicators: Traffic and congestion 2013. https://web.archive.org/web/20140408034906/http://wdi.worldbank.org/table/3.13 (accessed April 28, 2016).

[7] Nasdaq. www.nasdaq.com 2016. www.nasdaq.com/markets/ (accessed April 28, 2016).

[8] Lazard. Levelized cost of energy analysis, version 11.0 2017. https://www.lazard.com/perspective/levelized-cost-of-energy-2017/ (accessed February 18, 2018).

[9] Gröger O, Gasteiger HA, Suchsland J-P. Review-Electromobility: Batteries or fuel cells? J Electrochem Soc 2015;162:A2605–22.

[10] Schlögl R. Chemical energy storage. Göttingen: De Gruyter; 2013.

[11] Denholm P, O'Connell M, Brinkman G, Jorgenson J. Overgeneration from solar energy in California: A field guide to the duck chart. Technical report: NREL/TP-6A20-65023. 2015.

[12] Popp J, Lakner Z, Harangi-Rákos M, Fári M. The effect of bioenergy expansion: Food, energy, and environment. Renew Sustain Energy Rev 2014;32:559–78.

[13] Balat M. Production of bioethanol from lignocellulosic materials via the biochemical pathway: A review. Energy Convers Manag 2011;52:858–75.

[14] Roedl A. Production and energetic utilization of wood from short rotation coppice-a life cycle assessment. Int J Life Cycle Assess 2010;15:567–78.

[15] McKendry P. Energy production from biomass (part 1): Overview of biomass. Bioresour Technol 2002;83:37–46.

[16] Demirbas A. Biofuels sources, biofuel policy, biofuel economy and global biofuel projections. Energy Convers Manag 2008;49:2106–16.

[17] FAO, IFAD, WFP. The state of food insecurity in the world. The multiple dimensions of food security. Rome: 2013.

[18] O'Connor P. Chapter 1: A general introduction to biomass utilization possibilities. In: Triantafyllidis K, Lappas A, Stöcker M, editors. The role of catalysis for the sustainable

production of bio-fuels and bio-chemicals, E-Book: Elsevier; 2013, p. 1–25.

[19] Hayes DJM. Chapter 2: Biomass composition and its relevance to biorefining. In: Triantafyllidis K, Lappas A, Stöcker M, editors. The role of catalysis for the sustainable production of bio-fuels and bio-chemicals, E-Book: Elsevier; 2013, p. 27–65.

[20] Mortensen PM, Grunwaldt J-D, Jensen PA, Knudsen KG, Jensen AD. A review of catalytic upgrading of bio-oil to engine fuels. Appl Catal A Gen 2011;407:1–19.

[21] Linck M, Felix L, Marker T, Roberts M. Integrated biomass hydropyrolysis and hydrotreating: a brief review. WIREs Energy Environ 2014;3:575–81.

[22] Trinh TN, Jensen PA, Dam-Johansen K, Knudsen NO, Sørensen HR, Hvilsted S. Comparison of lignin, macroalgae, wood, and straw fast pyrolysis. Energy & Fuels 2013;27:1399–409.

[23] Bridgwater AV. Review of fast pyrolysis of biomass and product upgrading. Biomass and Bioenergy 2012;38:68–94.

[24] Czernik S, Bridgwater AV. Overview of applications of biomass fast pyrolysis oil. Energy & Fuels 2004;18:590–8.

[25] Bridgwater AV. Renewable fuels and chemicals by thermal processing of biomass. Chem Eng J 2003;91:87–102.

[26] Bridgwater AV. Principles and practice of biomass fast pyrolysis processes for liquids. J Anal Appl Pyrolysis 1999;51:3–22.

[27] Mohan D, Pittman CU, Steele PH. Pyrolysis of wood/biomass for bio-oil: A critical review. Energy & Fuels 2006;20:848–89.

[28] Butler E, Devlin G, Meier D, McDonnell K. A review of recent laboratory research and commercial developments in fast pyrolysis and upgrading. Renew Sustain Energy Rev 2011;15:4171–86.

[29] Yaman S. Pyrolysis of biomass to produce fuels and chemical feedstocks. Energy Convers Manag 2004;45:651–71.

[30] Venderbosch RH, Prins W. Fast pyrolysis technology development. Biofuels, Bioprod Biorefining 2010;4:178–208.

[31] Fahmi R, Bridgwater AV, Donnison I, Yates N, Jones JM. The effect of lignin and inorganic species in biomass on pyrolysis oil yields, quality and stability. Fuel 2008;87:1230–40.

[32] Azeez AM, Meier D, Odermatt J, Willner T. Fast pyrolysis of African and European lignocellulosic biomasses using Py-GC/MS and fluidized bed reactor. Energy & Fuels 2010;24:2078–85.

[33] Kang B-S, Lee KH, Park HJ, Park Y-K, Kim J-S. Fast pyrolysis of radiata pine in a bench scale plant with a fluidized bed: Influence of a char separation system and reaction conditions on the production of bio-oil. J Anal Appl Pyrolysis 2006;76:32–7.

[34] Garcia-Perez M, Wang XS, Shen J, Rhodes MJ, Tian F, Lee W-J, et al. Fast pyrolysis of oil mallee woody biomass: Effect of temperature on the yield and quality of pyrolysis products. Ind Eng Chem Res 2008;47:1846–54.

[35] Scott DS, Piskorz J, Radlein D. Liquid products from the continuous flash pyrolysis of biomass. Ind Eng Chem Process Des Dev 1985;24:581–8.

[36] Yildiz G, Lathouwers T, Toraman HE, Geem KM Van, Marin GB, Ronsse F, et al. Catalytic fast pyrolysis of pine wood: Effect of successive catalyst regeneration. Energy & Fuels 2014;28:4560–72.

[37] Asadieraghi M, Daud WMAW. In-situ catalytic upgrading of biomass pyrolysis vapor: Using a cascade system of various catalysts in a multi-zone fixed bed reactor. Energy Convers Manag 2015;101:151–63.

[38] Yung MM, Stanton AR, Iisa K, French RJ, Orton KA, Magrini KA. Multiscale evaluation of catalytic upgrading of biomass pyrolysis vapors on Ni- and Ga-modified ZSM-5. Energy & Fuels 2016;30:9471–9.

[39] Yang H, Coolman R, Karanjkar P, Wang H, Dornath P, Chen H, et al. The effects of contact time and coking on the catalytic fast pyrolysis of cellulose. Green Chem 2017;19:286–97.

[40] Mukarakate C, McBrayer JD, Evans TJ, Budhi S, Robichaud DJ, Iisa K, et al. Catalytic fast pyrolysis of biomass: the reactions of water and aromatic intermediates produces phenols. Green Chem 2015;17:4217–27.

[41] Asadieraghi M, Daud WMAW. In-situ catalytic upgrading of biomass pyrolysis vapor: Co-feeding with methanol in a multi-zone fixed bed reactor. Energy Convers Manag 2015;92:448–58.

[42] Iisa K, French RJ, Orton KA, Budhi S, Mukarakate C, Stanton AR, et al. Catalytic pyrolysis of pine over HZSM-5 with different binders. Top Catal 2016;59:94–108.

[43] Schultz EL, Mullen CA, Boateng AA. Aromatic hydrocarbon production from eucalyptus urophylla pyrolysis over several metal-modified ZSM-5 catalysts. Energy Technol 2017;5:196–204.

[44] Agblevor FA, Elliott DC, Santosa DM, Olarte M V., Burton SD, Swita M, et al. Red mud catalytic pyrolysis of pinyon juniper and single-stage hydrotreatment of oils. Energy & Fuels 2016;30:7947–58.

[45] Mante OD, Dayton DC, Gabrielsen J, Ammitzboll NL, Barbee D, Verdier S, et al. Integration of catalytic fast pyrolysis and hydroprocessing: a pathway to refinery intermediates and “drop-in” fuels from biomass. Green Chem 2016;18:6123–35.

[46] Nguyen TS, Duong TL, Pham TTT, Nguyen DT, Le PN, Nguyen HL, et al. Online catalytic deoxygenation of vapour from fast pyrolysis of Vietnamese sugarcane bagasse over sodium-based catalysts. J Anal Appl Pyrolysis 2017;127:436–43.

[47] Venderbosch RH. A critical view on catalytic pyrolysis of biomass. ChemSusChem 2015;8:1306–16.

[48] Yildiz G, Ronsse F, Duren R Van, Prins W. Challenges in the design and operation of processes for catalytic fast pyrolysis of woody biomass. Renew Sustain Energy Rev 2016;57:1596–610.

[49] Rezaei PS, Shafaghat H, Daud WMAW. Production of green aromatics and olefins by catalytic cracking of oxygenate compounds derived from biomass pyrolysis: A review.

Appl Catal A Gen 2014;469:490–511.

[50] Garcia-Nunez JA, Pelaez-Samaniego MR, Garcia-Perez ME, Fonts I, Abrego J, Westerhof RJM, et al. Historical developments of pyrolysis reactors: A review. Energy & Fuels 2017;31:5751–75.

[51] Lehmann J, Joseph S. Biochar for environmental management. Science and Technology. Sterling: Earthscan; 2009.

[52] Qian K, Kumar A, Zhang H, Bellmer D, Huhnke R. Recent advances in utilization of biochar. Renew Sustain Energy Rev 2015;42:1055–64.

[53] Ding Y, Liu Y, Liu S, Li Z, Tan X, Huang X, et al. Biochar to improve soil fertility. A review. Agron Sustain Dev 2016;36:1–18.

[54] Scott DS. Pyrolysis process CA 1241541 A1, 1988.

[55] Guda VK, Steele PH, Penmetsa VK, Li Q. Chapter 7: Fast pyrolysis of biomass: Recent advances in fast pyrolysis technology. Recent advances in thermo-chemical conversion of biomass, E-Book: Elsevier; 2015, p. 177–211.

[56] Scott DS, Majerski P, Piskorz J, Radlein D. A second look at fast pyrolysis of biomass-the RTI process. J Anal Appl Pyrolysis 1999;51:23–37.

[57] Envergent Tehcnologies. Envergent Technologies n.d. https://www.envergenttech.com/ (accessed January 28, 2018).

[58] Luo G, Chandler DS, Anjos LCA, Eng RJ, Jia P, Resende FLP. Pyrolysis of whole wood chips and rods in a novel ablative reactor. Fuel 2017;194:229–38.

[59] Wagenaar BM, Venderbosch RH, Carrasco J, Strenziok R, van der Aa BJ. Chapter 105: Rotating cone bio-oil production and applications. In: Bridgwater AV, editor. Progress in thermochemical biomass conversion, Oxford: Blackwell Science Ltd; 2001, p. 1268–80.

[60] Bech N, Larsen MB, Jensen PA, Dam-Johansen K. Modelling solid-convective flash pyrolysis of straw and wood in the pyrolysis centrifuge reactor. Biomass and Bioenergy 2009;33:999–1011.

[61] Trinh TN, Jensen PA, Dam-Johansen K, Knudsen NO, Sørensen HR. Influence of the pyrolysis temperature on sewage sludge product distribution, bio-oil, and char properties. Energy & Fuels 2013;27:1419–27.

[62] Trinh TN, Jensen PA, Sárossy Z, Dam-Johansen K, Knudsen NO, Sørensen HR, et al. Fast pyrolysis of lignin using a pyrolysis centrifuge reactor. Energy and Fuels 2013;27:3802–10.

[63] Hayes DJ. An examination of biorefining processes, catalysts and challenges. Catal Today 2009;145:138–51.

[64] Bridgwater AV. Biomass fast pyrolysis. Therm Sci 2004;8:21–49.

[65] Sun Y, Cheng J. Hydrolysis of lignocellulosic materials for ethanol production: A review. Bioresour Technol 2002;83:1–11.

[66] Lange J-P. Lignocellulose conversion: An introduction to chemistry, process and economics. Biofuels, Bioprod Biorefining 2007;1:39–48.

[67] Smith W, Tamutech Consultancy. Literature review: State of the art in biorefinery

developement (NFC 07/008). A report prepared for the National Non Food Crops Centre. 2007.

[68] Tang WK, Neill WK. Effect of flame retardants on pyrolysis and combustion of α-cellulose. J Polym Sci Part C 1964;6:65–81.

[69] Shafizadeh F, Fu YL. Pyrolysis of cellulose. Carbohydr Res 1973;29:113–22.

[70] Yang H, Yan R, Chen H, Lee DH, Zheng C. Characteristics of hemicellulose, cellulose and lignin pyrolysis. Fuel 2007;86:1781–8.

[71] Trinh TN. PhD Thesis: Fast Pyrolysis of Lignin, Macroalgae and Sewage Sludge. Technical University of Denmark, Dept. of Chemical and Biochemical Engineering, 2013.

[72] Lee K-H, Kang B-S, Park Y-K, Kim J-S. Influence of reaction temperature, pretreatment, and a char removal system on the production of bio-oil from rice straw by fast pyrolysis, using a fluidized bed. Energy & Fuels 2005;19:2179–84.

[73] Hwang H, Lee J, Moon J, Kim U, Choi I, Choi JW. Influence of K and Mg concentration on the storage stability of bio-oil. ACS Sustain Chem Eng 2016;4:4346–53.

[74] Nowakowski DJ, Bridgwater AV, Elliott DC, Meier D, de Wild P. Lignin fast pyrolysis: Results from an international collaboration. J Anal Appl Pyrolysis 2010;88:53–72.

[75] Park HJ, Park Y-K, Dong J-I, Kim J-S, Jeon J-K, Kim S-S, et al. Pyrolysis characteristics of Oriental white oak: Kinetic study and fast pyrolysis in a fluidized bed with an improved reaction system. Fuel Process Technol 2009;90:186–95.

[76] Piskorz J, Scott DS, Westerberg IB. Flash pyrolysis of sewage sludge. Ind Eng Chem Process Des Dev 1986;25:265–70.

[77] Demirbaş A. Relationships between lignin contents and heating values of biomass. Energy Convers Manag 2001;42:183–8.

[78] Liu Q, Wang S, Zheng Y, Luo Z, Cen K. Mechanism study of wood lignin pyrolysis by using TG-FTIR analysis. J Anal Appl Pyrolysis 2008;82:170–7.

[79] Yeh T-F, Chang H-M, Kadla JF. Rapid prediction of solid wood lignin content using transmittance near-infrared spectroscopy. J Agric Food Chem 2004;52:1435–9.

[80] Boroson ML, Howard JB, Longwell JP, Peters WA. Product yields and kinetics from the vapor phase cracking of wood pyrolysis tars. AIChE J 1989;35:120–8.

[81] Jensen A, Dam-Johansen K, Wójtowicz MA, Serio MA. TG-FTIR study of the influence of potassium chloride on wheat straw pyrolysis. Energy & Fuels 1998;12:929–38.

[82] Piskorz J, Majerski P, Radlein D, Scott DS, Bridgwater AV. Fast pyrolysis of sweet sorghum and sweet sorghum bagasse. J Anal Appl Pyrolysis 1998;46:15–29.

[83] biniti Ibrahim N. PhD Thesis: Bio-oil from Flash Pyrolysis of Agricultural Residues. Technical University of Denmark, Dept. of Chemical and Biochemical Engineering, 2012.

[84] Johansen JM, Jakobsen JG, Frandsen FJ, Glarborg P. Release of K, Cl, and S during pyrolysis and combustion of high-chlorine biomass. Energy & Fuels 2011;25:4961–71.

[85] Jung S-H, Kang B-S, Kim J-S. Production of bio-oil from rice straw and bamboo sawdust under various reaction conditions in a fast pyrolysis plant equipped with a fluidized bed and

a char separation system. J Anal Appl Pyrolysis 2008;82:240–7.

[86] Raveendran K, Ganesh A, Khilar KC. Influence of mineral matter on biomass pyrolysis characteristics. Fuel 1995;74:1812–22.

[87] de Wild PJ, Huijgen WJJ, Heeres HJ. Pyrolysis of wheat straw-derived organosolv lignin. J Anal Appl Pyrolysis 2012;93:95–103.

[88] Nikolaisen L, Jensen PD, Bech KS, Dahl J, Busk J, Brødsgaard T, et al. Energy production from marine biomass (Ulva lactuca). PSO Project No. 2008-1-0050. Danish Technological Institute. 2011.

[89] Kan T, Grierson S, de Nys R, Strezov V. Comparative assessment of the thermochemical conversion of freshwater and marine micro- and macroalgae. Energy & Fuels 2014;28:104–14.

[90] Ross AB, Jones JM, Kubacki ML, Bridgeman T. Classification of macroalgae as fuel and its thermochemical behaviour. Bioresour Technol 2008;99:6494–504.

[91] Roesijadi G, Jones SB, Snowden-Swan LJ, Zhu Y. Macroalgae as a biomass aeedstock : A preliminary analysis (PNNL- 19944). Pacific Northwest National Laboratory. 2010.

[92] Murphy F, Devlin G, Deverell R, McDonnell K. Biofuel production in Ireland-An approach to 2020 targets with a focus on algal biomass. Energies 2013;6:6391–412.

[93] Bae YJ, Ryu C, Jeon J-K, Park J, Suh DJ, Suh Y-W, et al. The characteristics of bio-oil produced from the pyrolysis of three marine macroalgae. Bioresour Technol 2011;102:3512–20.

[94] Milledge JJ, Smith B, Dyer PW, Harvey P. Macroalgae-derived biofuel: A review of methods of energy extraction from seaweed biomass. Energies 2014;7:7194–222.

[95] Cole AJ, Neveux N, Whelan A, Morton J, Vis M, de Nys R, et al. Adding value to the treatment of municipal wastewater through the intensive production of freshwater macroalgae. Algal Res 2016;20:100–9.

[96] Fonts I, Juan A, Gea G, Murillo MB, Sánchez JL. Sewage sludge pyrolysis in fluidized bed, 1: Influence of operational conditions on the product distribution. Ind Eng Chem Res 2008;47:5376–85.

[97] Shen L, Zhang D-K. An experimental study of oil recovery from sewage sludge by low-temperature pyrolysis in a fluidised-bed. Fuel 2003;82:465–72.

[98] Pokorna E, Postelmans N, Jenicek P, Schreurs S, Carleer R, Yperman J. Study of bio-oils and solids from flash pyrolysis of sewage sludges. Fuel 2009;88:1344–50.

[99] Toft AJ. PhD Thesis: A Comparison of Integrated Biomass to Electrocoty Systems. Univeristy of Aston in Birmingham, 1996.

[100] Di Blasi C. Modeling chemical and physical processes of wood and biomass pyrolysis. Prog Energy Combust Sci 2008;34:47–90.

[101] Bruchmüller J, van Wachem BGM, Gu S, Luo KH, Brown RC. Modeling the thermochemical degradation of biomass inside a fast pyrolysis fluidized bed reactor. AIChE J 2012;58:3030–42.

[102] Scott DS, Piskorz J. The flash pyrolysis of Aspen-poplar wood. Can J Chem Eng

1982;60:666–74.

[103] Westerhof RJM, Brilman DWF (Wim), Swaaij WPM Van, Kersten SRA. Effect of temperature in fluidized bed fast pyrolysis of biomass: Oil quality assessment in test units. Ind Eng Chem Res 2010;49:1160–8.

[104] Fagbemi L, Khezami L, Capart R. Pyrolysis products from different biomasses: application to the thermal cracking of tar. Appl Energy 2001;69:293–306.

[105] Hurt MR, Degenstein JC, Gawecki P, Borton II DJ, Vinueza NR, Yang L, et al. On-line mass spectrometric methods for the determination of the primary products of fast pyrolysis of carbohydrates and for their gas-phase manipulation. Anal Chem 2013;85:10927–34.

[106] Peacocke GVC. PhD Thesis: Ablative Pyrolysis of Biomass. Univeristy of Aston in Birmingham, 1994.

[107] Wang X, Kersten SRA, Prins W, van Swaaij WPM. Biomass pyrolysis in a fluidized bed reactor. Part 2: Experimental validation of model results. Ind Eng Chem Res 2005;44:8786–95.

[108] Ateş F, Pütün E, Pütün AE. Fast pyrolysis of sesame stalk: yields and structural analysis of bio-oil. J Anal Appl Pyrolysis 2004;71:779–90.

[109] Janse AMC, Westerhout RWJ, Prins W. Modelling of flash pyrolysis of a single wood particle. Chem Eng Process 2000;39:239–52.

[110] Shen J, Wang X-S, Garcia-Perez M, Mourant D, Rhodes MJ, Li C-Z. Effects of particle size on the fast pyrolysis of oil mallee woody biomass. Fuel 2009;88:1810–7.

[111] Westerhof RJM, Nygård HS, Van Swaaij WPM, Kersten SRA, Brilman DWF. Effect of particle geometry and microstructure on fast pyrolysis of beech wood. Energy and Fuels 2012;26:2274–80.

[112] Westerhof RJM, Kuipers NJM, Kersten SRA, Van Swaaij WPM. Controlling the water content of biomass fast pyrolysis oil. Ind Eng Chem Res 2007;46:9238–47.

[113] Gray MR, Corcoran WH, Gavalas GR. Pyrolysis of a wood-derived material. Effects of moisture and ash content. Ind Eng Chem Process Des Dev 1985;24:646–51.

[114] Negahdar L, Gonzalez-Quiroga A, Otyuskaya D, Toraman HE, Liu L, Jastrzebski JTBH, et al. Characterization and comparison of fast pyrolysis bio-oils from pinewood, rapeseed cake, and wheat straw using ^{13}C NMR and comprehensive GC × GC. ACS Sustain Chem Eng 2016;4:4974–85.

[115] Oasmaa A, Czernik S. Fuel oil quality of biomass pyrolysis oils-State of the art for the end users. Energy & Fuels 1999;13:914–21.

[116] Chiaramonti D, Oasmaa A, Solantausta Y. Power generation using fast pyrolysis liquids from biomass. Renew Sustain Energy Rev 2007;11:1056–86.

[117] Syntek Global Inc. Technical information: ASTM D975 diesel fuel specification test n.d. http://emotor-extreme.cl/assets/astm_d975_specification_test.pdf (accessed August 7, 2017).

[118] Mabanaft. Sulphur free diesel BS EN 590:2013 2015. https://www.mabanaft.com/fileadmin/content/global_content/downloads/mabanaft/Mabanaf

t-Ltd_Prod-Spec_Diesel.pdf (accessed August 7, 2017).

[119] Albertazzi S, Basile F, Fornasari G, Trifirò F, Vaccari A. Chapter 7: Thermal biomass conversion, Catalysis for renewables: From feedstock to energy production. Weinheim: Wiley-VCH Verlag GmbH & Co. KGaA; 2007.

[120] Boscagli C, Raffelt K, Zevaco TA, Olbrich W, Otto TN, Sauer J, et al. Mild hydrotreatment of the light fraction of fast-pyrolysis oil produced from straw over nickel-based catalysts. Biomass and Bioenergy 2015;83:525–38.

[121] Wang H, Male J, Wang Y. Recent advances in hydrotreating of pyrolysis bio-oil and its oxygen-containing model compounds. ACS Catal 2013;3:1047–70.

[122] Sipilä K, Kuoppala E, Fagernäs L, Oasmaa A. Characterization of biomass-based flash pyrolysis oils. Biomass and Bioenergy 1998;14:103–13.

[123] Branca C, Giudicianni P, Di Blasi C. GC/MS characterization of liquids generated from low-temperature pyrolysis of wood. Ind Eng Chem Res 2003;42:3190–202.

[124] Hassan EM, Steele PH, Ingram L. Characterization of fast pyrolysis bio-oils produced from pretreated pine wood. Appl Biochem Biotechnol 2009;154:182–92.

[125] Thangalazhy-Gopakumar S, Adhikari S, Gupta RB. Catalytic pyrolysis of biomass over H^+ZSM-5 under hydrogen pressure. Energy & Fuels 2012;26:5300–6.

[126] Oasmaa A, Elliott DC, Korhonen J. Acidity of biomass fast pyrolysis bio-oils. Energy & Fuels 2010;24:6548–54.

[127] Oasmaa A, Kuoppala E, Solantausta Y. Fast pyrolysis of forestry residue. 2. Physicochemical composition of product liquid. Energy & Fuels 2003;17:433–43.

[128] Piskorz J, Radlein DSAG, Scott DS, Czernik S. Liquid products from the fast pyrolysis of wood and cellulose. In: Bridgwater AV, Kuester JL, editors. Research in thermochemical biomass conversion, Elsevier Science Publishing Company Inc.; 1988, p. 557–71.

[129] Routray K, Barnett KJ, Huber GW. Hydrodeoxygenation of pyrolysis oils. Energy Technol 2017;5:80–93.

[130] Ruddy DA, Schaidle JA, Ferrell III JR, Wang J, Moens L, Hensley JE. Recent advances in heterogeneous catalysts for bio-oil upgrading via “ex situ catalytic fast pyrolysis”: catalyst development through the study of model compounds. Green Chem 2014;16:454–90.

[131] Milne T, Agblevor F, Davis M, Deutch S, Johnson D. A review of the chemical composition of fast-pyrolysis oils from biomass. In: Bridqwater AV, Boocock DGB, editors. Developments in thermochemical biomass conversion, Suffolk: Blackie A & P, an imprint of Chapman & Hall; 1997, p. 409–24.

[132] Mullen CA, Boateng AA. Chemical composition of bio-oils produced by fast pyrolysis of two energy crops. Energy & Fuels 2008;22:2104–9.

[133] Oasmaa A, Källi A, Lindfors C, Elliott DC, Springer D, Peacocke C, et al. Guidelines for transportation, handling, and use of fast pyrolysis bio-oil. 1. Flammability and toxicity. Energy & Fuels 2012;26:3864–73.

[134] Oasmaa A, Kuoppala E. Fast pyrolysis of forestry residue. 3. Storage stability of liquid fuel. Energy & Fuels 2003;17:1075–84.

[135] Czernik S, Johnson DK, Black S. Stability of wood fast pyrolysis oil. Biomass and Bioenergy 1994;7:187–92.

[136] Garcìa-Pérez M, Chaala A, Pakdel H, Kretschmer D, Rodrigue D, Roy C. Multiphase structure of bio-oils. Energy & Fuels 2006;20:364–75.

[137] Mortensen PM, Gardini D, Damsgaard CD, Grunwaldt J-D, Jensen PA, Wagner JB, et al. Deactivation of Ni-MoS_2 by bio-oil impurities during hydrodeoxygenation of phenol and octanol. Appl Catal A Gen 2016;523:159–70.

[138] Mortensen PM, Gardini D, de Carvalho HWP, Damsgaard CD, Grunwaldt J-D, Jensen PA, et al. Stability and resistance of nickel catalysts for hydrodeoxygenation: Carbon deposition and effects of sulfur, potassium, and chlorine in the feed. Catal Sci Technol 2014;4:3672–86.

[139] van de Beld B, Holle E, Florijn J. The use of a fast pyrolysis oil – Ethanol blend in diesel engines for chp applications. Biomass and Bioenergy 2018;110:114–22.

[140] Lee S, Kim T, Kang K. Performance and emission characteristics of a diesel engine operated with wood pyrolysis oil. Proc Inst Mech Eng Part D J Automob Eng 2014;228:180–9.

[141] Solantausta Y, Nylund N-O, Westerholm M, Koljonen T, Oasmaa A. Wood-pyrolysis oil as fuel in a diesel-power plant. Bioresour Technol 1993;46:177–88.

[142] Chiaramonti D, Bonini M, Fratini E, Tondi G, Gartner K, Bridgwater AV, et al. Development of emulsions from biomass pyrolysis liquid and diesel and their use in engines-Part 2: Tests in diesel engines. Biomass and Bioenergy 2003;25:101–11.

[143] Chiaramonti D, Bonini M, Fratini E, Tondi G, Gartner K, Bridgwater AV, et al. Development of emulsions from biomass pyrolysis liquid and diesel and their use in engines-Part 1: Emulsion production. Biomass and Bioenergy 2003;25:85–99.

[144] Shihadeh A, Hochgreb S. Impact of biomass pyrolysis oil process conditions on ignition delay in compression ignition engines. Energy & Fuels 2002;16:552–61.

[145] Shihadeh A, Hochgreb S. Diesel engine combustion of biomass pyrolysis oils. Energy & Fuels 2000;14:260–74.

[146] Juste GL, Monfort JJS. Preliminary test on combustion of wood derived fast pyrolysis oils in a gas turbine combustor. Biomass and Bioenergy 2000;19:119–28.

[147] Strenziok R. Bio-oil application in a small gas turbine. IEA bioenergy agreement task 34 newsletter - PyNe 32. Aston Univerisyt Bioenergy Group 2012:7–8.

[148] No S-Y. Application of bio-oils from lignocellulosic biomass to transportation, heat and power generation-A review. Renew Sustain Energy Rev 2014;40:1108–25.

[149] Khodier A, Kilgallon P, Legrave N, Simms N, Oakey J, Bridgwater T. Pilot-scale combustion of fast-pyrolysis bio-oil: Ash deposition and gaseous emissions. Environ Prog Sustain Energy 2009;28:397–403.

[150] Fortum. Joensuu CHP plant n.d. https://www3.fortum.com/about-us/our-company/our-energy-production/our-power-plants/joensuu-chp-plant (accessed April 27, 2018).

[151] BTG BioLiquids. Empyro BV n.d. https://www.btg-btl.com/en/company/projects/empyro

(accessed January 28, 2018).

[152] Thrän D, Peetz D, Schaubach K. Global wood pellet industry and trade study 2017. IEA Bioenergy Task 40. 2017.

[153] Raffelt K, Henrich E, Koegel A, Stahl R, Steinhardt J, Weirich F. The BTL2 process of biomass utilization entrained-flow gasification of pyrolyzed biomass slurries. Appl Biochem Biotechnol 2006;129–132:153–64.

[154] Dahmen N, Henrich E, Dinjus E, Weirich F. The bioliq® bioslurry gasification process for the production of biosynfuels, organic chemicals, and energy. Energy Sustain Soc 2012;2:3:1–44.

[155] Lappas AA, Bezergianni S, Vasalos IA. Production of biofuels via co-processing in conventional refining processes. Catal Today 2009;145:55–62.

[156] Pinho A d R, de Almeida MBB, Mendes FL, Ximenes VL, Casavechia LC. Co-processing raw bio-oil and gasoil in an FCC Unit. Fuel Process Technol 2015;131:159–66.

[157] Talmadge MS, Baldwin RM, Biddy MJ, McCormick RL, Beckham GT, Ferguson GA, et al. A Perspective on Oxygenated Species in the Refinery Integration of Pyrolysis Oil. Green Chem 2014;16:407–53.

[158] Alfke G, Irion WW, Neuwirth OS. Oil refining. Ullmann's encyclopedia of industrial chemistry, Weinheim, Germany: Wiley-VCH Verlag GmbH & Co. KGaA; 2007.

[159] Gueudré L, Chapon F, Mirodatos C, Schuurman Y, Venderbosch R, Jordan E, et al. Optimizing the bio-gasoline quantity and quality in fluid catalytic cracking co-refining. Fuel 2017;192:60–70.

[160] Lindfors C, Paasikallio V, Kuoppala E, Reinikainen M, Oasmaa A, Solantausta Y. Co-processing of dry bio-oil, catalytic pyrolysis oil, and hydrotreated bio-oil in a micro activity test unit. Energy & Fuels 2015;29:3707–14.

[161] Agblevor FA, Mante O, McClung R, Oyama ST. Co-processing of standard gas oil and biocrude oil to hydrocarbon fuels. Biomass and Bioenergy 2012;45:130–7.

[162] Pinho A de R, de Almeida MBB, Mendes FL, Casavechia LC, Talmadge MS, Kinchin CM, et al. Fast pyrolysis oil from pinewood chips co-processing with vacuum gas oil in an FCC unit for second generation fuel production. Fuel 2017;188:462–73.

[163] Topsøe H, Clausen BS, Massoth FE. Cataltsis - Science and Technology. Hydrotreating catalysis. Volume 11. Berlin Heidelberg, Germany: Springer-Verlag; 1996.

[164] Saidi M, Samimi F, Karimipourfard D, Nimmanwudipong T, Gates BC, Rahimpour MR. Upgrading of lignin-derived bio-oils by catalytic hydrodeoxygenation. Energy Environ Sci 2014;7:103–29.

[165] Web of Science. https://webofknowledge.com/ n.d. https://webofknowledge.com/ (accessed January 13, 2018).

[166] Elliott DC. Historical developments in hydroprocessing bio-oils. Energy & Fuels 2007;21:1792–815.

[167] Zacher AH, Olarte MV, Santosa DM, Elliott DC, Jones SB. A review and perspective of recent bio-oil hydrotreating research. Green Chem 2014;16:491–515.

[168] Furimsky E. Catalytic hydrodeoxygenation. Appl Catal A Gen 2000;199:147–90.

[169] Furimsky E. Hydroprocessing challenges in biofuels production. Catal Today 2013;217:13–56.

[170] He Z, Wang X. Hydrodeoxygenation of model compounds and catalytic systems for pyrolysis bio-oils upgrading. Catal Sustain Energy 2012;1:28–52.

[171] Ruinart de Brimont M, Dupont C, Daudin A, Geantet C, Raybaud P. Deoxygenation mechanisms on Ni-promoted MoS_2 bulk catalysts: A combined experimental and theoretical study. J Catal 2012;286:153–64.

[172] Romero Y, Richard F, Brunet S. Hydrodeoxygenation of 2-ethylphenol as a model compound of bio-crude over sulfided Mo-based catalysts: Promoting effect and reaction mechanism. Appl Catal B Environ 2010;98:213–23.

[173] Romero Y, Richard F, Renème Y, Brunet S. Hydrodeoxygenation of benzofuran and its oxygenated derivatives (2,3-dihydrobenzofuran and 2-ethylphenol) over $NiMoP/Al_2O_3$ catalyst. Appl Catal A Gen 2009;353:46–53.

[174] Nelson RC, Baek B, Ruiz P, Goundie B, Brooks A, Wheeler MC, et al. Experimental and theoretical insights into the hydrogen-efficient direct hydrodeoxygenation mechanism of phenol over Ru/TiO_2. ACS Catal 2015;5:6509–23.

[175] Runnebaum RC, Nimmanwudipong T, Block DE, Gates BC. Catalytic conversion of compounds representative of lignin-derived bio-oils: A reaction network for guaiacol, anisole, 4-methylanisole, and cyclohexanone conversion catalysed by $Pt/\gamma\text{-}Al_2O_3$. Catal Sci Technol 2012;2:113–8.

[176] Zanuttini MS, Lago CD, Gross MS, Peralta MA, Querini CA. Hydrodeoxygenation of anisole with Pt catalysts. Ind Eng Chem Res 2017;56:6419–31.

[177] Popov A, Kondratieva E, Goupil JM, Mariey L, Bazin P, Gilson J-P, et al. Bio-oils hydrodeoxygenation: Adsorption of phenolic molecules on oxidic catalyst supports. J Phys Chem C 2010;114:15661–70.

[178] Centeno A, Laurent E, Delmon B. Influence of the support of CoMo sulfide catalysts and of the addition of potassium and platinum on the catalytic performances for the hydrodeoxygenation of carbonyl, carboxyl, and guaiacol-type molecules. J Catal 1995;154:288–98.

[179] Echeandia S, Arias PL, Barrio VL, Pawelec B, Fierro JLG. Synergy effect in the HDO of phenol over Ni-W catalysts supported on active carbon: Effect of tungsten precursors. Appl Catal B Environ 2010;101:1–12.

[180] Elliott DC, Hart TR. Catalytic hydroprocessing of chemical models for bio-oil. Energy & Fuels 2009;23:631–7.

[181] Ternan M, Furimsky E, Parsons BI. Coke formation on hydrodesulphurization catalysts. Fuel Process Technol 1979;2:45–55.

[182] Bui VN, Laurenti D, Afanasiev P, Geantet C. Hydrodeoxygenation of guaiacol with CoMo catalysts. Part I: Promoting effect of cobalt on HDO selectivity and activity. Appl Catal B Environ 2011;101:239–45.

[183] Yin W, Kloekhorst A, Venderbosch RH, Bykova M V., Khromova SA, Yakovlev VA, et al.

Catalytic hydrotreatment of fast pyrolysis liquids in batch and continuous set-ups using a bimetallic Ni-Cu catalyst with a high metal content. Catal Sci Technol 2016;6:5899–915.

[184] Grange P, Laurent E, Maggi R, Centeno A, Delmon B. Hydrotreatment of pyrolysis oils from biomass: Reactivity of the various categories of oxygenated compounds and preliminary techno-economical study. Catal Today 1996;29:297–301.

[185] de Souza PM, Rabelo-Neto RC, Borges LEP, Jacobs G, Davis BH, Sooknoi T, et al. Role of keto intermediates in the hydrodeoxygenation of phenol over Pd on oxophilic supports. ACS Catal 2015;5:1318–29.

[186] Boscagli C, Raffelt K, Grunwaldt J-D. Reactivity of platform molecules in pyrolysis oil and in water during hydrotreatment over nickel and ruthenium catalysts. Biomass and Bioenergy 2017;106:63–73.

[187] Wang H, Wang Y. Characterization of deactivated bio-oil hydrotreating catalysts. Top Catal 2016;59:65–72.

[188] Venderbosch RH, Ardiyanti AR, Wildschut J, Oasmaa A, Heeres HJ. Stabilization of biomass-derived pyrolysis oils. J Chem Technol Biotechnol 2010;85:674–86.

[189] Pham TN, Shi D, Resasco DE. Evaluating strategies for catalytic upgrading of pyrolysis oil in liquid phase. Appl Catal B Environ 2014;145:10–23.

[190] Jahangiri H, Osatiashtiani A, Bennett JA, Isaacs MA, Gu S, Lee AF, et al. Zirconia catalysed acetic acid ketonisation for pre-treatment of biomass fast pyrolysis vapours. Catal Sci Technol 2018;8:1134–41.

[191] Puértolas B, Keller TC, Mitchell S, Pérez-Ramírez J. Deoxygenation of bio-oil over solid base catalysts: From model to realistic feeds. Appl Catal B Environ 2016;184:77–86.

[192] Edelman MC, Maholland MK, Baldwin RM, Cowley SW. Vapor-phase catalytic hydrodeoxygenation of benzofuran. J Catal 1988;111:243–53.

[193] Dwiatmoko AA, Lee S, Ham HC, Choi J-W, Suh DJ, Ha J-M. Effects of carbohydrates on the hydrodeoxygenation of lignin-derived phenolic compounds. ACS Catal 2015;5:433–7.

[194] Ryymin E-M, Honkela ML, Viljava T-R, Krause AOI. Competitive reactions and mechanisms in the simultaneous HDO of phenol and methyl heptanoate over sulphided NiMo/γ-Al_2O_3. Appl Catal A Gen 2010;389:114–21.

[195] Wildschut J. PhD Thesis: Pyrolysis Oil Upgrading to Transportation Fuels by Catalytic Hydrotreatment. University of Groningen, 2009.

[196] Wildschut J, Mahfud FH, Venderbosch RH, Heeres HJ. Hydrotreatment of fast pyrolysis oil using heterogeneous noble-metal catalysts. Ind Eng Chem Res 2009;48:10324–34.

[197] Bridgwater AV. Production of high grade fuels and chemicals from catalytic pyrolysis of biomass. Catal Today 1996;29:285–95.

[198] Samolada MC, Baldauf W, Vasalos IA. Production of a bio-gasoline by upgrading biomass flash pyrolysis liquids via hydrogen processing and catalytic cracking. Fuel 1998;77:1667–75.

[199] Lloyd WG, Davenport DA. Applying thermodynamics to fossil fuels: Heats of combustion from elemental compositions. J Chem Educ 1980;57:56–60.

[200] Baldauf W, Balfanz U, Rupp M. Upgrading of flash pyrolysis oil and utilization in refineries. Biomass and Bioenergy 1994;7:237–44.

[201] Sheu Y-HE, Anthony RG, Soltes EJ. Kinetic studies of upgrading pine pyrolytic oil by hydrotreatment. Fuel Process Technol 1988;19:31–50.

[202] Wang Y, Lin H, Zheng Y. Hydrotreatment of lignocellulosic biomass derived oil using a sulfided NiMo/γ-Al_2O_3 catalyst. Catal Sci Technol 2014;4:109–19.

[203] Mortensen PM. PhD Thesis: Catalytic Conversion of Bio-oil to Fuel for Transportation. Technical University of Denmark, Dept. of Chemical and Biochemical Engineering, 2013.

[204] Cheng S, Wei L, Julson J, Rabnawaz M. Upgrading pyrolysis bio-oil through hydrodeoxygenation (HDO) using non-sulfided Fe-Co/SiO_2 catalyst. Energy Convers Manag 2017;150:331–42.

[205] Guo C, Rao KTV, Yuan Z, He S (Quan), Rohani S, Xu C (Charles). Hydrodeoxygenation of fast pyrolysis oil with novel activated carbon-supported NiP and CoP catalysts. Chem Eng Sci 2018;178:248–59.

[206] Elliott DC, Hart TR, Neuenschwander GG, Rotness LJ, Zacher AH. Catalytic hydroprocessing of biomass fast pyrolysis bio-oil to produce hydrocarbon products. Environ Prog Sustain Energy 2009;28:441–9.

[207] Cordero-Lanzac T, Palos R, Arandes JM, Castaño P, Rodríguez-Mirasol J, Cordero T, et al. Stability of an acid activated carbon based bifunctional catalyst for the raw bio-oil hydrodeoxygenation. Appl Catal B Environ 2017;203:389–99.

[208] Dayton DC, Carpenter JR, Kataria A, Peters JE, Barbee D, Mante OD, et al. Design and operation of a pilot-scale catalytic biomass pyrolysis unit. Green Chem 2015;17:4680–9.

[209] Dabros TMH, Gaur A, Pintos DG, Sprenger P, Høj M, Hansen TW, et al. Influence of H2O and H2S on the composition, activity, and stability of sulfided Mo, CoMo, and NiMo supported on MgAl2O4 for hydrodeoxygenation of ethylene glycol. Appl Catal A Gen 2018;551:106–21.

[210] Kwon KC, Mayfield H, Marolla T, Nichols B, Mashburn M. Catalytic deoxygenation of liquid biomass for hydrocarbon fuels. Renew Energy 2011;36:907–15.

[211] Su-Ping Z, Yong-Jie Y, Zhengwei R, Tingchen L. Study of hydrodeoxygenation of bio-oil from the fast pyrolysis of biomass. Energy Sources 2003;25:57–65.

[212] Furimsky E, Mikhlin JA, Jones DQ, Adley T, Baikowitz H. On the mechanism of hydrodeoxygenation of ortho substituted phenols. Can J Chem Eng 1986;64:982–5.

[213] Badawi M, Paul J-F, Cristol S, Payen E, Romero Y, Richard F, et al. Effect of water on the stability of Mo and CoMo hydrodeoxygenation catalysts: A combined experimental and DFT study. J Catal 2011;282:155–64.

[214] Badawi M, Paul J-F, Cristol S, Payen E. Guaiacol derivatives and inhibiting species adsorption over MoS_2 and CoMoS catalysts under HDO conditions: A DFT study. Catal Commun 2011;12:901–5.

[215] Laurent E, Delmon B. Study of the hydrodeoxygenation of carbonyl, carboxylic and guaiacyl groups over sulfided CoMo/γ-Al_2O_3 and NiMo/γ-Al_2O_3 catalyst: II. Influence of water, ammonia and hydrogen sulfide. Appl Catal A Gen 1994;109:97–115.

[216] Şenol Oİ, Ryymin E-M, Viljava T-R, Krause AOI. Effect of hydrogen sulphide on the hydrodeoxygenation of aromatic and aliphatic oxygenates on sulphided catalysts. J Mol Catal A Chem 2007;277:107–12.

[217] Şenol Oİ, Viljava T-R, Krause AOI. Effect of sulphiding agents on the hydrodeoxygenation of aliphatic esters on sulphided catalysts. Appl Catal A Gen 2007;326:236–44.

[218] Bui VN, Laurenti D, Delichère P, Geantet C. Hydrodeoxygenation of guaiacol. Part II: Support effect for CoMoS catalysts on HDO activity and selectivity. Appl Catal B Environ 2011;101:246–55.

[219] Gutierrez A, Turpeinen E-M, Viljava T-R, Krause O. Hydrodeoxygenation of model compounds on sulfided CoMo/γ-Al_2O_3 and NiMo/γ-Al_2O_3 catalysts; Role of sulfur-containing groups in reaction networks. Catal Today 2017;285:125–34.

[220] Bouvier C, Romero Y, Richard F, Brunet S. Effect of H_2S and CO on the transformation of 2-ethylphenol as a model compound of bio-crude over sulfided Mo-based catalysts: propositions of promoted active sites for deoxygenation pathways based on an experimental study. Green Chem 2011;13:2441–51.

[221] Massoth FE, Politzer P, Concha MC, Murray JS, Jakowski J, Simons J. Catalytic hydrodeoxygenation of methyl-substituted phenols: Correlations of kinetic parameters with molecular properties. J Phys Chem B 2006;110:14283–91.

[222] Liu G, Robertson AW, Li MM-J, Kuo WCH, Darby MT, Muhieddine MH, et al. MoS_2 monolayer catalyst doped with isolated Co atoms for the hydrodeoxygenation reaction. Nat Chem 2017;9:810–6.

[223] Horáček J, Kubička D. Bio-oil hydrotreating over conventional CoMo & NiMo catalysts: The role of reaction conditions and additives. Fuel 2017;198:49–57.

[224] Sepúlveda C, García R, Reyes P, Ghampson IT, Fierro JLG, Laurenti D, et al. Hydrodeoxygenation of guaiacol over ReS_2/activated carbon catalysts. Support and Re loading effect. Appl Catal A Gen 2014;475:427–37.

[225] Ruiz PE, Leiva K, Garcia R, Reyes P, Fierro JLG, Escalona N. Relevance of sulfiding pretreatment on the performance of Re/ZrO_2 and Re/ZrO_2-sulfated catalysts for the hydrodeoxygenation of guayacol. Appl Catal A Gen 2010;384:78–83.

[226] Leiva K, Sepúlveda C, García R, Fierro JLG, Escalona N. Effect of water on the conversions of 2-methoxyphenol and phenol as bio-oil model compounds over ReS_2/SiO_2 catalyst. Catal Commun 2014;53:33–7.

[227] Infantes-Molina A, Pawelec B, Fierro JLG, Loricera CV, Jiménez-López A, Rodríguez-Castellón E. Effect of Ir and Pt addition on the HDO performance of RuS_2/SBA-15 sulfide catalysts. Top Catal 2015;58:247–57.

[228] Zhu Y, Ramasse QM, Brorson M, Moses PG, Hansen LP, Topsøe H, et al. Location of Co and Ni promoter atoms in multi-layer MoS_2 nanocrystals for hydrotreating catalysis. Catal Today 2015;261:75–81.

[229] Besenbacher F, Brorson M, Clausen BS, Helveg S, Hinnemann B, Kibsgaard J, et al. Recent STM, DFT and HAADF-STEM studies of sulfide-based hydrotreating catalysts: Insight into mechanistic, structural and particle size effects. Catal Today 2008;130:86–96.

[230] Lauritsen JV, Kibsgaard J, Olesen GH, Moses PG, Hinnemann B, Helveg S, et al. Location and coordination of promoter atoms in Co-and Ni-promoted MoS_2-based hydrotreating catalysts. J Catal 2007;249:220–33.

[231] van Haandel L, Bremmer GM, Hensen EJM, Weber T. Influence of sulfiding agent and pressure on structure and performance of $CoMo/Al_2O_3$ hydrodesulfurization catalysts. J Catal 2016;342:27–39.

[232] Kibsgaard J, Tuxen A, Knudsen KG, Brorson M, Topsøe H, Lægsgaard E, et al. Comparative atomic-scale analysis of promotional effects by late 3d-transition metals in MoS_2 hydrotreating catalysts. J Catal 2010;272:195–203.

[233] Lauritsen JV, Helveg S, Lægsgaard E, Stensgaard I, Clausen BS, Topsøe H, et al. Atomic-scale structure of Co–Mo–S nanoclusters in hydrotreating catalysts. J Catal 2001;197:1–5.

[234] Lauritsen JV, Bollinger MV, Lægsgaard E, Jacobsen KW, Nørskov JK, Clausen BS, et al. Atomic-scale insight into structure and morphology changes of MoS_2 nanoclusters in hydrotreating catalysts. J Catal 2004;221:510–22.

[235] Moses PG, Hinnemann B, Topsøe H, Nørskov JK. The effect of Co-promotion on MoS_2 catalysts for hydrodesulfurization of thiophene: A density functional study. J Catal 2009;268:201–8.

[236] Lauritsen JV, Besenbacher F. Atom-resolved scanning tunneling microscopy investigations of molecular adsorption on MoS_2 and CoMoS hydrodesulfurization catalysts. J Catal 2015;328:49–58.

[237] Travert A, Nakamura H, van Santen RA, Cristol S, Paul J-F, Payen E. Hydrogen activation on Mo-based sulfide catalysts, a periodic DFT study. J Am Chem Soc 2002;124:7084–95.

[238] Topsøe N-Y, Topsøe H. FTIR studies of Mo/Al_2O_3-based catalysts. II. Evidence for the presence of SH groups and their role in acidity and activity. J Catal 1993;139:641–51.

[239] Lauritsen JV, Nyberg M, Nørskov JK, Clausen BS, Topsøe H, Lægsgaard E, et al. Hydrodesulfurization reaction pathways on MoS_2 nanoclusters revealed by scanning tunneling microscopy. J Catal 2004;224:94–106.

[240] Lauritsen JV, Nyberg M, Vang RT, Bollinger MV, Clausen BS, Topsøe H, et al. Chemistry of one-dimensional metallic edge states in MoS_2 nanoclusters. Nanotechnology 2003;14:385–9.

[241] Tuxen AK, Füchtbauer HG, Temel B, Hinnemann B, Topsøe H, Knudsen KG, et al. Atomic-scale insight into adsorption of sterically hindered dibenzothiophenes on MoS_2 and Co-Mo-S hydrotreating catalysts. J Catal 2012;295:146–54.

[242] Badawi M, Cristol S, Paul J-F, Payen E. DFT study of furan adsorption over stable molybdenum sulfide catalyst under HDO conditions. CR Chim 2009;12:754–61.

[243] Şenol Oİ, Viljava T-R, Krause AOI. Hydrodeoxygenation of aliphatic esters on sulphided $NiMo/\gamma\text{-}Al_2O_3$ and $CoMo/\gamma\text{-}Al_2O_3$ catalyst: The effect of water. Catal Today 2005;106:186–9.

[244] Stanislaus A, Marafi A, Rana MS. Recent advances in the science and technology of ultra low sulfur diesel (ULSD) production. Catal Today 2010;153:1–68.

[245] Ryymin E-M, Honkela ML, Viljava T-R, Krause AOI. Insight to sulfur species in the

hydrodeoxygenation of aliphatic esters over sulfided NiMo/γ-Al_2O_3 catalyst. Appl Catal A Gen 2009;358:42–8.

[246] Şenol Oİ, Ryymin E-M, Viljava T-R, Krause AOI. Reactions of methyl heptanoate hydrodeoxygenation on sulphided catalysts. J Mol Catal A Chem 2007;268:1–8.

[247] Raybaud P, Hafner J, Kresse G, Kasztelan S, Toulhoat H. Structure, energetics, and electronic properties of the surface of a promoted MoS_2 catalyst: An ab initio local density functional study. J Catal 2000;190:128–43.

[248] Leliveld BRG, van Dillen JAJ, Geus JW, Koningsberger DC, de Boer M. Structure and nature of the active sites in CoMo hydrotreating catalysts. An EXAFS study of the reaction with selenophene. J Phys Chem B 1997;101:11160–71.

[249] Gonçalves VOO, Brunet S, Richard F. Hydrodeoxygenation of cresols over Mo/Al_2O_3 and CoMo/Al_2O_3 sulfided catalysts. Catal Letters 2016;146:1562–73.

[250] Schachtl E, Yoo JS, Gutiérrez OY, Studt F, Lercher JA. Impact of Ni promotion on the hydrogenation pathways of phenanthrene on MoS_2/γ-Al_2O_3. J Catal 2017;352:171–81.

[251] Dupont C, Lemeur R, Daudin A, Raybaud P. Hydrodeoxygenation pathways catalyzed by MoS_2 and NiMoS active phases: A DFT study. J Catal 2011;279:276–86.

[252] Prasomsri T, Nimmanwudipong T, Román-Leshkov Y. Effective hydrodeoxygenation of biomass-derived oxygenates into unsaturated hydrocarbons by MoO_3 using low H_2 pressures. Energy Environ Sci 2013;6:1732–8.

[253] Moberg DR, Thibodeau TJ, Amar FG, Frederick BG. Mechanism of Hydrodeoxygenation of Acrolein on a Cluster Model of MoO_3. J Phys Chem C 2010;114:13782–95.

[254] Whiffen VML, Smith KJ. Hydrodeoxygenation of 4-methylphenol over unsupported MoP, MoS_2, and MoO_x catalysts. Energy & Fuels 2010;24:4728–37.

[255] Prasomsri T, Shetty M, Murugappan K, Román-Leshkov Y. Insights into the catalytic activity and surface modification of MoO_3 during the hydrodeoxygenation of lignin-derived model compounds into aromatic hydrocarbons under low hydrogen pressures. Energy Environ Sci 2014;7:2660–9.

[256] Shetty M, Murugappan K, Prasomsri T, Green WH, Román-Leshkov Y. Reactivity and stability investigation of supported molybdenum oxide catalysts for the hydrodeoxygenation (HDO) of m-cresol. J Catal 2015;331:86–97.

[257] Shetty M, Buesser B, Román-Leshkov Y, Green WH. Computational investigation on hydrodeoxygenation (HDO) of acetone to propylene on α-MoO_3 (010) surface. J Phys Chem C 2017;121:17848–55.

[258] Ranga C, Lødeng R, Alexiadis VI, Rajkhowa T, Bjørkan H, Chytil S, et al. Effect of composition and preparation on supported MoO_3 catalysts for anisole hydrodeoxygenation. Chem Eng J 2018;335:120–32.

[259] Ghampson IT, Sepúlveda C, García R, Fierro JLG, Escalona N. Carbon nanofiber-supported ReO_x catalysts for the hydrodeoxygenation of lignin-derived compounds. Catal Sci Technol 2016;6:4356–69.

[260] Auroux A, Gervasini A. Microcalorimetric study of the acidity and basicity of metal oxide surfaces. J Phys Chem 1990;94:6371–9.

[261] Li S, Dixon DA. Molecular and electronic structures, Brönsted basicities, and Lewis acidities of group VIB transition metal oxide clusters. J Phys Chem A 2006;110:6231–44.

[262] Busca G. Chapter 9: The surface acidity and basicity of solid oxides and zeolites. In: J.L.G. Fierro, editor. Metal oxides. Chemistry and applications, Boca Raton: CRC Press, Taylor & Francis Group; 2006, p. 247–318.

[263] Rodriguez JA, Hrbek J. Interaction of sulfur with well-defined metal and oxide surfaces: unraveling the mysteries behind catalyst poisoning and desulfurization. Acc Chem Res 1999;32:719–28.

[264] Chorkendorff I, Niemantsverdriet JW. Chapter 8: Heterogeneous catalysis in practice: Hydrogen. Concepts of modern catalysis and kinetics. 2nd ed., Darmstadt: Wiley-VCH Verlag GmbH & Co. KGaA; 2010, p. 305–52.

[265] Mortensen PM, Grunwaldt J-D, Jensen PA, Jensen AD. Screening of catalysts for hydrodeoxygenation of phenol as a model compound for bio-oil. ACS Catal 2013;3:1774–85.

[266] Tan Q, Wang G, Long A, Dinse A, Buda C, Shabaker J, et al. Mechanistic analysis of the role of metal oxophilicity in the hydrodeoxygenation of anisole. J Catal 2017;347:102–15.

[267] Kordouli E, Kordulis C, Lycourghiotis A, Cole R, Vasudevan PT, Pawelec B, et al. HDO activity of carbon-supported Rh, Ni and Mo-Ni catalysts. Mol Catal 2017;441:209–20.

[268] Garcia-Pintos D, Voss J, Jensen AD, Studt F. Hydrodeoxygenation of phenol to benzene and cyclohexane on Rh(111) and Rh(211) surfaces: Insights from density functional theory. J Phys Chem C 2016;120:18529–37.

[269] Lee CR, Yoon JS, Suh Y-W, Choi J-W, Ha J-M, Suh DJ, et al. Catalytic roles of metals and supports on hydrodeoxygenation of lignin monomer guaiacol. Catal Commun 2012;17:54–8.

[270] Zhao C, Kou Y, Lemonidou AA, Li X, Lercher JA. Highly selective catalytic conversion of phenolic bio-oil to alkanes. Angew Chemie Int Ed 2009;48:3987–90.

[271] Tan Q, Wang G, Nie L, Dinse A, Buda C, Shabaker J, et al. Different product distributions and mechanistic aspects of the hydrodeoxygenation of m-cresol over platinum and ruthenium catalysts. ACS Catal 2015;5:6271–83.

[272] de Souza PM, Rabelo-Neto RC, Borges LEP, Jacobs G, Davis BH, Graham UM, et al. Effect of zirconia morphology on hydrodeoxygenation of phenol over Pd/ZrO_2. ACS Catal 2015;5:7385–98.

[273] Nie L, de Souza PM, Noronha FB, An W, Sooknoi T, Resasco DE. Selective conversion of m-cresol to toluene over bimetallic Ni–Fe catalysts. J Mol Catal A Chem 2014;388–389:47–55.

[274] de Souza PM, Rabelo-Neto RC, Borges LEP, Jacobs G, Davis BH, Resasco DE, et al. Hydrodeoxygenation of phenol over Pd catalysts. Effect of support on reaction mechanism and catalyst deactivation. ACS Catal 2017;7:2058–73.

[275] Griffin MB, Ferguson GA, Ruddy DA, Biddy MJ, Beckham GT, Schaidle JA. Role of the support and reaction conditions on the vapor-phase deoxygenation of m-cresol over Pt/C and Pt/TiO_2 catalysts. ACS Catal 2016;6:2715–27.

[276] Hellinger M, Carvalho HWP, Baier S, Wang D, Kleist W, Grunwaldt J-D. Catalytic hydrodeoxygenation of guaiacol over platinum supported on metal oxides and zeolites. Appl Catal A Gen 2015;490:181–92.

[277] Nie L, Resasco DE. Kinetics and mechanism of m-cresol hydrodeoxygenation on a Pt/SiO_2 catalyst. J Catal 2014;317:22–9.

[278] Oh S, Hwang H, Choi HS, Choi JW. The effects of noble metal catalysts on the bio-oil quality during the hydrodeoxygenative upgrading process. Fuel 2015;153:535–43.

[279] Saidi M, Rahimpour MR, Raeissi S. Upgrading process of 4-methylanisole as a lignin-derived bio-oil catalyzed by $Pt/\gamma\text{-}Al_2O_3$: Kinetic investigation and reaction network development. Energy & Fuels 2015;29:3335–44.

[280] Saidi M, Rostami P, Rahimpour MR, Gates BC, Raeissi S. Upgrading of lignin-derived bio-oil components catalyzed by $Pt/\gamma\text{-}Al_2O_3$: Kinetics and reaction pathways characterizing conversion of cyclohexanone with H_2. Energy & Fuels 2015;29:191–9.

[281] Gutierrez A, Kaila RK, Honkela ML, Slioor R, Krause AOI. Hydrodeoxygenation of guaiacol on noble metal catalysts. Catal Today 2009;147:239–46.

[282] Yohe SL, Choudhari HJ, Mehta DD, Dietrich PJ, Detwiler MD, Akatay CM, et al. High-pressure vapor-phase hydrodeoxygenation of lignin-derived oxygenates to hydrocarbons by a PtMo bimetallic catalyst: Product selectivity, reaction pathway, and structural characterization. J Catal 2016;344:535–52.

[283] Hensley AJR, Wang Y, McEwen J-S. Phenol deoxygenation mechanisms on Fe(110) and Pd(111). ACS Catal 2015;5:523–36.

[284] Sun J, Karim AM, Zhang H, Kovarik L, Li XS, Hensley AJ, et al. Carbon-supported bimetallic Pd–Fe catalysts for vapor-phase hydrodeoxygenation of guaiacol. J Catal 2013;306:47–57.

[285] Sitthisa S, Resasco DE. Hydrodeoxygenation of furfural over supported metal catalysts: A comparative study of Cu, Pd and Ni. Catal Letters 2011;141:784–91.

[286] Luo J, Monai M, Yun H, Arroyo-Ramírez L, Wang C, Murray CB, et al. The H_2 pressure dependence of hydrodeoxygenation selectivities for furfural over Pt/C catalysts. Catal Letters 2016;146:711–7.

[287] Wildschut J, Arentz J, Rasrendra CB, Venderbosch RH, Heeres HJ. Catalytic hydrotreatment of fast pyrolysis oil: Model studies on reaction pathways for the carbohydrate fraction. Environ Prog Sustain Energy 2009;28:450–460.

[288] Vesborg PCK, Jaramillo TF. Addressing the terawatt challenge: Scalability in the supply of chemical elements for renewable energy. RSC Adv 2012;2:7933–47.

[289] Jin S, Xiao Z, Li C, Chen X, Wang L, Xing J, et al. Catalytic hydrodeoxygenation of anisole as lignin model compound over supported nickel catalysts. Catal Today 2014;234:125–32.

[290] Yakovlev VA, Khromova SA, Sherstyuk OV, Dundich VO, Ermakov DY, Novopashina VM, et al. Development of new catalytic systems for upgraded bio-fuels production from bio-crude-oil and biodiesel. Catal Today 2009;144:362–6.

[291] Khromova SA, Smirnov AA, Bulavchenko OA, Saraev AA, Kaichev VV, Reshetnikov SI,

et al. Anisole hydrodeoxygenation over Ni–Cu bimetallic catalysts: The effect of Ni/Cu ratio on selectivity. Appl Catal A Gen 2014;470:261–70.

[292] Mortensen PM, Grunwaldt J-D, Jensen PA, Jensen AD. Influence on nickel particle size on the hydrodeoxygenation of phenol over Ni/SiO_2. Catal Today 2016;259:277–84.

[293] Zhang X, Zhang Q, Wang T, Ma L, Yu Y, Chen L. Hydrodeoxygenation of lignin-derived phenolic compounds to hydrocarbons over Ni/SiO_2-ZrO_2 catalysts. Bioresour Technol 2013;134:73–80.

[294] Ardiyanti AR, Bykova M V., Khromova SA, Yin W, Venderbosch RH, Yakovlev VA, et al. Ni-based catalysts for the hydrotreatment of fast pyrolysis oil. Energy and Fuels 2016;30:1544–54.

[295] Dongil AB, Ghampson IT, García R, Fierro JLG, Escalona N. Hydrodeoxygenation of guaiacol over Ni/carbon catalysts: effect of the support and Ni loading. RSC Adv 2016;6:2611–23.

[296] Fang H, Zheng J, Luo X, Du J, Roldan A, Leoni S, et al. Product tunable behavior of carbon nanotubes-supported Ni–Fe catalysts for guaiacol hydrodeoxygenation. Appl Catal A Gen 2017;529:20–31.

[297] Zhao HY, Li D, Bui P, Oyama ST. Hydrodeoxygenation of guaiacol as model compound for pyrolysis oil on transition metal phosphide hydroprocessing catalysts. Appl Catal A Gen 2011;391:305–10.

[298] Moon J-S, Kim E-G, Lee Y-K. Active sites of Ni_2P/SiO_2 catalyst for hydrodeoxygenation of guaiacol: A joint XAFS and DFT study. J Catal 2014;311:144–52.

[299] Li K, Wang R, Chen J. Hydrodeoxygenation of anisole over silica-supported Ni_2P, MoP, and NiMoP catalysts. Energy & Fuels 2011;25:854–63.

[300] Wu S-K, Lai P-C, Lin Y-C, Wan H-P, Lee H-T, Chang Y-H. Atmospheric hydrodeoxygenation of guaiacol over alumina-, zirconia-, and silica-supported nickel phosphide catalysts. ACS Sustain Chem Eng 2013;1:349–58.

[301] Moon J-S, Lee Y-K. Support effects of Ni_2P catalysts on the hydrodeoxygenation of guaiacol: In situ XAFS studies. Top Catal 2015;58:211–8.

[302] Gonçalves VOO, de Souza PM, da Silva VT, Noronha FB, Richard F. Environmental kinetics of the hydrodeoxygenation of cresol isomers over Ni_2P/SiO_2: Proposals of nature of deoxygenation active sites based on an experimental study. Appl Catal A Gen 2017;205:357–67.

[303] Bui P, Cecilia JA, Oyama ST, Takagaki A, Infantes-Molina A, Zhao H, et al. Studies of the synthesis of transition metal phosphides and their activity in the hydrodeoxygenation of a biofuel model compound. J Catal 2012;294:184–98.

[304] Choi J, Zacher AH, Wang H, Olarte M V, Armstrong BL, Meyer HM, et al. Molybdenum carbides, active and in situ regenerable catalysts in hydroprocessing of fast pyrolysis bio-oil. Energy & Fuels 2016;30:5016–25.

[305] Li Z, Choi J, Wang H, Lepore AW, Connatser RM, Lewis SA, et al. Sulfur-tolerant molybdenum carbide catalysts enabling low-temperature stabilization of fast pyrolysis bio-oil. Energy & Fuels 2017;31:9585–94.

[306] Engelhardt J, Lyu P, Nachtigall P, Schüth F, García ÁM. The influence of water on the performance of molybdenum carbide catalysts in hydrodeoxygenation reactions: A combined theoretical and experimental study. ChemCatChem 2017;9:1985–91.

[307] Jiang H, Yu X, Peng X, Zhang H, Nie R, Lu X, et al. Efficient aqueous hydrodeoxygenation of vanillin over a mesoporous carbon nitride-modified Pd nanocatalyst. RSC Adv 2016;6:69045–51.

[308] Arun N, Maley J, Chen N, Sammynaiken R, Hu Y, Dalai AK. NiMo nitride supported on γ-Al_2O_3 for hydrodeoxygenation of oleic acid: Novel characterization and activity study. Catal Today 2017;291:153–9.

[309] Furimsky E. Metal carbides and nitrides as potential catalysts for hydroprocessing. Appl Catal A Gen 2003;240:1–28.

[310] Kelly TG, Chen JG. Metal overlayer on metal carbide substrate: Unique bimetallic properties for catalysis and electrocatalysis. Chem Soc Rev 2012;41:8021–34.

[311] Mortensen PM, de Carvalho HWP, Grunwaldt J-D, Jensen PA, Jensen AD. Activity and stability of Mo_2C/ZrO_2 as catalyst for hydrodeoxygenation of mixtures of phenol and 1-octanol. J Catal 2015;328:208–15.

[312] Liu C, Sun J, Brown HM, Marin-Flores OG, Bays JT, Karim AM, et al. Aqueous phase hydrodeoxygenation of polyols over Pd/WO_3-ZrO_2: Role of Pd-WO_3 interaction and hydrodeoxygenation pathway. Catal Today 2016;269:103–9.

[313] Dickinson JG, Savage PE. Development of NiCu catalysts for aqueous-phase hydrodeoxygenation. ACS Catal 2014;4:2605–15.

[314] Ahmadi S, Yuan Z, Rohani S, Xu C. Effects of nano-structured CoMo catalysts on hydrodeoxygenation of fast pyrolysis oil in supercritical ethanol. Catal Today 2016;269:182–94.

[315] Weng Y, Wang T, Qiu S, Wang C, Ma L. Aqueous-phase hydrodeoxygenation of biomass sugar alcohol into renewable alkanes over a carbon-supported ruthenium with phosphoric acid catalytic system. ChemCatChem 2017;9:774–81.

[316] Wang W, Yang Y, Luo H, Peng H, Wang F. Effect of La on Ni-W-B amorphous catalysts in hydrodeoxygenation of phenol. Ind Eng Chem Res 2011;50:10936–42.

[317] Laurent E, Delmon B. Influence of water in the deactivation of a sulfided NiMo/γ-Al_2O_3 catalyst during hydrodeoxygenation. J Catal 1994;146:281–91.

[318] Idriss H, Barteau MA. Active sites on oxides: From single crystals to catalysts. Adv Catal 2000;45:261–331.

[319] Kung HH. Chapter 4: Surface coordinative unsaturation. Studies in surface science and catalysis. Transition metal oxides: Surface chemistry and catalysis, vol. 45. 1st ed., Amsterdam: Elsevier Science Publishing Company Inc.; 1989, p. 53–71.

[320] Popov A, Kondratieva E, Mariey L, Goupil JM, El Fallah J, Gilson J-P, et al. Bio-oil hydrodeoxygenation: Adsorption of phenolic compounds on sulfided (Co)Mo catalysts. J Catal 2013;297:176–86.

[321] Sankaranarayanan TM, Berenguer A, Ochoa-Hernández C, Moreno I, Jana P, Coronado JM, et al. Hydrodeoxygenation of anisole as bio-oil model compound over supported Ni

and Co catalysts: Effect of metal and support properties. Catal Today 2015;243:163–72.

[322] Chen H, Wang Q, Zhang X, Wang L. Effect of support on the NiMo phase and its catalytic hydrodeoxygenation of triglycerides. Fuel 2015;159:430–5.

[323] Selvaraj M, Shanthi K, Maheswari R, Ramanathan A. Hydrodeoxygenation of guaiacol over MoO_3-NiO/mesoporous silicates: Effect of incorporated heteroatom. Energy & Fuels 2014;28:2598−2607.

[324] Dundich VO, Khromova SA, Ermakov DY, Lebedev MY, Novopashina VM, Sister VG, et al. Nickel catalysts for the hydrodeoxygenation of biodiesel. Kinet Catal 2010;51:704–9.

[325] Phan BMQ, Ha QLM, Le NP, Ngo PT, Nguyen TH, Dang TT, et al. Influences of various supports, γ-Al_2O_3, CeO_2, and SBA-15 on HDO performance of NiMo catalyst. Catal Letters 2015;145:662–7.

[326] Schimming SM, Foo GS, LaMont OD, Rogers AK, Yung MM, D'Amico AD, et al. Kinetics of hydrogen activation on ceria–zirconia. J Catal 2015;329:335–47.

[327] Schimming SM, LaMont OD, König M, Rogers AK, D'Amico AD, Yung MM, et al. Hydrodeoxygenation of guaiacol over ceria-zirconia catalysts. ChemSusChem 2015;8:2073–83.

[328] Vivier L, Duprez D. Ceria-based solid catalysts for organic chemistry. ChemSusChem 2010;3:654–78.

[329] Foraita S, Fulton JL, Chase ZA, Vjunov A, Xu P, Baráth E, et al. Impact of the oxygen defects and the hydrogen concentration on the surface of tetragonal and monoclinic ZrO_2 on the reduction rates of stearic acid on Ni/ZrO_2. Chem Eur J 2015;21:2423–34.

[330] Elliott DC, Neuenschwander GG, Hart TR. Hydroprocessing bio-oil and products separation for coke production. ACS Sustain Chem Eng 2013;1:389–92.

[331] Elliott DC, Wang H, French R, Deutch S, Iisa K. Hydrocarbon liquid production from biomass via hot-vapor-filtered fast pyrolysis and catalytic hydroprocessing of the bio-oil. Energy & Fuels 2014;28:5909–17.

[332] Zacher AH, Elliott DC, Olarte M V., Santosa DM, Preto F, Iisa K. Pyrolysis of woody residue feedstocks: Upgrading of bio-oils from mountain-pine-beetle-killed trees and hog fuel. Energy & Fuels 2014;28:7510–6.

[333] Olarte M V., Padmaperuma AB, Ferrell III JR, Christensen ED, Hallen RT, Lucke RB, et al. Characterization of upgraded fast pyrolysis oak oil distillate fractions from sulfided and non-sulfided catalytic hydrotreating. Fuel 2017;202:620–30.

[334] McCall MJ, Brandvold TA. Fuel and fuel blending components from biomass derived pyrolysis oil US 2009/0253948 A1, 2009.

[335] Mercader F de M, Groeneveld MJ, Kersten SRA, Way NWJ, Schaverien CJ, Hogendoorn JA. Production of advanced biofuels: Co-processing of upgraded pyrolysis oil in standard refinery units. Appl Catal B Environ 2010;96:57–66.

[336] Furimsky E, Massoth FE. Deactivation of hydroprocessing catalysts. Catal Today 1999;52:381–495.

[337] Boscagli C, Yang C, Welle A, Wang W, Behrens S, Raffelt K, et al. Effect of pyrolysis oil

components on the activity and selectivity of nickel-based catalysts during hydrotreatment. Appl Catal A Gen 2017;544:161–72.

[338] Fonseca A, Zeuthen P, Nagy JB. ^{13}C n.m.r. quantitative analysis of catalyst carbon deposits. Fuel 1996;75:1363–76.

[339] Fonseca A, Zeuthen P, Nagy JB. Assignment of an average chemical structure to catalyst carbon deposits on the basis of quantitative ^{13}C n.m.r. spectra. Fuel 1996;75:1413–23.

[340] Zhang J, Wang K, Nolte MW, Choi YS, Brown RC, Shanks BH. Catalytic deoxygenation of bio-oil model compounds over acid-base bifunctional catalysts. ACS Catal 2016;6:2608–21.

[341] Weber RS, Olarte MV, Wang H. Modeling the kinetics of deactivation of catalysts during the upgrading of bio-oil. Energy & Fuels 2015;29:273−277.

[342] Yamamoto Y, Kumata F, Massoth FE. Hydrotreating catalyst deactivation by coke from SRC-II oil. Fuel Process Technol 1988;19:253–63.

[343] Pieck CL, Jablonski EL, Parera JM. Sintering-redispersion of Pt-Re/Al_2O_3 during regeneration. Appl Catal 1990;62:47–60.

[344] Dufresne P. Hydroprocessing catalysts regeneration and recycling. Appl Catal A Gen 2007;322:67–75.

[345] Resende FLP. Recent advances on fast hydropyrolysis of biomass. Catal Today 2016;269:148–55.

[346] Meesuk S, Cao J-P, Sato K, Ogawa Y, Takarada T. Fast pyrolysis of rice husk in a fluidized bed: Effects of the gas atmosphere and catalyst on bio-oil with a relatively low content of oxygen. Energy & Fuels 2011;25:4113–21.

[347] Meesuk S, Cao J-P, Sato K, Ogawa Y, Takarada T. Study of catalytic hydropyrolysis of rice husk under nickel-loaded brown coal char. Energy & Fuels 2011;25:5438–43.

[348] Meesuk S, Cao J-P, Sato K, Ogawa Y, Takarada T. The effects of temperature on product yields and composition of bio-oils in hydropyrolysis of rice husk using nickel-loaded brown coal char catalyst. J Anal Appl Pyrolysis 2012;94:238–45.

[349] Zhang H, Xiao R, Wang D, He G, Shao S, Zhang J, et al. Biomass fast pyrolysis in a fluidized bed reactor under N_2, CO_2, CO, CH_4 and H_2 atmospheres. Bioresour Technol 2011;102:4258–64.

[350] Dayton DC, Carpenter J, Farmer J, Turk B, Gupta R. Biomass hydropyrolysis in a pressurized fluidized bed reactor. Energy & Fuels 2013;27:3778–85.

[351] Melligan F, Hayes MHB, Kwapinski W, Leahy JJ. Hydro-pyrolysis of biomass and online catalytic vapor upgrading with Ni-ZSM-5 and Ni-MCM-41. Energy & Fuels 2012;26:6080–90.

[352] Melligan F, Hayes MHB, Kwapinski W, Leahy JJ. A study of hydrogen pressure during hydropyrolysis of Miscanthus x giganteus and online catalytic vapour upgrading with Ni on ZSM-5. J Anal Appl Pyrolysis 2013;103:369–77.

[353] Gamliel DP, Bollas GM, Valla JA. Bifunctional Ni-ZSM-5 catalysts for the pyrolysis and hydropyrolysis of biomass. Energy Technol 2017;5:172–82.

[354] Gamliel DP, Wilcox L, Valla JA. The effects of catalyst properties on the conversion of biomass via catalytic fast hydropyrolysis. Energy & Fuels 2017;31:679–87.

[355] Jan O, Marchand R, Anjos LCA, Seufitelli GVS, Nikolla E, Resende FLP. Hydropyrolysis of lignin using Pd/HZSM-5. Energy & Fuels 2015;29:1793–800.

[356] Thangalazhy-Gopakumar S, Adhikari S, Gupta RB, Tu M, Taylor S. Production of hydrocarbon fuels from biomass using catalytic pyrolysis under helium and hydrogen environments. Bioresour Technol 2011;102:6742–9.

[357] Dayton DC, Hlebak J, Carpenter JR, Wang K, Mante OD, Peters JE. Biomass hydropyrolysis in a fluidized bed reactor. Energy & Fuels 2016;30:4879–87.

[358] Agrawal R, Singh NR. Synergistic routes to liquid fuel for a petroleum-deprived future. AIChE J 2009;55:1898–905.

[359] Singh NR, Delgass WN, Ribeiro FH, Agrawal R. Estimation of liquid fuel yields from biomass. Environ Sci Technol 2010;44:5298–305.

[360] Singh NR, Mallapragada DS, Agrawal R, Tyner WE. Economic analysis of novel synergistic biofuel (H_2Bioil) processes. Biomass Convers Biorefinery 2012;2:141–8.

[361] Venkatakrishnan VK, Delgass WN, Ribeiro FH, Agrawal R. Oxygen removal from intact biomass to produce liquid fuel range hydrocarbons via fast-hydropyrolysis and vapor-phase catalytic hydrodeoxygenation. Green Chem 2015;17:178–83.

[362] Venkatakrishnan VK, Degenstein JC, Smeltz AD, Delgass WN, Agrawal R, Ribeiro FH. High-pressure fast-pyrolysis, fast-hydropyrolysis and catalytic hydrodeoxygenation of cellulose: Production of liquid fuel from biomass. Green Chem 2014;16:792–802.

[363] Marker TL, Felix LG, Linck MB, Roberts MJ. Integrated hydropyrolysis and hydroconversion (IH^2) for the direct production of gasoline and diesel fuels or blending components from biomass, Part 1: Proof of principle testing. Environ Prog Sustain Energy 2012;31:191–9.

[364] Marker TL, Felix LG, Linck MB, Roberts MJ, Ortiz-Toral P, Wangerow J. Integrated hydropyrolysis and hydroconversion ($IH^{2®}$) for the direct production of gasoline and diesel fuels or blending components from biomass, Part 2: Continuous testing. Environ Prog Sustain Energy 2014;33:762–8.

[365] Maleche E, Glaser R, Marker T, Shonnard D. A preliminary life cycle assessment of biofuels produced by the $IH^{2\ TM}$ process. Environ Prog Sustain Energy 2014;33:322–9.

[366] Tan ECD, Marker TL, Roberts MJ. Direct production of gasoline and diesel fuels from biomass via integrated hydropyrolysis and hydroconversion process-A techno-economic analysis. Environ Prog Sustain Energy 2014;33:609–17.

[367] Independent Statistics & Analysis - U.S. Energy Information Administration. Refiner gasoline prices by grade and sales type 2017. https://www.eia.gov/dnav/pet/pet_pri_refmg_dcu_nus_a.htm (accessed July 5, 2017).

[368] Zhang L, Gong K, Lai J, Alvey P. Chemical composition and stability of renewable hydrocarbon products generated from a hydropyrolysis vapor upgrading process. Green Chem 2017;19:3628–41.

[369] Lai J, Zhang L, Gong K. Nuclear magnetic resonance characterization of renewable

products from a two-step ex-situ hydropyrolysis vapor upgrading process. ChemistrySelect 2018;3:297–307.

[370] Stummann, M.Z.; Høj, M.; Schandel, C.B.; Hansen, A.B.; Wiwel, P.; Gabrielsen, J.; Jensen, P.A.; Jensen AD. Hydrogen assisted catalytic biomass pyrolysis. Effect of temperature and pressure. Biomass and Bioenergy 2018;115:97–107.

[371] Badger PC, Fransham P. Use of mobile fast pyrolysis plants to densify biomass and reduce biomass handling costs-A preliminary assessment. Biomass and Bioenergy 2006;30:321–5.

[372] Jones SB, Valkenburg C, Walton CW, Elliot DC, Holladay JE, Stevens DJ, et al. Production of gasoline and diesel from biomass via fast pyrolysis, hydrotreating and hydrocracking: A design case (PNNL-18284). Pacific Northwest National Laboratory. 2009.

[373] Marker T, Roberts M, Linck M, Felix L, Ortiz-Toral P, Wangerow J, et al. Long term processing using integrated hydropyrolysis plus hydroconversion (IH^2) for the production of gasoline and diesel from biomass. gti. Technical Report. 2013.

[374] Dagaut P. On the kinetics of hydrocarbons oxidation from natural gas to kerosene and diesel fuel. Phys Chem Chem Phys 2002;4:2079–94.